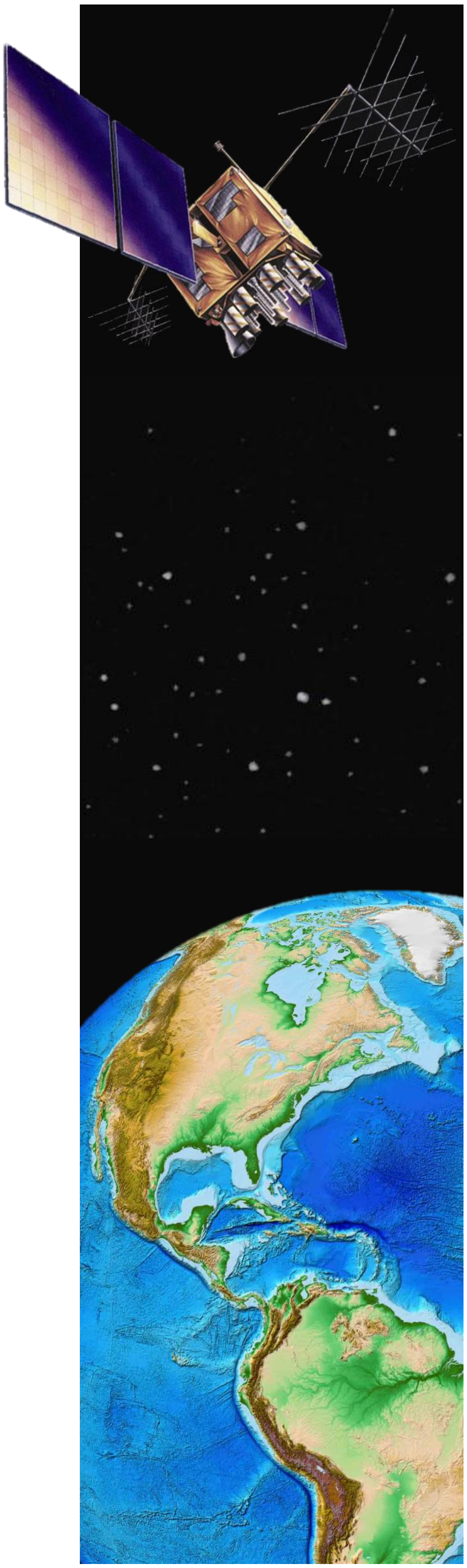

An Analysis of Global Positioning System (GPS) Standard Positioning Service (SPS) Performance for 2017

TR-SGL-18-02

March 20, 2018

Space and Geophysics Laboratory
Applied Research Laboratories
The University of Texas at Austin
P.O. Box 8029
Austin, TX 78713-8029

Brent A. Renfro,
Miquela Stein,
Nicholas Boeker,
Audric Terry

Contract: NAVSEA Contract N00024-01-D-6200
Task Order: 5101165

Distribution A: Approved for public release; Distribution is unlimited.

This Page Added for Document Spacing

Executive Summary

Applied Research Laboratories, The University of Texas at Austin (ARL:UT) examined the performance of the Global Positioning System (GPS) throughout 2017 for the Global Positioning Systems Directorate (SMC/GP). This report details the results of that performance analysis. This material is based upon work supported by the US Air Force Space & Missile Systems Center Global Positioning Systems Directorate through Naval Sea Systems Command Contract N00024-01-D-6200, task order 5101165, "GPS Data Collection and Performance Analysis."

Performance is defined by the 2008 Standard Positioning Service (SPS) Performance Standard (SPS PS) [1]. The performance standard provides the U.S. government's assertions regarding the expected performance of GPS. This report does not address all of the assertions in the performance standards. This report emphasizes those assertions which can be verified by anyone with knowledge of standard GPS data analysis practices, familiarity with the relevant signal specification, and access to a Global Navigation Satellite System (GNSS) data archive.

The assertions evaluated include those of accuracy, integrity, continuity, and availability of the GPS signal-in-space (SIS) along with the assertions on accuracy of positioning and time transfer. Chapter 1 is an introduction to the report. Chapter 2 of the report includes a tabular summary of the assertions that were evaluated and a summary of the results. The remaining chapters present details on the analysis associated with each assertion.

All the SPS PS assertions examined in the report were met in 2017 with one exception. The exception was the report notification requirement for scheduled interruptions. This was met in only 36 of 47 cases (81%).

Contents

List of Figures

List of Tables

Chapter 1

Introduction

Applied Research Laboratories, The University of Texas at Austin (ARL:UT)[1] examined the performance of the Global Positioning System (GPS) throughout 2017 for the Global Positioning Systems Directorate (SMC/GP). This report details the results of that analysis. This material is based upon work supported by the US Air Force Space & Missile Systems Center Global Positioning Systems Directorate through Naval Sea Systems Command Contract N00024-01-D-6200, task order 5101165, "GPS Data Collection and Performance Analysis."

Performance is assessed relative to selected assertions in the 2008 Standard Positioning Service (SPS) Performance Standard (SPS PS) [1]. (Hereafter the term SPS PS, or SPSPS08, is used when referring to the 2008 SPS PS.) Chapter 2 contains a tabular summary of performance stated in terms of the metrics provided in the performance standard. Chapter 3 presents a more detailed explanation of the analysis conducted in evaluating each assertion. The assertions are presented in the order of appearance in the performance standards. Chapter 4 details additional findings of the performance analysis.

The performance standards define the services delivered through the L1 C/A code signal. The metrics are limited to characterizing the signal-in-space (SIS) and do not address atmospheric errors, receiver errors, or errors due to the user environment (e.g. multipath errors, terrain masking, and foliage). This report addresses assertions in the SPS PS that can be verified by anyone with knowledge of standard GPS data analysis practices, familiarity with the relevant signal specification [2], and access to a data archive (such as that available via the International Global Navigation Satellite System (GNSS) Service (IGS)) [3]. The assertions examined include those related to user range error (URE), availability of service, and position domain standards.

[1] *A complete list of abbreviations found in this document is provided in Appendix G.*

The majority of the assertions related to URE values are evaluated by comparison of the space vehicle (SV) clock and position representations as computed from the broadcast Legacy Navigation (LNAV) message data against the SV truth clock and position data as provided by a precise orbit calculated after the time of interest. The broadcast clock and position data is denoted in this report by BCP and the truth clock and position data by TCP. The process by which the URE values are calculated is described in Appendix B of this report.

Observation data from tracking stations are used to cross-check the URE values and to evaluate non-URE assertions. Examples of the latter application include the areas of Continuity (3.3), Availability (3.4), and Position/Time Availability (3.5). In these cases, data from two networks are used. The two networks considered are the National Geospatial-Intelligence Agency (NGA) Monitor Station Network (MSN) [4] and a subset of the tracking stations that contribute to the IGS. The geographic distribution of these stations is shown in Figure 1.1. The selection of these sets of stations ensure continuous simultaneous observation of all space vehicles by multiple stations.

Navigation message data used in this report were collected from the NGA MSN. The collection and selection of navigation message data are described in general terms in Appendix B.2.

Several metrics in the performance standards are stated in terms of either the Base 24 constellation which consists of six orbital planes and four slots per plane or the Expandable 24 constellation in which three of the 24 slots may be occupied by two SVs. Currently, there are more than 32 GPS SVs on-orbit. Of these, at most 31 SVs may be operationally broadcasting at any time. Of the SVs on-orbit, 27 are located in the Expandable 24 constellation. The SVs in excess of those located in defined slots are assigned to locations in various planes in accordance with operational considerations.

The majority of the metrics in this report are evaluated on either a per-SV basis or for the full constellation. The metrics associated with continuity and availability are defined with respect to the slot definitions.

Each of the GPS SVs are identified by pseudo-random noise ID (PRN) and by space vehicle number (SVN). PRN IDs are assigned to SVs for periods of time. A given SV may be assigned different PRNs at different times during its operational life. The SVN represents the permanent unique identifier for the vehicle under discussion. As the number of active SVs has increased to nearly the total available, PRNs are now being used by multiple SVs within a given year (but by no more than one SV at a time). In general, we list the SVN first and the PRN second because the SVN is the unique identifier of the two. The SVN-to-PRN relationships were provided by the Master Control Station (MCS), however other useful summaries of this information may be found on the U.S. Coast Guard Navigation Center website [5] and the U.S. Naval Observatory (USNO) website [6].

The authors acknowledge and appreciate the effort of several ARL:UT staff members who reviewed these results. For 2017 this included Jon Little, Scott Sellers, Jason Vestuto, and Johnathan York.

Karl Kovach of Aerospace Corporation provided valuable assistance in interpreting the SPSPS08 assertions. John Lavrakas of Advanced Research Corporation and P.J. Mendicki of Aerospace Corporation have long been interested in GPS performance metrics and have provided valuable comments on the final draft. However, the results presented in this report are derived by ARL:UT, and any errors in this report are the responsibility of ARL:UT.

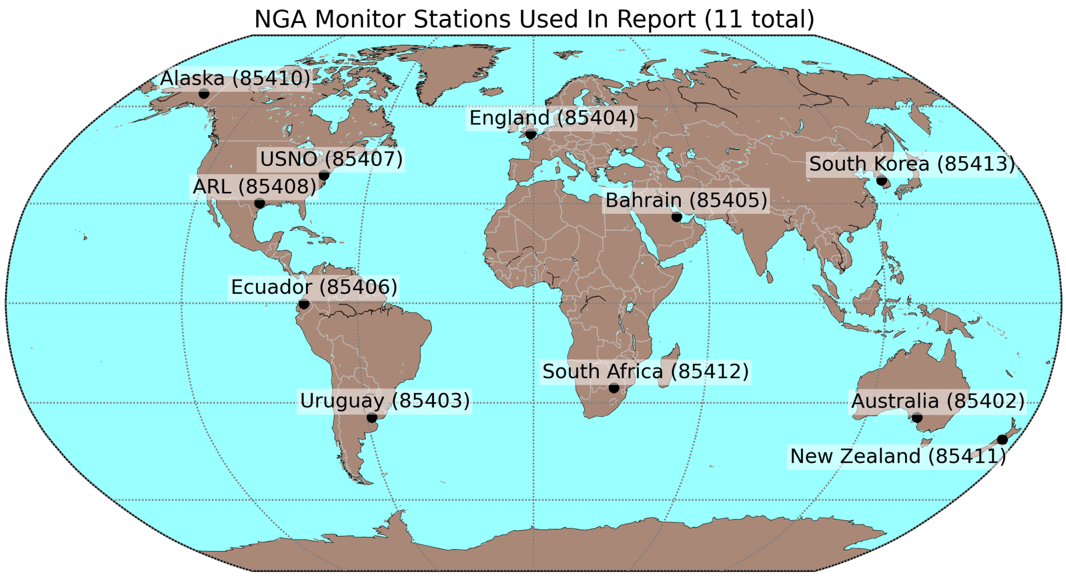

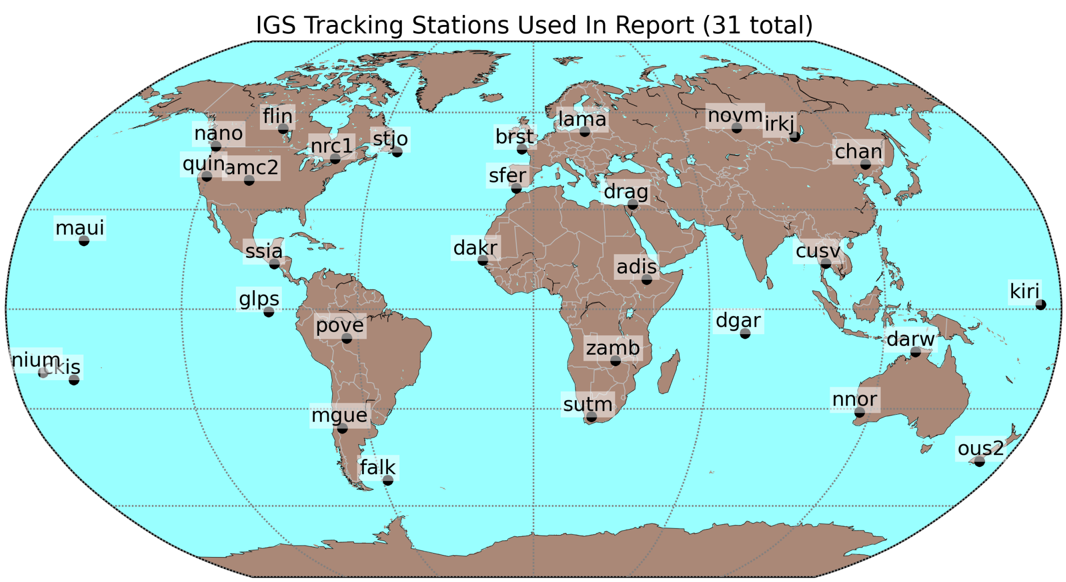

Figure 1.1: Maps of the Network of Stations Used in this Report

Chapter 2

Summary of Results

Table 2.1 provides a summary of the assertions defined in the performance standards. The table is annotated to show which assertions are evaluated in this report and the status of each assertion.

Of the assertions evaluated, only one was not met in 2017. The exception is associated with the notification time for scheduled interruptions. The assertion that at least 48 hours notice will be provided for scheduled interruptions was met in only 36 of 47 cases (81%).

Details regarding each result may be found in Chapter 3. All abbreviations used in Table 2.1 may be found in Appendix G.

Table 2.1: Summary of SPS PS Metrics Examined for 2017

SPSPS08 Section	SPS PS Assertion	2017 Status
3.4.1 SIS URE Accuracy	$\leq$ 7.8 m 95% Global average URE during normal operations over all AODs	✔
	$\leq$ 6.0 m 95% Global average URE during normal operations at zero AOD	✔
	$\leq$ 12.8 m 95% Global average URE during normal operations at any AOD	✔
	$\leq$ 30 m 99.94% Global average URE during normal operations	✔
	$\leq$ 30 m 99.79% Worst case single point average URE during normal operations	✔
	$\leq$ 388 m 95% Global average URE after 14 days without upload	N/A
3.4.2 SIS URRE Accuracy	$\leq$ 0.006 m/s 95% Global average at any AOD	not eval.
3.4.3 SIS URAE Accuracy	$\leq$ 0.002 m/s^2 95% Global average at any AOD	not eval.
3.4.4 SIS UTCOE Accuracy	$\leq$ 40 nsec 95% Global average at any AOD	✔
3.5.1 SIS Instantaneous URE Integrity	$\leq 1X10^{-5}$ Probability over any hour of exceeding the NTE tolerance without a timely alert	✔
3.5.4 SIS Instantaneous UTCOE Integrity	$\leq 1X10^{-5}$ Probability over any hour of exceeding the NTE tolerance without a timely alert	✔
3.6.1 SIS Continuity - Unscheduled Failure Interruptions	$\geq$ 0.9998 Probability over any hour of not losing the SPS SIS availability from the slot due to unscheduled interruption	✔
3.6.3 Status and Problem Reporting	Appropriate NANU issue at least 48 hours prior to a scheduled event	not met
3.7.1 SIS Per-Slot Availability	$\geq$ 0.957 Probability that (a.) a slot in the baseline 24-slot will be occupied by a satellite broadcasting a healthy SPS SIS, or (b.) a slot in the expanded configuration will be occupied by a pair of satellites each broadcasting a healthy SIS	✔
3.7.2 SIS Constellation Availability	$\geq$ 0.98 Probability that at least 21 slots out of the 24 slots will be occupied by a satellite (or pair of satellites for expanded slots) broadcasting a healthy SIS	✔
	$\geq$ 0.99999 Probability that at least 20 slots out of the 24 slots will be occupied by a satellite (or pair of satellites for expanded slots) broadcasting a healthy SIS	✔
3.7.3 Operational Satellite Counts	$\geq$ 0.95 Probability that the constellation will have at least 24 operational satellites regardless of whether those operational satellites are located in slots or not	✔
3.8.1 PDOP Availability	$\geq$ 98% Global PDOP of 6 or less	✔
	$\geq$ 88% Worst site PDOP of 6 or less	✔
3.8.2 Position Service Availability	$\geq$ 99% Horizontal, average location	✔
	$\geq$ 99% Vertical, average location	
	$\geq$ 90% Horizontal, worst-case location	
	$\geq$ 90% Vertical, worst-case location	
3.8.3 Position Accuracy	$\leq$ 9 m 95% Horizontal, global average	✔
	$\leq$ 15 m 95% Vertical, global average	
	$\leq$ 17 m 95% Horizontal, worst site	
	$\leq$ 37 m 95% Vertical, worst site	
	$\leq$ 40 nsec time transfer error 95% of the time	✔

✔ - Met

N/A - No SVs were in this mode in 2017

Chapter 3

Discussion of Performance Standard Metrics and Results

While Chapter 2 summarizes the status of the SPSPS08 metrics for 2017, the statistics and trends reported in this chapter provide both additional information and support for these conclusions.

3.1 SIS Accuracy

SIS URE accuracy is asserted in Section 3.4 of the SPSPS08. The following standards (from Table 3.4-1 in the SPS PS) are considered in this report:

- *"$\leq$ 7.8 m 95% Global Average URE during Normal Operations over all AODs"*
- *"$\leq$ 6.0 m 95% Global Average URE during Normal Operations at Zero AOD"*
- *"$\leq$ 12.8 m 95% Global Average URE during Normal Operations at any AOD"*
- *"$\leq$ 30 m 99.94% Global Average URE during Normal Operations"*
- *"$\leq$ 30 m 99.79% Worst Case Single Point Average URE during Normal Operations"*
- *"$\leq$ 40 nsec 95% Global Average UTCOE during Normal Operations at Any AOD"*

The remaining standard associated with operations after extended periods without an upload are not applicable in 2017 as periods of extended operations were very limited. (This is discussed in Section 4.4.)

The URE statistics presented in this report are based on a comparison of the BCP against the TCP. (Refer to Appendix B for further details on the process by which the URE are computed.) This is a useful approach, but one that has specific limitations, the most significant being that the TCP may not capture the effect of individual discontinuities or large effects over short time scales (e.g. a frequency step or clock run-off).

Nonetheless, this approach is appropriate given the 30 day period of averaging implemented in determining URE compared to brief (less than an hour) periods of the rare discontinuities. Briefly, this approach allows the computation of URE without direct reference to observations from any particular ground sites, though the TCP carries an implicit network dependency based on the set of ground stations used to derive the precise orbits from which the TCP is derived.

In the case of this report, the BCP and TCP are both referenced to the L1/L2 P(Y)-code signal. As a result, the resulting URE values are best characterized as Precise Positioning Service (PPS) dual-frequency URE values. The SPS results are derived from the PPS dual-frequency results by a process described in Appendix F.

Throughout this section and the next, there are references to several distinct SIS URE expressions. Each of these SIS URE expressions means something slightly different. It is important to pay careful attention to the particular SIS URE expression being used in each case to avoid misinterpreting the associated URE numbers. Appendix C of the SPSPS08 provides definitions for the two ways SIS URE are computed, *Instantaneous SIS URE*, which expresses URE on an instantaneous basis and *root mean square (RMS) SIS URE*, which expresses URE on a statistical basis. When the BCP and TCP are used to estimate the range residual along a specific satellite-to-receiver line-of-sight vector at a given instant in time, then that is an "Instantaneous SIS URE." Some of the primary differences between Instantaneous basis SIS UREs and statistical basis SIS UREs are given below.

Table 3.1: Characteristics of SIS URE Methods

Instantaneous Basis SIS URE	**Statistical Basis SIS URE**
Always algebraically signed (±) number	Never an algebraic sign
Never a statistical qualifier	Always a statistical qualifier (RMS, 95%, etc.)
Specific to a particular time and place	Statistic over span of times, or places, or both
Next section of this report (Section 3.2)	This section of this report (Section 3.1)

Throughout this section, there are references to the "Instantaneous RMS SIS URE." This is a statistical basis SIS URE (note the "RMS" statistical qualifier), where the measurement quantity is the Instantaneous SIS URE, and the span of the statistic covers that one particular point ("instant") in time across a large range of spatial points. This is effectively the evaluation of the Instantaneous SIS URE across every spatial point in the area of the service volume visible to the SV at that particular instant in time. Put another way; consider the signal from a given SV at a given point in time. That signal intersects the surface of the Earth over an area, and at each point in that area there is a unique Instantaneous SIS URE value based on geometric relationship between the SV and the point of interest. In the name "Instantaneous RMS SIS URE," the "Instantaneous" means that no time averaging occurs. The "RMS" refers to taking the RMS of all the individual Instantaneous SIS URE values across the area visible to the SV for a single time. This concept is explained in SPSPS08 Section A.4.11, and the relevant equation is presented in Appendix B.1.2 of this report.

3.1.1 URE Over All AOD

The performance standard URE metric that is most closely related to a user's observations is the calculation of the 95^{th} percentile Global Average URE over all ages of data (AODs). This is associated with the SPSPS08 Section 3.4 metrics:

- *"≤ 7.8 m 95% Global Average URE during Normal Operations over all AODs"*

These metrics can be decomposed into several pieces to better understand the process. For example, the first metric may be decomposed as follows:

- *7.8 m* - This is the limit against which to test. The value is unique to the signal under evaluation.
- *95^{th} percentile* - This is the statistical measure applied to the data to determine the actual URE. In this case, there are a sufficiently large number of samples to allow direct sorting of the results across time and selection of the 95^{th} percentile.
- *Global Average URE* - This is another term for the Instantaneous RMS SIS URE, a statistical quantity representing the average URE across the area of the service volume visible to the SV at a given point in time. The expression used to compute this quantity is provided in Appendix B.1.2.
- *Normal Operations* - This is a constraint related to normal vs. extended mode operations. See IS-GPS-200 20.3.4.4 [2].
- *over all AODs* - This constraint means that the Global Average URE is considered at each evaluation time regardless of the AOD at the evaluation time. A more detailed explanation of the AOD and how this quantity is computed can be found in Section 4.2.

In addition, there are three general statements in Section 3.4 of SPSPS08 that have a bearing on this calculation:

- These statistics include data only from periods when each SV was healthy.
- These statistics are "per SV" - that is, they apply to the signal from each satellite, not for averages across the constellation.
- *"The ergodic period contains the minimum number of samples such that the sample statistic is representative of the population statistic. Under a one-upload-per-day scenario, for example, the traditional approximation of the URE ergodic period is 30 days."* (SPSPS08 Section 3.4, Note 1)

The statistics are computed over monthly periods and not daily. Monthly periods approximate the suggested 30 day period while conforming to a familiar time scale and avoiding the complication that a year is not evenly divisible by 30. We have computed the monthly statistic regardless of the number of days of availability in each month. (In reports for previous years, months with less than 25 days of availability have been indicated in Table 3.2, however in 2017 all SVs were available for more the 25 days for each month.)

Table 3.2 contains the monthly 95^{th} percentile values of the RMS SIS URE based on the assumptions and constraints described above. For each SV, the worst value across the year is marked in red. In all cases, no values exceed 7.8 m, and so this requirement is met for 2017.

Figure 3.1 provides a summary of these results for the entire constellation. For each SV, shown along the horizontal axis, the median value of the monthly 95^{th} percentile SIS URE is displayed as a point. The full range of the monthly 95^{th} percentile SIS URE is shown by the vertical bars. Color distinguishes between the Block IIR, Block IIR-M, and Block IIF SVs. The red horizontal line at 7.8 m is the performance threshold asserted by the SPSPS08 Section 3.4 performance metric.

A number of points are evident from Table 3.2 and Figure 3.1:

1. All SVs meet the performance assertion of the SPSPS08, even when only the worst performing month is considered. Even the worst value for each SV (indicated by the upper extent of the range bars) is more than factor of 2 smaller than the threshold.
2. For most of the SVs, the value of the 95^{th} percentile SIS URE metric is relatively stable over the course of the year, as indicated by relatively small range bars.
3. The “best” SVs appear to be those which cluster below the 1.0 m level and whose range variation is small.
4. SVN 44 has the highest values among the Block IIR SVs. Several of the Block IIA SVs were at this level prior to their retirement.
5. The values for SVN 65 and SVN 72 are noticeably different than the other Block IIF SVs. These are the only Block IIF SVs operating on a Cesium frequency standard.

Table 3.2: Monthly 95^{th} Percentile Values of SIS RMS URE for All SVs in Meters

SVN	PRN	Block	Jan.	Feb.	Mar.	Apr.	May	Jun.	Jul.	Aug.	Sept.	Oct.	Nov.	Dec.	2017
41	14	IIR	1.23	1.03	1.03	0.98	0.96	1.01	1.18	1.19	1.00	0.98	0.94	1.06	1.06
43	13	IIR	1.10	1.19	1.02	1.19	1.09	1.17	1.09	1.23	1.10	1.17	1.42	1.13	1.14
44	28	IIR	2.43	2.31	2.25	2.49	2.13	2.58	2.45	2.38	2.10	2.16	2.36	2.29	2.35
45	21	IIR	1.16	1.09	1.13	1.02	1.01	0.98	1.07	1.02	1.01	0.95	1.00	1.22	1.06
46	11	IIR	1.79	1.63	1.61	1.51	1.14	1.39	1.31	1.64	1.35	1.44	1.40	1.26	1.50
47	22	IIR	0.95	0.96	0.91	0.94	0.98	0.95	0.94	0.97	0.96	0.91	0.97	1.04	0.96
48	7	IIR-M	1.27	1.15	1.14	1.13	1.38	1.29	1.14	1.27	1.26	1.15	1.10	1.17	1.21
50	5	IIR-M	0.93	0.96	0.96	0.95	0.91	0.96	0.96	1.02	1.04	1.05	0.91	0.97	0.97
51	20	IIR	0.93	1.01	0.98	0.97	0.96	0.98	0.99	0.94	0.99	0.92	0.99	1.01	0.97
52	31	IIR-M	1.24	1.31	1.18	1.26	1.28	1.23	1.17	1.22	1.12	1.22	1.33	1.21	1.24
53	17	IIR-M	1.25	1.47	1.60	1.58	1.31	1.48	1.85	1.80	2.03	1.42	1.78	1.59	1.61
54	18	IIR	0.94	1.20	1.17	1.38	1.23	1.16	1.49	1.20	0.97	1.48	1.04	1.19	1.20
55	15	IIR-M	0.90	0.90	0.95	0.94	0.91	0.92	0.89	0.93	0.96	1.00	0.99	0.91	0.94
56	16	IIR	0.94	0.95	0.95	0.94	0.90	0.93	0.95	0.92	0.95	0.91	0.91	0.93	0.93
57	29	IIR-M	1.32	1.31	1.35	1.35	1.41	1.22	1.46	1.37	1.40	1.32	1.49	1.67	1.38
58	12	IIR-M	0.93	0.93	0.94	0.93	0.94	0.93	0.95	1.01	1.11	1.06	0.99	1.00	0.98
59	19	IIR	0.99	0.95	0.95	0.94	0.97	0.98	0.94	1.02	0.95	1.01	0.95	1.00	0.97
60	23	IIR	0.95	0.93	0.99	0.94	0.95	0.97	0.98	0.92	0.95	0.95	0.94	0.95	0.95
61	2	IIR	1.18	1.01	0.95	0.97	0.94	0.98	0.98	1.02	1.00	0.94	0.99	0.96	1.00
62	25	IIF	1.03	0.99	1.12	0.95	1.09	1.12	1.11	1.16	1.09	1.14	1.01	0.95	1.08
63	1	IIF	1.24	1.13	1.00	1.21	0.96	1.01	1.09	1.00	1.00	1.18	1.21	1.10	1.10
64	30	IIF	0.98	1.03	0.96	0.99	0.96	0.98	0.98	0.96	0.97	0.98	1.08	1.13	1.00
65	24	IIF	2.40	2.12	2.46	2.58	2.58	2.57	2.72	2.58	2.62	2.33	2.66	2.65	2.56
66	27	IIF	0.95	0.95	1.01	1.10	1.00	0.96	0.99	0.96	0.95	0.99	0.96	0.93	0.98
67	6	IIF	0.97	1.03	1.08	1.02	1.07	1.07	1.04	1.14	1.02	0.97	1.00	1.00	1.04
68	9	IIF	0.89	0.97	1.06	1.19	1.02	1.02	0.98	0.99	1.03	1.04	1.01	1.45	1.04
69	3	IIF	1.09	1.65	1.68	1.41	1.35	1.29	1.02	1.17	1.18	1.23	1.23	1.25	1.34
70	32	IIF	0.97	0.94	0.99	1.04	0.94	0.92	0.92	0.94	1.08	1.07	1.02	0.97	0.98
71	26	IIF	1.00	1.08	1.07	0.96	1.01	1.07	1.04	1.09	1.04	0.96	1.02	1.11	1.04
72	8	IIF	2.36	2.11	2.34	1.87	2.32	2.33	2.28	2.04	2.10	1.98	2.06	1.98	2.16
73	10	IIF	0.98	1.08	1.04	0.98	0.90	0.94	1.01	1.01	1.07	1.00	0.96	0.98	1.00
Block IIR			1.21	1.21	1.19	1.19	1.13	1.14	1.20	1.25	1.17	1.18	1.21	1.19	1.19
Block IIF			1.42	1.39	1.48	1.39	1.51	1.46	1.47	1.39	1.39	1.39	1.48	1.44	1.43
All SVs			1.27	1.28	1.30	1.27	1.26	1.25	1.27	1.30	1.24	1.25	1.30	1.27	1.27

Notes: Months with the highest SIS RMS URE for a given SV are colored red. The column labeled "2017" is the 95^{th} *percentile over all the days in the year. The three rows at the bottom are the monthly* 95^{th} *percentile values over various sets of SVs.*

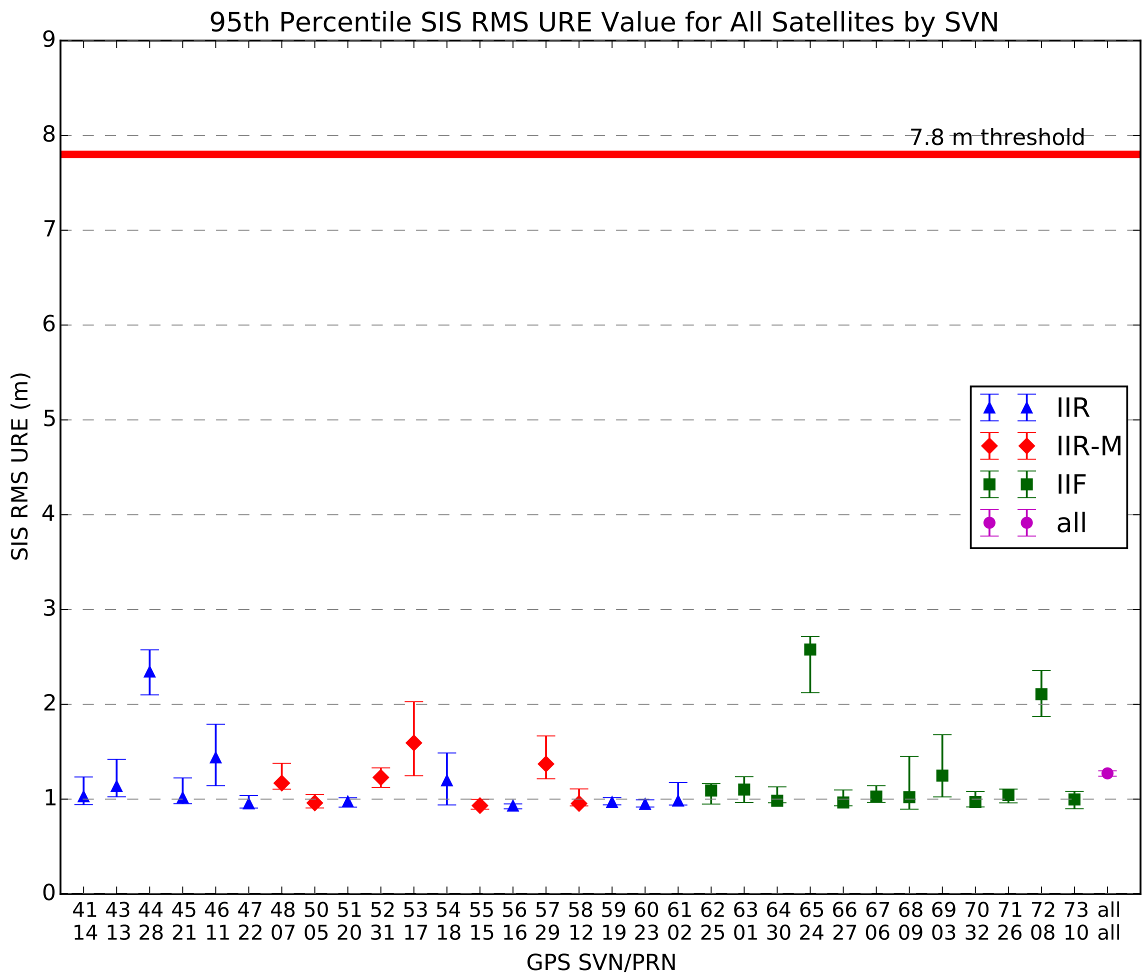

Figure 3.1: Range of the Monthly 95^{th} Percentile Values for All SVs

Notes: Each SVN with valid data is shown sequentially along the horizontal axis. The median value of the monthly 95^{th} *percentile SIS URE displayed as a point along the vertical axis. The minimum and maximum of the monthly* 95^{th} *percentile SIS URE for 2017 are shown by whiskers on the vertical bars. Color distinguishes between the Block IIR, Block IIR-M, and Block IIF SVs. The red horizontal line at 7.8 m indicates the upper bound given by the SPSPS08 Section 3.4 performance metric. The marker for "all" represents the monthly* 95^{th} *percentile values across all satellites.*

3.1.1.1 An Alternate Method

As described toward the end of Section 3.1, the 95^{th} percentile Global Average URE values are formed by first deriving the Instantaneous RMS SIS URE at a succession of time points, then picking the 95^{th} percentile value over that set of results. This has the computational advantage that the Instantaneous RMS SIS URE is derived from a single equation in radial, along-track, cross-track, and time errors at a given instant in time (as explained in Appendix B.1.2). However, it leads to a two-step implementation under which we first compute an RMS over a spatial area at a series of time points, then compute a 95^{th} percentile statistic over time.

Given current computation and storage capability, it is practical to compute a set of 95^{th} percentile URE values in which the Instantaneous SIS URE values are computed over a sufficiently dense grid and at fixed time intervals separated by uniform time steps throughout the period of interest. The 95^{th} percentile value is then selected from the entire set of Instantaneous SIS URE values. This was done in parallel to the process that produced the results shown in Section 3.1.1. The evaluation was performed at a 5 minute cadence. For each SV at each evaluation time, the point on the Earth immediately below the SV was used as the center of the uniformly spaced 577 point grid that extends over the area visible to the satellite above the 5° minimum elevation angle. Further details on the implementation are provided in Appendix B.1.3.

Table 3.3 presents a summary of the results obtained by this alternate method. This table is in the same format as Table 3.2. Figure 3.2 (which is in the same format as Figure 3.1) presents the values in Table 3.3 in a graphical manner. The values in Table 3.3 are larger than the values in Table 3.2 by an average of 0.03 m. The maximum difference [alternate - original] for a given SV-month is 0.11 m; the minimum difference is -0.07 m.

Figure 3.3 is an illustration of the differences between the Monthly 95^{th} percentile SIS URE values calculated by the two different methods. Each pair of monthly values for a given SV found in Table 3.2 and Table 3.3 were taken and the difference computed as the quantity [alternate - original]. The median, maximum, and minimum differences were then selected from each set and plotted in Figure 3.3. Figure 3.3 illustrates that the two methods agree to within 20 cm and generally a good deal less with the alternate method typically being a few cm larger.

None of the values in Table 3.3 exceed the threshold of 7.8 m. Therefore, the threshold is met for 2017 even under this alternate interpretation of the metric.

Table 3.3: Monthly 95^{th} Percentile Values of SIS Instantaneous URE for All SVs in Meters (via Alternate Method)

SVN	PRN	Block	Jan.	Feb.	Mar.	Apr.	May	Jun.	Jul.	Aug.	Sept.	Oct.	Nov.	Dec.	2017
41	14	IIR	1.28	1.07	1.04	1.02	0.99	1.04	1.27	1.26	1.04	1.02	0.97	1.08	1.09
43	13	IIR	1.14	1.22	1.05	1.20	1.12	1.22	1.11	1.24	1.12	1.18	1.42	1.12	1.17
44	28	IIR	2.44	2.34	2.29	2.50	2.16	2.54	2.49	2.40	2.14	2.14	2.36	2.29	2.35
45	21	IIR	1.20	1.13	1.14	1.04	1.02	1.00	1.13	1.06	1.04	0.99	1.02	1.26	1.08
46	11	IIR	1.79	1.67	1.59	1.56	1.15	1.40	1.34	1.67	1.39	1.51	1.40	1.29	1.51
47	22	IIR	0.96	0.99	0.93	0.97	0.99	0.98	0.96	1.00	0.98	0.95	0.99	1.08	0.98
48	7	IIR-M	1.32	1.16	1.20	1.18	1.38	1.33	1.16	1.28	1.28	1.18	1.12	1.17	1.23
50	5	IIR-M	0.96	0.98	0.98	0.96	0.92	0.99	0.98	1.05	1.08	1.05	0.92	0.97	0.99
51	20	IIR	0.96	1.06	1.00	1.00	0.99	1.03	1.01	0.95	1.00	0.95	1.02	1.04	1.00
52	31	IIR-M	1.28	1.33	1.21	1.28	1.29	1.25	1.20	1.25	1.15	1.25	1.36	1.24	1.26
53	17	IIR-M	1.27	1.50	1.61	1.58	1.34	1.50	1.78	1.83	2.09	1.44	1.84	1.56	1.62
54	18	IIR	0.97	1.22	1.19	1.40	1.27	1.20	1.49	1.19	1.00	1.52	1.06	1.21	1.22
55	15	IIR-M	0.93	0.92	0.97	0.99	0.92	0.96	0.92	0.95	1.00	1.06	1.04	0.95	0.97
56	16	IIR	0.97	0.97	0.96	0.95	0.91	0.95	0.96	0.94	0.97	0.93	0.93	0.95	0.95
57	29	IIR-M	1.44	1.36	1.37	1.39	1.42	1.25	1.42	1.43	1.45	1.43	1.52	1.70	1.43
58	12	IIR-M	0.97	0.96	0.97	0.97	0.97	0.97	0.97	1.04	1.14	1.10	1.02	1.06	1.01
59	19	IIR	1.00	0.97	0.98	0.97	0.99	1.00	0.97	1.03	0.97	1.05	0.98	1.01	0.99
60	23	IIR	0.98	0.96	1.01	0.96	0.97	0.99	0.99	0.94	0.99	0.97	0.96	0.97	0.97
61	2	IIR	1.21	1.04	0.98	0.99	0.97	1.00	1.00	1.07	1.04	0.96	1.02	0.99	1.02
62	25	IIF	1.06	1.03	1.14	0.98	1.13	1.20	1.15	1.19	1.12	1.22	1.03	0.98	1.12
63	1	IIF	1.30	1.18	1.02	1.24	0.98	1.03	1.14	1.05	1.05	1.22	1.23	1.16	1.14
64	30	IIF	1.00	1.05	0.99	1.02	0.98	1.01	0.99	1.00	0.98	1.00	1.09	1.18	1.02
65	24	IIF	2.42	2.13	2.47	2.58	2.62	2.61	2.79	2.60	2.67	2.35	2.68	2.68	2.58
66	27	IIF	0.97	0.97	1.05	1.13	1.03	0.97	1.02	0.98	0.97	1.01	0.99	0.95	1.01
67	6	IIF	1.00	1.08	1.11	1.05	1.09	1.15	1.08	1.17	1.05	1.00	1.05	1.04	1.08
68	9	IIF	0.91	1.00	1.07	1.21	1.04	1.04	1.00	1.00	1.05	1.05	1.03	1.49	1.06
69	3	IIF	1.11	1.67	1.69	1.46	1.39	1.29	1.06	1.25	1.23	1.24	1.25	1.27	1.37
70	32	IIF	1.02	0.98	1.02	1.07	0.96	0.95	0.95	0.98	1.11	1.09	1.04	1.00	1.02
71	26	IIF	1.03	1.10	1.10	0.98	1.03	1.08	1.07	1.11	1.06	1.00	1.05	1.13	1.07
72	8	IIF	2.36	2.10	2.32	1.87	2.37	2.38	2.30	2.08	2.10	1.98	2.11	2.02	2.18
73	10	IIF	1.00	1.09	1.05	1.01	0.91	0.99	1.03	1.04	1.09	1.04	1.00	1.03	1.03
Block IIR			1.24	1.23	1.20	1.21	1.15	1.17	1.22	1.27	1.20	1.21	1.23	1.23	1.22
Block IIF			1.43	1.40	1.50	1.41	1.51	1.49	1.48	1.41	1.41	1.41	1.48	1.45	1.45
All SVs			1.30	1.30	1.31	1.29	1.28	1.27	1.30	1.32	1.27	1.28	1.31	1.31	1.30

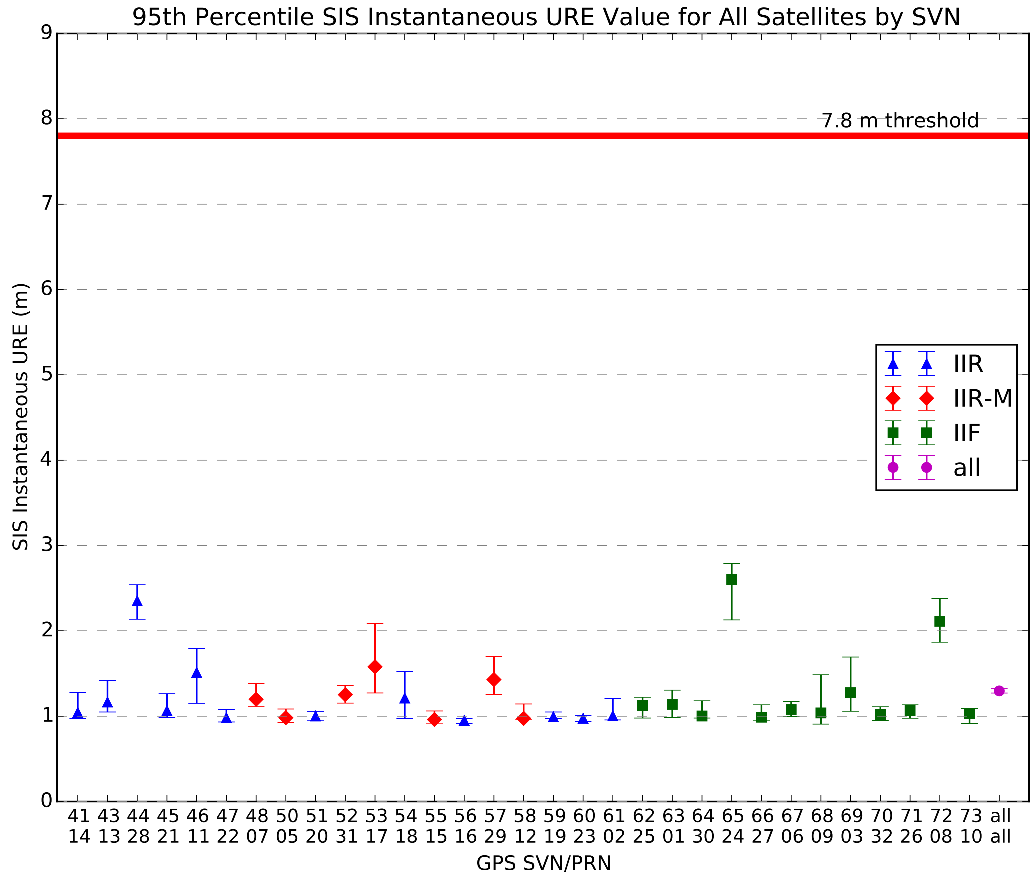

Figure 3.2: Range of the Monthly 95^{th} Percentile Values for All SVs (via Alternate Method)

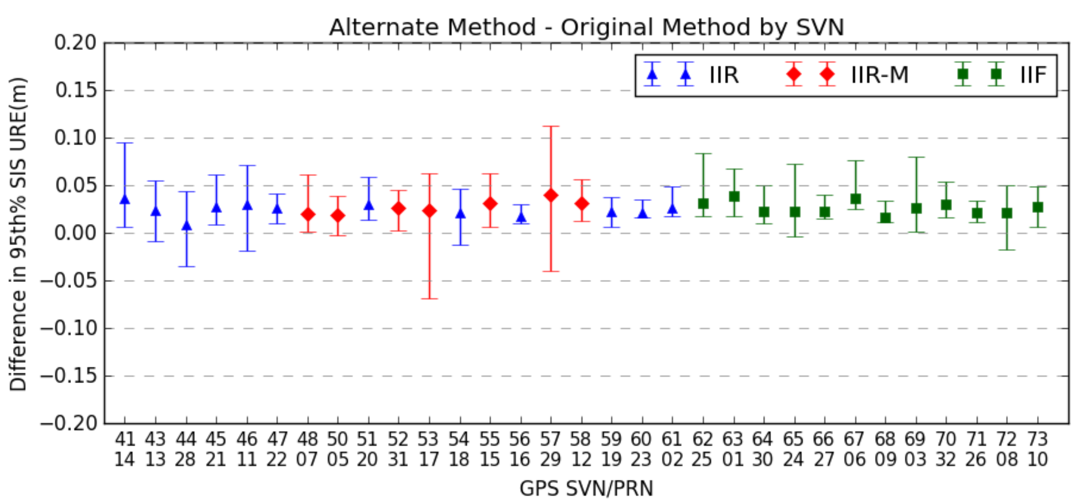

Figure 3.3: Range of Differences in Monthly Values for All SVs

3.1.2 URE at Any AOD

The next URE metric considered is the calculation of URE at any AOD. This is associated with the following SPSPS08 Section 3.4 metrics:

- *"$\leq$ 12.8 m 95% Global Average URE during Normal Operations at Any AOD"*

This metric may be decomposed in a manner similar to the previous metrics. The key differences are the term "at any AOD" and the change in the threshold values. The phrase "at any AOD" is interpreted to mean that at any AOD where sufficient data can be collected to constitute a reasonable statistical set the value of the required statistic should be $\leq$ 12.8 m. See Section 4.2 for a discussion of how the AOD is computed.

To examine this requirement, the set of 30 s Instantaneous RMS SIS URE values used in Section 3.1.1 was analyzed as described in Appendix A. In summary, the RMS SIS URE values for each satellite for the entire year were divided into bins based on 15 minute intervals of AOD. The 95^{th} percentile values for each bin were selected and the results were plotted as a function of the AOD.

Figures 3.4 through 3.7 show two curves: shown in blue is the 95^{th} percentile URE vs. AOD (in hours), and shown in green the count of points in each bin as a function of AOD. For satellites that are operating on the normal pattern (roughly one upload per day), the count of points in each bin is roughly equal from the time the upload becomes available until about 24 hours AOD. In fact, the nominal number of points can be calculated by multiplying the number of expected 30 s estimates in a 15 minute bin (30 estimates per bin) by the number of days in the year. There are just under 11000 points in each bin. This corresponds well to the plateau area of the green curve for the well-performing satellites (e.g. Figures 3.4 and 3.5). For satellites that are uploaded more frequently, the green curve will show a left-hand peak higher than the nominal count decreasing to the right. This is a result of the fact that there will be fewer points at higher AOD due to the more frequent uploads. The vertical scales on Figure 3.4 through 3.7 and the figures in Appendix A have been constrained to a constant value to aid in comparisons between the charts. For 2017, all SVs were operational throughout the year, so the total number of samples is very consistent across SVs.

The best performers for Block IIR/IIR-M and Block IIF are shown in Figures 3.4 and 3.5. For both blocks, several SVs have similar good results. These figures show a very flat distribution of AODs, and the UREs appear to degrade roughly linearly with time, at least out to the point that the distribution (represented by the green curve) shows a marked reduction in the number of points. Figures 3.6 and 3.7 show the worst performing (i.e. highest URE values) Block IIR/IIR-M, and Block IIF SVs. Note that the distribution of AOD samples for SVN 65 is biased toward shorter values of AOD, which indicates that uploads are occurring more frequently than once/day on occasion.

The plots for all satellites are contained in Appendix A. A review of the full set leads to the conclusion that the rate of URE growth in the Block IIF SVs is noticeably higher for the two satellites that use a Cesium frequency standard. While there are noticeable differences between individual satellites, all the results are well within the assertion for this metric.

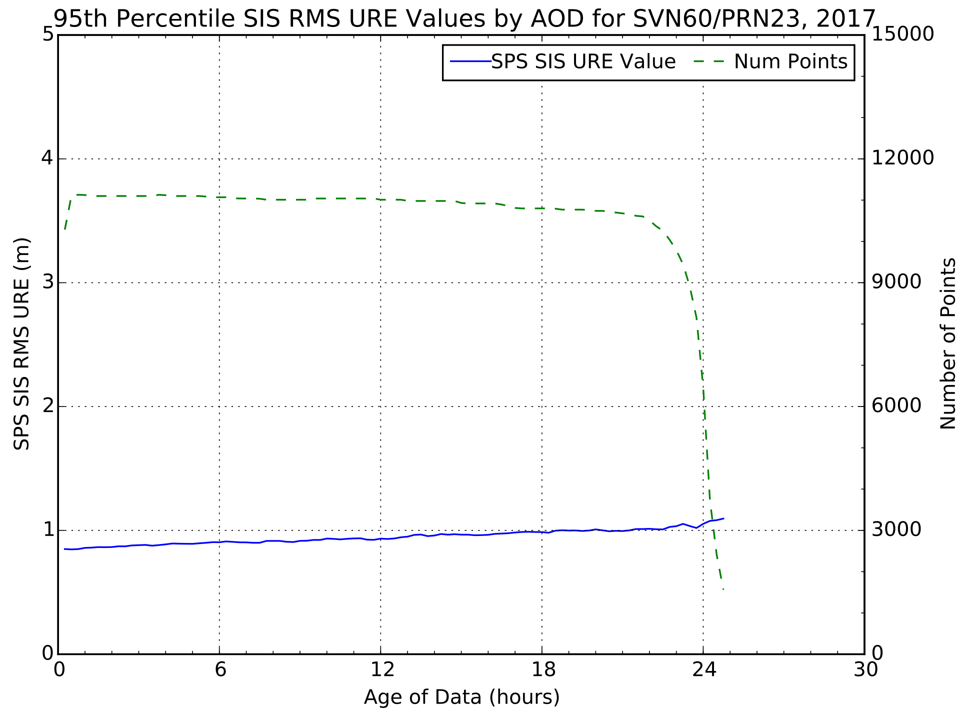

Figure 3.4: Best Performing Block IIR/IIR-M SV in Terms of Any AOD (SVN 60/PRN 23)

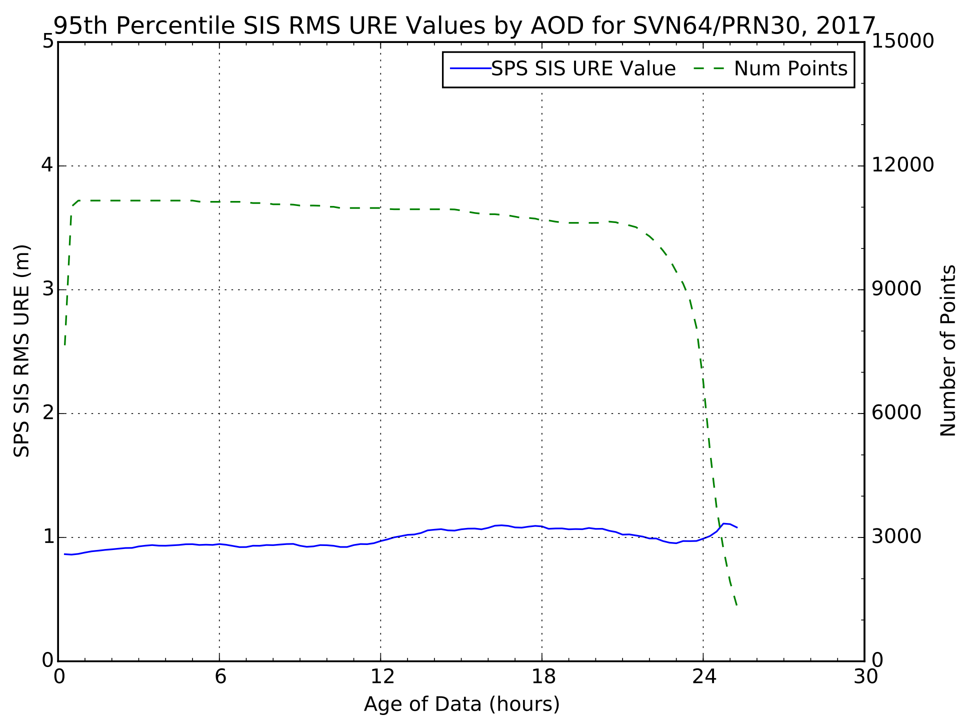

Figure 3.5: Best Performing Block IIF SV in Terms of Any AOD (SVN 64/PRN 30)

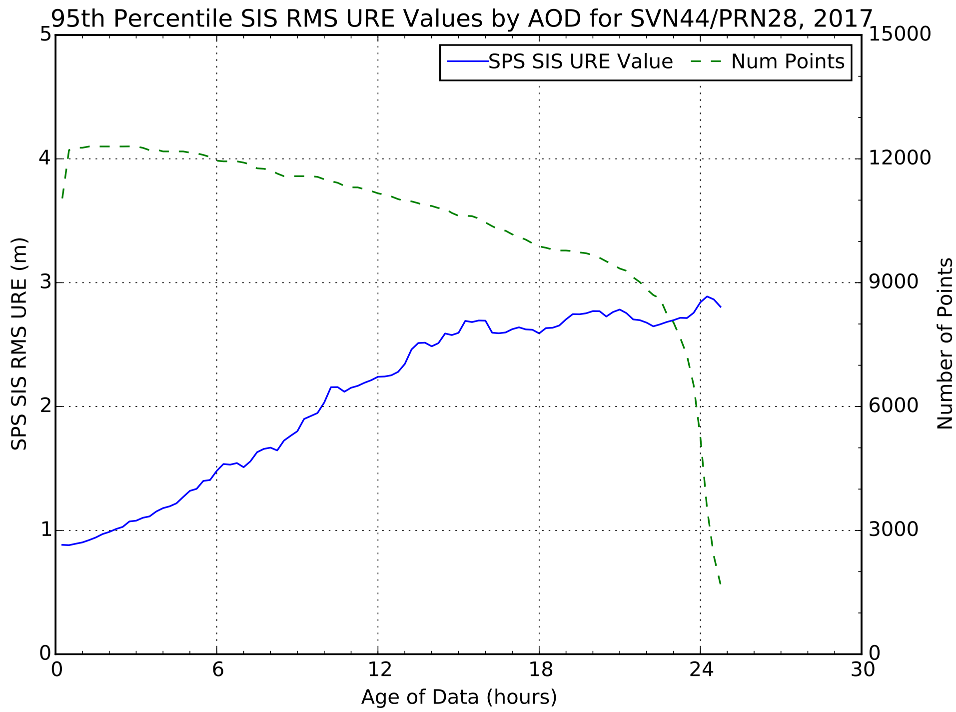

Figure 3.6: Worst Performing Block IIR/IIR-M SV in Terms of Any AOD (SVN 44/PRN 28)

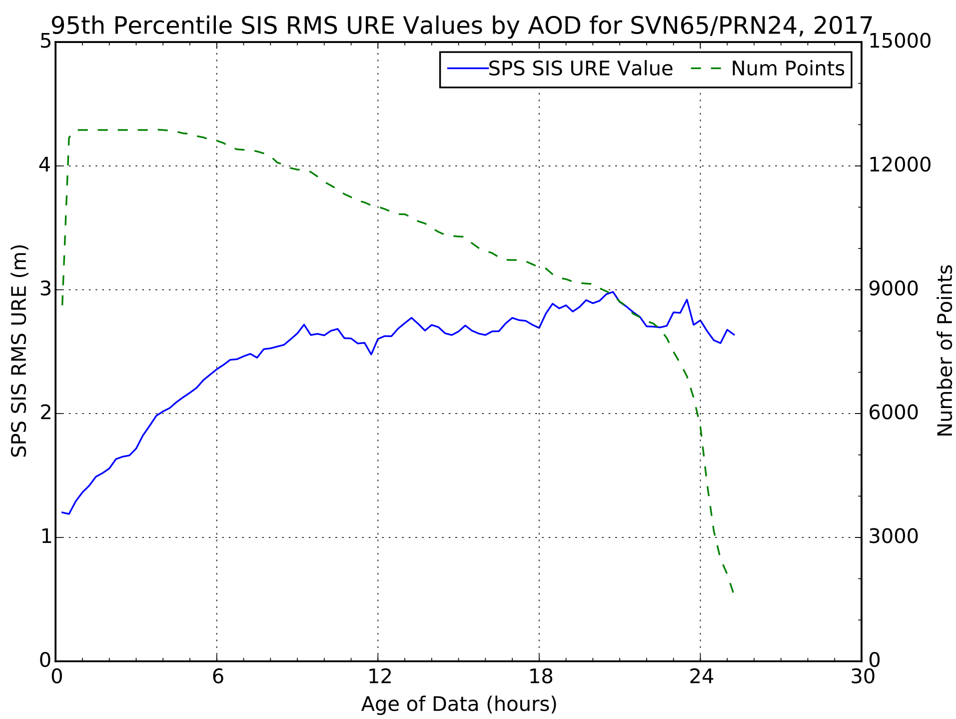

Figure 3.7: Worst Performing Block IIF SV in Terms of Any AOD (SVN 65/PRN 24)

3.1.3 URE at Zero AOD

Another URE metric considered is the calculation of URE at Zero Age of Data (ZAOD). This is associated with the SPSPS08 Section 3.4 metric:

- *"$\leq$ 6.0 m 95% Global Average URE during Normal Operations at Zero AOD"*

This metric may be decomposed in a manner similar to the previous two metrics. The key differences are the term "at Zero AOD" and the change in the threshold values.

The broadcast ephemeris is never available to user equipment at ZAOD simply due to the delays inherent in preparing the broadcast ephemeris and uploading it to the SV. However, we can still make a case that this assertion is met by examining the 95^{th} percentile SIS RMS URE value at 15 minutes AOD. These values are represented by the left-most data point on the red lines shown in Figure 3.6 through Figure 3.5. The ZAOD values should be slightly better than the 15 minute AOD values, or at worst roughly comparable. Inspection of the 15 minute AOD values shows that the values for all SVs are well within the 6.0 m value associated with the assertion. Therefore the assertion is considered fulfilled.

3.1.4 URE Bounding

The SPSPS08 asserts the following requirements for single-frequency C/A code:

- *"$\leq$ 30 m 99.94% Global Average URE during Normal Operations"*
- *"$\leq$ 30 m 99.79% Worst Case Single Point Average URE during Normal Operations"*

Note that the first assertion states "Global Average URE", which is interpreted to mean the Instantaneous SIS RMS URE values, while the second assertion states "Worst Case Single Point Average URE", which is interpreted to mean the Instantaneous SIS URE. Therefore, to evaluate the first assertion, the 30 s Instantaneous SIS RMS URE values computed as part of evaluation described in Section 3.1.1 were checked to determine whether any exceeded the 30 m threshold.

To evaluate the second assertion, the Instantaneous SIS URE values computed as part of the evaluation described in Section 3.1.1.1 were checked to determine whether any exceeded the 30 m threshold. This provides a set of 577 Instantaneous SIS URE values distributed across the area visible to a given SV at each 30 s epoch.(The 577 point grid and the distribution of the points is described in Appendix B.1.3.) This yields a set of over 60 million Instantaneous SIS URE values per SV per year. (577 values/300 s epoch * 288 30 s epochs/day * 365 days/year.)

However, there are limitations to our technique of estimating UREs that are worth noting such as fits across orbit/clock discontinuities, thrust events, and clock run-offs.

These are discussed in Appendix B.1.4. As a result of these limitations, a set of observed range deviations (ORDs) was also examined as a cross-check.

The ORDs were formed using the observation data collected to support the position accuracy analysis described in Section 3.5.4. In the case of ORDs, the observed range is differenced from the range predicted by the geometric distance from the known station position to the SV location derived from the broadcast ephemeris. The ORDs are similar to the Instantaneous SIS URE in that both represent the error along a specific line-of-sight. However, the ORDs are not true SIS measurements due to the presence of residual atmospheric effects and receiver noise. The selected stations are geographically distributed such that at least two sets of observations are available for each SV at all times. As a result, any actual SV problems that would lead to a violation of this assertion will produce large ORDs from multiple stations.

None of these three checks found any values that exceeded the 30m threshold. Based on these results, these assertions are considered satisfied.

3.1.5 UTC Offset Error Accuracy

The SPS PS provides the following assertion regarding the UTC offset error (UTCOE) Accuracy:

- *"$\leq$ 40 nsec 95% Global Average UTCOE during Normal Operations at Any AOD"*

The conditions and constraints state that this assertion should be true for any healthy SPS SIS.

This assertion was evaluated by calculating the global average UTCOE at each 15 minute interval in the year. The GPS-UTC offset available to the user was calculated based on the GPS broadcast navigation message data available from the SV at that time. The GPS-UTC offset truth information was provided by the USNO daily GPS-UTC offset values. A multi-day spline was fit to the daily truth values and the USNO value for GPS-UTC at each evaluation epoch was derived from this fit.

The selection and averaging algorithms are a key part of this process. The global average at each 15 minute epoch is determined by evaluating the UTCOE across the surface of the earth at each point on a 111 km $\times$ 111 km grid. (This grid spacing corresponds to roughly 1° at the Equator.) At each grid point, the algorithm determines the set of SVs visible at or above the 5° minimum elevation angle that are broadcasting a healthy indication in the navigation message. For each of these SVs, the UTC offset information in subframe 4 page 18 of the navigation message is compared to determine the data set that has an epoch time (t_{ot}) that is the latest of those that fall in the range $current\ time \leq t_{ot} \leq current\ time + 72\ hours$. These data are used to form the UTC offset and UTCOE for that time-grid point. (The 72 hour value comes from IS-GPS-200 Table 20-XIII [2])

The global averages at each evaluation epoch are assembled into monthly data sets. The 95^{th} percentile values are then selected from these sets.

Table 3.4 provides the results for each month of 2017. None of these values exceed the assertion of 40 nsec. Therefore the assertion is verified for 2017.

Table 3.4: 95^{th} Percentile Global Average UTCOE for 2017

Month	95^{th} Percentile Global Avg. UTCOE (nsec)
Jan.	1.754
Feb.	1.498
Mar.	1.325
Apr.	1.122
May	1.504
Jun.	1.300
Jul.	1.048
Aug.	1.564
Sep.	1.569
Oct.	1.315
Nov.	1.592
Dec.	1.495

3.2 SIS Integrity

3.2.1 URE Integrity

Under the heading of SIS Integrity, the SPSPS08 makes the following assertion in Section 3.5.1, Table 3.5-1:

- *"$\leq 1 \times 10^{-5}$ Probability Over Any Hour of the SPS SIS Instantaneous URE Exceeding the NTE Tolerance Without a Timely Alert During Normal Operations"*

The associated conditions and constraints include a limitation to healthy SIS, a Not to Exceed (NTE) tolerance ± 4.42 times the upper bound on the user range accuracy (URA) currently broadcast, and a worst case for a delayed alert of 6 hours.

The reference to "a Timely Alert" in the assertion refers to any of a number of ways to issue an alert to the user through the GPS signal or navigation message. See SPSPS08 Section A.5.5 for a complete description.

To estimate the worst-case probability of users experiencing misleading signal information (MSI), note that immediately below SPSPS08 Table 3.5-1 is an explanation that for a 32 SV constellation (full broadcast almanac) the corresponding average annual number of SPS SIS Instantaneous URE integrity losses is 3. Assuming each of the 3 losses lasts no more than 6 hours over one year, the fraction of time in which MSI will occur is 0.002.

This assertion was verified using two methods:

- The Instantaneous SIS URE values at the worst case location in view of each SV at each 30 s interval were examined to determine the number of values that exceed ±4.42 times the URA. (The worst location was selected from the set of Instantaneous SIS URE values computed for each SV as described in Section 3.1.1.1.)
- ORDs from a network of tracking stations were examined to determine the number of values that exceed ±4.42 times the URA.

Two methods were used due to the fact that each method may result in false positives in rare cases. For example, the URE values may be incorrect near discontinuities in the URE (as described in Appendix B). Similarly, the ORD values may be incorrect due to receiver or reception issues. Therefore, all reported violations are examined manually to determine whether a violation actually occurred, and if so, the extent of the violation.

Screening the 30 s instantaneous SIS URE values and the ORD data did not reveal any events for which this threshold was exceeded. Therefore the assertion is verified for 2017.

3.2.2 UTCOE Integrity

The SPS PS provides the following assertion regarding SPS PS UTCOE Integrity in Section 3.5.4:

- *"$\leq 1 \times 10^{-5}$ Probability Over Any Hour of the SPS SIS Instantaneous UTCOE Exceeding the NTE Tolerance Without A Timely Alert during Normal Operations"*

The associated conditions and constraints include a limitation to healthy SIS, a NTE tolerance of ±120 nsec, and the note that this holds true for any healthy SPS SIS. The reference to "a Timely Alert" in the assertion refers to any of a number of ways to issue an alert. See SPSPS08 Section A.5.5 for a complete description.

This assertion was evaluated by calculating the UTC offset for the navigation message subframe 4 page 18 data broadcast by each SV transmitting a healthy indication in the navigation message at each 15 minute interval. As in Section 3.1.5, only UTC offset information with an epoch time (t_{ot}) that is in the range $current\ time \leq t_{ot} \leq current\ time + 72\ hours$ were considered valid. That offset was used to compute the corresponding UTCOE from truth data obtained from the USNO [7]. Any UTCOE values that exceed the NTE threshold of ±120 nsec were investigated to determine if they represent actual violations of the NTE threshold or were artifacts of data processing.

No values exceeding the NTE threshold were found in 2017. The value farthest from zero for the year was -5.393 nsec (during January). Therefore the assertion is verified for 2017.

3.3 SIS Continuity

3.3.1 Unscheduled Failure Interruptions

The metric is stated in SPSPS08 Table 3.6-1 as follows:

- *"$\geq$ 0.9998 Probability Over Any Hour of Not Losing the SPS SIS Availability from a Slot Due to Unscheduled Interruption"*

The conditions and constraints note the following:

- The empirical estimate of the probability is calculated as an average over all slots in the 24-slot constellation, normalized annually.
- The SPS SIS is available from the slot at the start of the hour.

The notion of SIS continuity is slightly more complex for an expandable slot, because multiple SVs are involved. Following SPSPS08 Section A.6.5, a loss of continuity is considered to occur when,

> *"The expandable slot is in the expanded configuration, and either one of the pair of satellites occupying the orbital locations defined in Table 3.2-2 for the slot loses continuity."*

Hence, the continuity of signal of the expanded slot will be determined by whether either SV loses continuity.

Another point is that there is some ambiguity in this metric, which is stated in terms of "a slot" while the associated conditions and constraints note that this is an average over all slots. Therefore both the per-slot and 24-slot constellation averages have been computed. As discussed below, while the per-slot values are interesting, the constellation average is the correct value to compare to the SPS PS metric.

Three factors must be considered in looking at this metric:

1. We must establish which SVs were assigned to which slots during the period of the evaluation.
2. We must determine when SVs were not transmitting (or not transmitting a PRN available to users).
3. We must determine which interruptions were scheduled vs. unscheduled.

The derivation of the SV/Slot assignments is described in Appendix E.

For purposes of this report, interruptions were considered to have occurred if one or more of the SVs assigned to the given slot are unhealthy in the sense of SPSPS08 Section 2.3.2.

The following specific indications were considered:

- If the health bits in navigation message subframe 1 are set to anything other than all zeros.
- If an appropriately distributed worldwide network of stations failed to collect any pseudorange data sets for a given measurement interval.

The latter case (failure to collect any data) indicates that the satellite signal was removed from service (e.g. non-standard code or some other means). The NGA MSN provides at least two-station visibility (and at least 90% three-station visibility) with redundant receivers at each station, both continuously monitoring up to 12 SVs in view. Therefore, if no data for a satellite are received for a specific time, it is highly likely that the satellite was not transmitting on the assigned PRN at that time. The 30 s Receiver Independent Exchange format (RINEX) [8] observation files from this network were examined for each measurement interval (i.e. every 30 s) for each SV. If at least one receiver collected a pseudorange data set on L1 C/A, L1 P(Y), and L2 P(Y) with a signal-to-noise level of at least 25 dB-Hz on all frequencies and no loss-of-lock flags, the SV is considered trackable at that moment. In addition, the 30 s IGS data collected to support the position accuracy estimates (Section 3.5.4) were examined in a similar fashion to guard against any MSN control center outages that could have led to missing data across multiple stations simultaneously. This allows us to define an epoch-by-epoch availability for each satellite. Then, for each slot, each hour in the year was examined, and if an SV occupying the slot was not available at the start of the hour, the hour was not considered as part of the evaluation of the metric. If the slot was determined to be available, then the remaining data was examined to determine if an outage occurred during the hour.

The preceding criteria were applied to determine the times and durations of interruptions. After this was done, the Notice Advisories to Navstar Users (NANUs) effective in 2017 were reviewed to determine which of these interruptions could be considered scheduled interruptions as defined in SPSPS08 Section 3.6. The scheduled interruptions were removed from consideration for purposes of assessing continuity of sevice. When a slot was available at the start of an hour but a scheduled interruption occurred during the hour, the hour was assessed based on whether data were available prior to the scheduled outage.

Scheduled interruptions as defined in the ICD-GPS-240 [9] have a nominal notification time of 96 hours prior to the outage. Following the SPSPS08 Section 2.3.5, scheduled interruptions announced 48 hours in advance are not to be considered as contributing to the loss of continuity. So to contribute to a loss of continuity, the notification time for a scheduled interruption must occur less than 48 hours in advance of the interruption. In the case of an interruption not announced in a timely manner, the time from the start of the interruption to the moment 48 hours after notification time can be considered as a potential unscheduled interruption (for continuity purposes).

The following NANU types are considered to represent (or modify) scheduled interruptions (assuming the 48-hour advance notice is met):

- FCSTDV - Forecast Delta-V
- FCSTMX - Forecast Maintenance
- FCSTEXTD - Forecast Extension
- FCSTRESCD - Forecast Rescheduled
- FCSTUUFN - Forecast Unusable Until Further Notice

The FCSTSUMM (Forecast Summary) NANU that occurs after the outage is referenced to confirm the actual beginning and ending time of the outage.

For scheduled interruptions that extend beyond the period covered by a FCSTDV or FCSTMX NANU, the uncovered portion will be considered an unscheduled interruption. However, if a FCSTEXTD NANU extending the length of a scheduled interruption is published 48 hours in advance of the effective time of extension, the interruption will remain categorized as scheduled. It is worth reiterating that, for the computation of the metric, only those hours for which a valid SIS is available from the slot at the start of the hour are actually considered in the computation of the values.

The results of the assessment of SIS continuity are summarized in Table 3.5. The metric is averaged over the constellation, therefore the value in the bottom row (labeled "All Slots") must be greater than 0.9998 in order to meet the assertion.

To put this in perspective, there are 8760 hours in a year (8784 for a leap year). The required probability of not losing SPS SIS availability is calculated as an average over all slots in the 24-slot constellation, which implies that the maximum number of unscheduled interruptions over the year is given by $8760 \times (1 - 0.9998) \times 24 = 42$ unscheduled hours that experience interruptions. This is less than two unscheduled interruptions per SV per year but allows for the possibility that some SVs may have no unscheduled interruptions while others may have more than one.

Returning to Table 3.5, across the slots in the Expanded 24 constellation the total number of hours lost was 21. This is smaller than the maximum number of hours of unscheduled interruptions (42) available to meet the metric (see the previous paragraph) and leads to empirical value for the fraction of hours in which SIS continuity was maintained of 0.9999. Therefore, this assertion is considered fulfilled in 2017.

Table 3.5: Probability Over Any Hour of Not Losing Availability Due to Unscheduled Interruption in 2017 (SPS)

Plane-Slot	# of Hours with the SPS SIS available at the start of the hour[b]	# of Hours with Unscheduled Interruption[c]	Fraction of Hours in Which Availability was Not Lost
A1	8760	0	1.000000
A2	8759	1	0.999886
A3	8757	1	0.999886
A4	8677	3	0.999654
B1[a]	8760	1	0.999886
B2	8756	1	0.999886
B3	8760	0	1.000000
B4	8760	1	0.999886
C1	8760	1	0.999886
C2	8755	1	0.999886
C3	8760	0	1.000000
C4	8758	2	0.999772
D1	8760	0	1.000000
D2[a]	8742	3	0.999657
D3	8760	0	1.000000
D4	8760	0	1.000000
E1	8760	1	0.999886
E2	8760	1	0.999886
E3	8760	1	0.999886
E4	8760	0	1.000000
F1	8755	1	0.999886
F2[a]	8760	1	0.999886
F3	8757	1	0.999886
F4	8760	0	1.000000
All Slots	210116	21	0.999900

[a] *When B1, D2, and F2 are configured as expandable slots, both slot locations must be occupied by an available satellite for the slot to be counted as available.*

[b] *There were 8760 hours in 2017.*

[c] *Number of hours in which SPS SIS was available at the start of the hour and during the hour either (1.) an SV transmitted navigation message with subframe 1 health bits set to other than all zeroes without a scheduled outage, (2.) signal lost without a scheduled outage, or (3.) the URE NTE tolerance was violated.*

3.3.2 Status and Problem Reporting Standards

3.3.2.1 Scheduled Events

The SPSPS08 makes the following assertion in Section 3.6.3 regarding notification of scheduled events affecting service:

- *"Appropriate NANU issued to Coast Guard and the FAA at least 48 hours prior to the event"*

While beyond the assertion in the performance standards, ICD-GPS-240 [9] states a nominal notification time of 96 hours prior to outage start and an objective of 7 days (168 hours) prior to outage start.

This metric was evaluated by comparing the NANU periods to outages observed in the data. In general, scheduled events are described in a pair of NANUs. The first NANU is a forecast of when the outage will occur. The second NANU is provided after the outage and summarizes the actual start and end times of the outage. (This is described in ICD-GPS-240 Section 10.1.1.)

Table 3.6 summarizes the pairs found for 2017. The two leftmost columns provide the SVN/PRN of the subject SV. The next three columns specify the NANU #, type, and date/time of the NANU for the forecast NANU. These are followed by three columns that specify the NANU #, the date/time of the NANU for the FCSTSUMM NANU provided after the outage, and the date/time of the beginning of the outage. The final column is the time difference between the time the forecast NANU was released and the beginning of the actual outage (in hours). This represents the length of time between the release of the forecast and the actual start of the outage.

To meet the assertion in the performance standard, the number of hours in the rightmost column of Table 3.6 should always be greater than 48.0. The average notice was over 134 hours. However, there were nine cases in which the forecast was less than the 48 hour assertion. These are shown in red in Table 3.6. Therefore, the assertion has been met in only 38 of 47 cases (81%).

All nine of the NANUs that did not meet the 48 hour assertion referenced SVs in the 24+3 constellation definition. These have been treated as unscheduled interruptions for purposes of the evaluation in the previous section. They are also marked as "Scheduled (Short Notice $<$ 48 hrs)" in Appendix D.

No satellites were decommissioned in 2017. Table 3.7 is empty but retained to maintain similarity of table numbering with reports from other years.

Table 3.6: Scheduled Events Covered in NANUs for 2017

SVN	PRN	Prediction NANU			Summary NANU (FCSTSUMM)			Notice
		NANU #	TYPE	Release Time	NANU #	Release Time	Start Of Outage	(hrs)
69	03	2016076	FCSTDV	29 Dec 2035Z	2017002	10 Jan 2046Z	10 Jan 1536Z	283.02
60	23	2017003	FCSTDV	12 Jan 1744Z	2017004	17 Jan 2123Z	17 Jan 1526Z	117.70
53	17	2017008	FCSTMX	25 Jan 0410Z	2017009	25 Jan 0626Z	25 Jan 0449Z	0.65
53	17	2017010	FCSTMX	06 Feb 2221Z	2017011	07 Feb 0559Z	07 Feb 0502Z	6.68
58	12	2017012	FCSTMX	07 Feb 0605Z	2017013	07 Feb 0829Z	07 Feb 0801Z	1.93
50	05	2017014	FCSTMX	07 Feb 0841Z	2017015	07 Feb 1131Z	07 Feb 1104Z	2.38
55	15	2017016	FCSTMX	07 Feb 1135Z	2017017	07 Feb 1430Z	07 Feb 1401Z	2.43
52	31	2017018	FCSTMX	07 Feb 1437Z	2017021	07 Feb 2011Z	07 Feb 1930Z	4.88
48	07	2017019	FCSTMX	07 Feb 1808Z	2017022	07 Feb 2259Z	07 Feb 2230Z	4.37
57	29	2017020	FCSTMX	07 Feb 1814Z	2017023	08 Feb 1235Z	08 Feb 1204Z	17.83
48	07	2017028	FCSTDV	16 Mar 1733Z	2017029	23 Mar 2139Z	23 Mar 1456Z	165.38
59	19	2017030	FCSTMX	14 Apr 1541Z	2017031	19 Apr 1935Z	19 Apr 1505Z	119.40
41	14	2017034	FCSTMX	25 Apr 2121Z	2017038	03 May 2309Z	03 May 1945Z	190.40
47	22	2017037	FCSTDV	28 Apr 1643Z	2017039	05 May 1311Z	05 May 0803Z	159.33
46	11	2017041	FCSTMX	12 May 1551Z	2017043	18 May 2039Z	18 May 1655Z	145.07
58	12	2017040	FCSTDV	12 May 1544Z	2017044	19 May 0605Z	19 May 0008Z	152.40
54	18	2017047	FCSTDV	26 May 1448Z	2017048	02 Jun 0709Z	02 Jun 0141Z	154.88
44	28	2017049	FCSTMX	02 Jun 1501Z	2017051	07 Jun 2232Z	07 Jun 1819Z	123.30
54	18	2017050	FCSTMX	07 Jun 1348Z	2017055	13 Jun 1838Z	13 Jun 1449Z	145.02
55	15	2017052	FCSTDV	09 Jun 1742Z	2017056	16 Jun 0108Z	15 Jun 1842Z	145.00
47	22	2017053	FCSTMX	13 Jun 1642Z	2017057	21 Jun 0140Z	20 Jun 2256Z	174.23
43	13	2017054	FCSTMX	13 Jun 1647Z	2017058	22 Jun 0310Z	22 Jun 0031Z	199.73
56	16	2017059	FCSTMX	22 Jun 1542Z	2017061	27 Jun 2235Z	27 Jun 1925Z	123.72
51	20	2017060	FCSTMX	22 Jun 1558Z	2017063	30 Jun 0214Z	29 Jun 2329Z	175.52
61	02	2017062	FCSTDV	29 Jun 1800Z	2017066	07 Jul 0014Z	06 Jul 1841Z	168.68
60	23	2017064	FCSTMX	06 Jul 1747Z	2017067	12 Jul 0214Z	11 Jul 2345Z	125.97
50	05	2017065	FCSTMX	06 Jul 1752Z	2017069	14 Jul 0035Z	13 Jul 2136Z	171.73
48	07	2017068	FCSTMX	12 Jul 1702Z	2017071	19 Jul 0336Z	18 Jul 2127Z	148.42
62	25	2017072	FCSTDV	27 Jul 1715Z	2017075	03 Aug 2136Z	03 Aug 1614Z	166.98
53	17	2017073	FCSTMX	02 Aug 1426Z	2017076	09 Aug 0410Z	08 Aug 2345Z	153.32
55	15	2017074	FCSTMX	02 Aug 1430Z	2017079	10 Aug 1802Z	10 Aug 1439Z	192.15
52	31	2017077	FCSTMX	09 Aug 1434Z	2017084	15 Aug 1726Z	15 Aug 1502Z	144.47
61	02	2017078	FCSTMX	09 Aug 1437Z	2017088	18 Aug 0545Z	18 Aug 0312Z	204.58
57	29	2017085	FCSTMX	16 Aug 2157Z	2017091	22 Aug 2223Z	22 Aug 2008Z	142.18
58	12	2017086	FCSTMX	16 Aug 2203Z	2017092	24 Aug 0838Z	24 Aug 0613Z	176.17
68	09	2017087	FCSTDV	17 Aug 1938Z	2017093	25 Aug 1406Z	25 Aug 0847Z	181.15
45	21	2017089	FCSTMX	22 Aug 1617Z	2017094	29 Aug 2028Z	29 Aug 1738Z	169.35
50	05	2017090	FCSTDV	22 Aug 1620Z	2017096	01 Sep 0125Z	31 Aug 1956Z	219.60
43	13	2017095	FCSTDV	30 Aug 1631Z	2017097	07 Sep 1817Z	07 Sep 1050Z	186.32
70	32	2017108	FCSTDV	03 Oct 2257Z	2017111	04 Oct 1620Z	04 Oct 1123Z	12.43
57	29	2017112	FCSTDV	05 Oct 1823Z	2017113	12 Oct 1735Z	12 Oct 1421Z	163.97
71	26	2017114	FCSTDV	13 Oct 1944Z	2017115	20 Oct 0043Z	19 Oct 1646Z	141.03
52	31	2017116	FCSTDV	20 Oct 1826Z	2017118	27 Oct 0639Z	27 Oct 0101Z	150.58
57	29	2017117	FCSTDV	25 Oct 2223Z	2017119	02 Nov 1904Z	02 Nov 1341Z	183.30
56	16	2017120	FCSTDV	06 Nov 1932Z	2017121	09 Nov 2132Z	09 Nov 1624Z	68.87
45	21	2017123	FCSTDV	07 Dec 1546Z	2017125	14 Dec 1922Z	14 Dec 1329Z	165.72
67	06	2017124	FCSTDV	07 Dec 1551Z	2017126	19 Dec 1435Z	19 Dec 0924Z	281.55
Average Notice Period								134.76

Table 3.7: Decommissioning Events Covered in NANUs for 2017

SVN	PRN	FCSTUUFN NANU		DECOM NANU			Notice
		NANU #	Release Time	NANU #	Release Time	End of Unusable Period	(hrs)
Average Notice Period							– [a]

[a]There were no decommisioning events in 2017.

3.3.2.2 Unscheduled Outages

The SPS PS provides the following assertion in Section 3.6.3 regarding notification of unscheduled outages or problems affecting service:

- *"Appropriate NANU issued to Coast Guard and the FAA as soon as possible after the event"*

The ICD-GPS-240 states that the nominal notification time is less than 1 hour after the start of the outage with an objective of 15 minutes.

This metric was evaluated by examining the NANUs provided throughout the year and comparing the NANU periods to outages observed in the data. Unscheduled events may be covered by either a single NANU or a pair of NANUs. In the case of a brief outage, a NANU with type UNUNOREF (unusable with no reference) is provided to detail the period of the outage. In the case of longer outages, a UNUSUFN (unusable until further notice) is provided to inform users of an ongoing outage or problem. This is followed by a NANU with type UNUSABLE after the outage is resolved. (This is described in detail in ICD-GPS-240 Section 10.1.2.)

Table 3.8 provides a list of the unscheduled outages found in the NANU information for 2017. The two leftmost columns provide the SVN/PRN of the subject SV. The third column provides the plane-slot of the SV to assist in relating these events to the information in Table 3.5. The next two columns provide the NANU #, and date/time of the UNUSUFN NANU. These are followed by three columns that specify the NANU #, the date/time of the NANU for the UNUSABLE NANU provided after the outage, and the date/time of the beginning of the outage. The final column is the time difference between the outage start time and the UNUSUFN NANU release time (in minutes). Values shown in red in the final column have a lag time of greater than 60 minutes.

Table 3.8: Unscheduled Events Covered in NANUs for 2017

SVN	PRN	Plane-Slot[a]	UNUSUFN NANU		UNUSABLE/UNUNOREF NANU			Lag Time (minutes)
			NANU #	Release Time	NANU #	Release Time	Start Of Event	
64	30	A3	2017024	08 Mar 0948Z	2017025	08 Mar 1114Z	08 Mar 0708Z	160.00
46	11	D2F	2017026	16 Mar 0307Z	2017027	16 Mar 0832Z	16 Mar 0255Z	12.00
56	16	B1A	2017032	22 Apr 1638Z	2017033	22 Apr 1656Z	22 Apr 1637Z	1.00
66	27	C2	2017035	28 Apr 0002Z	2017036	28 Apr 0451Z	27 Apr 2327Z	35.00
68	09	F3	2017080	11 Aug 1117Z	2017081	11 Aug 1345Z	11 Aug 1058Z	19.00
48	07	A4	2017099	12 Sep 0633Z	2017100	12 Sep 1012Z	12 Sep 0625Z	8.00
63	01	D2A	2017102	14 Sep 0039Z	2017103	14 Sep 0926Z	14 Sep 0021Z	18.00
48	07	A4	2017101	12 Sep 1355Z	2017104	15 Sep 2008Z	12 Sep 1342Z	13.00
62	25	B2	2017105	17 Sep 1553Z	2017106	17 Sep 1839Z	17 Sep 1500Z	53.00
63	01	D2A	2017109	04 Oct 0946Z	2017110	04 Oct 1313Z	04 Oct 0937Z	9.00
Average Lag Time								32.80

[a] *Only plane is specified for SVs that are not in a defined slot.*

Because the performance standard states only "as soon as possible after the event," there is no evaluation to be performed. However, the data are provided for information. With respect to the nominal notification times provided in ICD-GPS-240, the nominal times are met in 2017 except for NANU 2017024.

3.4 SIS Availability

3.4.1 Per-slot Availability

The SPSPS08 Section 3.7.1 makes two linked statements in this area:

- *"$\geq$ 0.957 Probability that a Slot in the Baseline Configuration will be Occupied by a Healthy Navstar Satellite Broadcasting a Useable SPS SIS"*
- *"$\geq$ 0.957 Probability that a Slot in the Expanded Configuration will be Occupied by a pair of Healthy Navstar Satellites Each Broadcasting a Useable SPS SIS"*

The constraints include the note that this is to be calculated as an average over all slots in the 24-slot constellation, normalized annually (SPS PS).

The derivation of the SV/Slot assignments is described in Appendix E.

This metric was verified by examining the status of each SV in the Baseline 24-Slot configuration (or pair of SVs in an Expandable Slot) at every 30 s interval throughout the year. The health status was determined from the subframe 1 health bits of the ephemeris being broadcast at the time of interest. In addition, data from both the MSN and the IGS monitor station networks were examined to verify that the SV was broadcasting a trackable signal at the time. The results are summarized in Table 3.9. The metric is averaged over the constellation, therefore the value in the bottom row (labeled "All Slots") must be greater than 0.957 in order for the assertion to be met.

Regardless of the individual slot availabilities, the average SPS PS availability for the constellation was 0.998703, above the threshold of 0.957. Therefore the assertion being tested in this section was met.

3.4.2 Constellation Availability

The SPSPS08 makes two linked statements in this area:

- *"$\geq$ 0.98 Probability that at least 21 Slots out of the 24 Slots will be Occupied Either by a Satellite Broadcasting a Healthy SPS SIS in the Baseline 24-Slot Configuration or by a Pair of Satellites Each Broadcasting a Healthy SPS SIS in the Expanded Slot Configuration"*
- *"$\geq$ 0.99999 Probability that at least 20 Slots out of the 24 Slots will be Occupied Either by a Satellite Broadcasting a Healthy SPS SIS in the Baseline 24-Slot Configuration or by a Pair of Satellites Each Broadcasting a Healthy SPS SIS in the Expanded Slot Configuration"*

Table 3.9: Per-Slot Availability in 2017 (SPS)

Plane-Slot	# Missing Epochs	Available
A1	0	1.000000
A2	1039	0.999012
A3	456	0.999566
A4	11418	0.989138
B1[a]	1918	0.998175
B2	1039	0.999012
B3	492	0.999532
B4	1035	0.999015
C1	1313	0.998751
C2	645	0.999386
C3	0	1.000000
C4	741	0.999295
D1	940	0.999106
D2[a]	2598	0.997529
D3	985	0.999063
D4	606	0.999424
E1	578	0.999450
E2	7	0.999993
E3	1008	0.999041
E4	1037	0.999014
F1	583	0.999445
F2[a]	2340	0.997774
F3	946	0.999100
F4	1008	0.999041
All Slots	32732	0.998703

Note: For each slot there were 1051200 total 30 s epochs in 2017.

[a] *When B1, D2, and F2 are configured as expandable slots, both slot locations must be occupied by an available satellite for the slot to be counted as available.*

To evaluate this metric the subframe 1 health condition and the availability of signal were evaluated for each SV every 30 s for all of 2017. Following a literal reading of the requirement, the number of SVs broadcasting a healthy SIS was examined for each measurement interval and assigned to the correct slot. For non-expanded baseline slots, if an SV qualified as being in the slot and was transmitting a healthy signal, the slot was counted as occupied. For expanded slots, the slot was counted as occupied if two healthy SVs were found: one in each of the two portions of the expanded slot. If the count of occupied slots was greater than 20, the measurement interval was counted as a 1; otherwise the measurement interval was assigned a zero. The sum of the 1 values was then divided by the total number of measurement intervals. The value for 2017 is 1.00. Thus, both requirements are satisfied.

While this satisfies the metric, it does not provide much information on exactly how many SVs are typically healthy. To address this, at each 30 s interval the number of SVs broadcasting a healthy SIS was counted. This was done for both the count of occupied slots and for the number of SVs. The daily averages as a function of time are shown in Figure 3.8. As is clear, the number of occupied slots always exceeds 21.

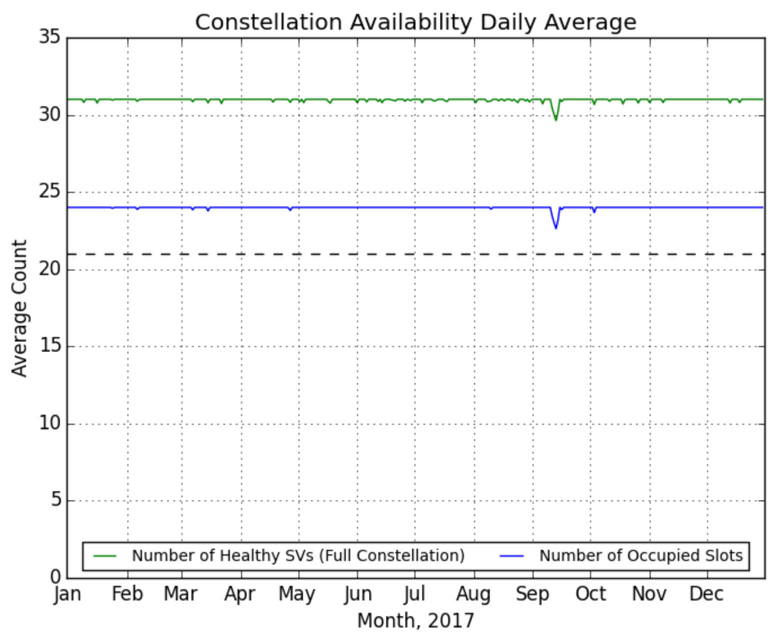

Figure 3.8: Daily Average Number of Occupied Slots

3.4.3 Operational Satellite Counts

Table 3.7-3 of the SPSPS08 states:

- *"$\geq$ 0.95 Probability that the Constellation will Have at least 24 Operational Satellites Regardless of Whether Those Operational Satellites are Located in Slots or Not"*

Under "Conditions and Constraints" the term Operational is defined as

> *"any satellite which appears in the transmitted navigation message almanac... regardless of whether that satellite is currently broadcasting a healthy SPS SIS or not or whether the broadcast SPS SIS also satisfies the other performance standards in this SPS PS or not."*

Given the information presented in Sections 3.4.1 and 3.4.2, we conclude that 24 SVs were operational 100% of the time for 2017. However, to evaluate this more directly, the almanac status was examined directly. The process consisted of selecting an almanac for each day in 2017. IS-GPS-200 Section 20.3.3.5.1.3 [2] assigns a special meaning to the SV health bits in the almanac's subframe 4 page 25 and subframe 5 page 25 (Data ID 51 and 63). When these bits are set to all ones it indicates "the SV which has that ID is not available, and there might be no data regarding that SV in that page of subframes 4 and 5..." Given this definition, the process examines the subframe 4 and 5 health bits for the individual SVs and counts the number of SVs for which the health bits are other than all ones. The results are shown in Figure 3.9. This plot is very similar to the full constellation healthy satellite count shown in Figure 3.8. The almanac health data are not updated as frequently as those in subframe 1. As a result, the plot in Figure 3.9 contains only integer values. Therefore, on days when it appears the operational SV count is lower than the number of healthy SVs in the constellation, these reflect cases where an SV was set unhealthy for a small portion of the day. In Figure 3.8, such effects are averaged over the day, yielding a higher availability.

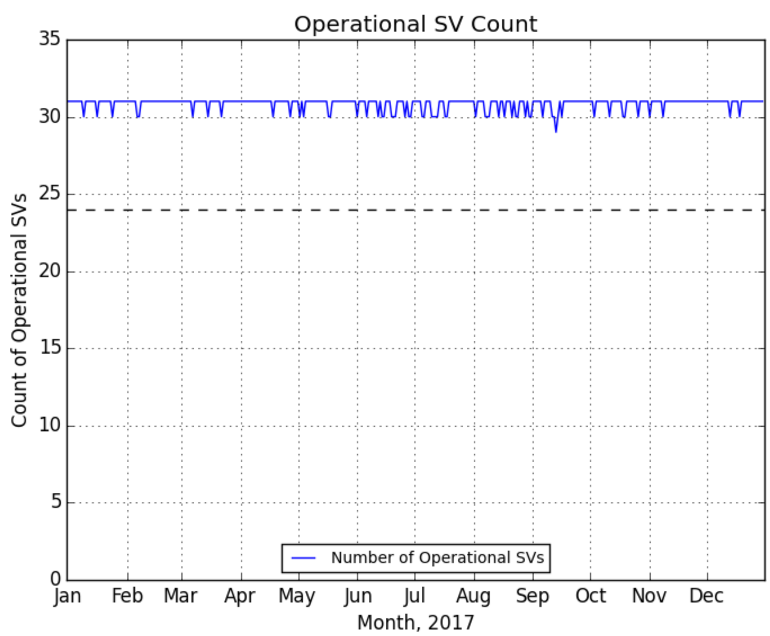

Figure 3.9: Count of Operational SVs by Day

3.5 Position/Time Domain Standards

3.5.1 PDOP Availability

Given representative user conditions and considering any 24 hour interval the SPSPS08 calls for:

- *"$\geq$ 98% global PDOP of 6 or less"*
- *"$\geq$ 88% worst site PDOP of 6 or less"*

Based on the definition of a representative receiver contained in SPS PS Section 3.8, a 5° minimum elevation angle is used for this evaluation.

These assertions were verified empirically throughout 2017 using a uniformly-spaced grid, containing N_{grid} points, to represent the terrestrial service volume at zero altitude and an archive of the broadcast ephemerides transmitted by the SVs throughout the year. All healthy, transmitting SVs were considered. The grid was 111 km $\times$ 111 km (roughly 1° $\times$ 1° at the Equator). The time started at 0000Z each day and stepped through the entire day at one minute intervals (1440 points/day, defined as $1 \leq N_t \leq 1440$). The overall process followed is similar to that defined in Section 5.4.6 of the GPS Civil Monitoring Performance Specification (CMPS) [10].

The Position Dilution of Precision (PDOP) values were formed using the traditional PDOP algorithm [11], without regard for the impact of terrain. The coordinates of the grid locations provided the ground positions at which the PDOP was computed. The position of each SV was computed from the broadcast ephemeris available to a receiver at the time of interest. The only filtering performed was the exclusion of any unhealthy SVs (those with subframe 1 health bits set to other than all 0's). The results of each calculation were tested with respect to the threshold of PDOP $\leq$ 6. If the condition was violated, a bad PDOP counter associated with the particular grid point, b_i for $1 \leq i \leq N_{grid}$, was incremented.

At least four SVs must be available to a receiver for a valid PDOP computation. This condition was fulfilled for all grid points at all times in 2017.

Once the PDOPs had been computed across all grid points, for each of the 1440 time increments during the day, the percentage of time the PDOP was less than or equal to 6 for the day was computed using the formula:

$$(\%PDOP \leq 6) = 100 \left(1 - \frac{\sum_{i=1}^{N_{grid}} b_i}{N_{grid} N_t} \right)$$

The worst site for a given day was identified from the same set of counters by finding the site with the maximum bad count: $b_{max} = \max_i(b_i)$. The ratio of b_{max} to N_t is an estimate of the fraction of time the worst site PDOP exceeds the threshold. This value was averaged over the year, and the percentage of time the PDOP is less than or equal to 6 was computed.

Table 3.10 summarizes the results of this analysis for the configurations of all SVs available. The second column ("Average daily % over 2017") provides the values for the assertions. The additional column is provided to verify that no single-day value actually dropped below the goal. From this table we conclude that the PDOP availability metrics are met for 2017.

Table 3.10: Summary of PDOP Availability

Metric	Average daily % over 2017	Minimum daily % over 2017
$\geq$ 98% Global Average PDOP $\leq$ 6	100.000	99.651
$\geq$ 88% Worst site PDOP $\leq$ 6	99.998	98.611

In addition to verifying the standard, several additional analyses go beyond the direct question and speak to the matter of how well the system is performing on a more granular basis. The remainder of this chapter describes those analyses and results.

3.5.2 Additional DOP Analysis

There are several ways to look at Dilution of Precision (DOP) values when various averaging techniques are taken into account. Assuming a set of DOP values, each identified by latitude (λ), longitude (θ), and time (t), then each individual value is represented by $DOP_{\lambda,\theta,t}$.

The global average DOP for a day, $\langle DOP\rangle(day)$, is defined to be

$$\langle DOP\rangle(day) = \frac{\sum_t \sum_\theta \sum_\lambda DOP_{\lambda,\theta,t}}{N_{grid} \times N_t}$$

Another measure of performance is the average DOP over the day at the worst site,$\langle DOP\rangle_{worst\,site}$. In this case the average over a day is computed for each unique latitude/longitude combination and the worst average of the day is taken as the result.

$$\langle DOP\rangle_{worst\,site}(day) = \max_{\lambda,\theta}\left(\frac{\sum_t DOP_{\lambda,\theta,t}}{N_t}\right)$$

This statistic is the most closely related to the description of worst site used in Section 3.5.1.

The average of worst site DOP, $\langle DOP_{worst\,site}\rangle$, is calculated by obtaining the worst DOP in the latitude/longitude grid at each time, then averaging these values over the day.

$$\langle DOP_{worst\,site}\rangle(day) = \frac{\sum_t \max_{\lambda,\theta}\left(DOP_{\lambda,\theta,t}\right)}{N_t}$$

This represents a measure of the worst DOP performance. It is not particularly useful from the user's point of view because the location of the worst site varies throughout the day.

Finally, the absolute worst time-point in a day is given by taking the maximum of the individual DOP values for all locations and all times.

$$DOP_{abs.\,worst}(day) = \max_{\lambda,\theta,t}\left(DOP_{\lambda,\theta,t}\right)$$

Given that the $\langle DOP\rangle_{worst\,site}(day)$ is most closely related to the worse site definition used in Section 3.5.1, this is the statistic that will be used for "worst site" in the remainder of this section. For 2017, both $\langle DOP\rangle_{worst\,site}(day)$ and $\langle DOP_{worst\,site}\rangle(day)$ satisfy the SPS PS assertions.

It is worth noting the following mathematical relationship between these quantities:

$$\langle DOP\rangle \leq \langle DOP\rangle_{worst\,site} \leq \langle DOP_{worst\,site}\rangle \leq DOP_{abs.\,worst}$$

This serves as a sanity check on the DOP results in general and establishes that these metrics are increasingly sensitive to outliers in $DOP_{\lambda,\theta,t}$.

In calculating the percentage of the time that the $\langle DOP\rangle$ and $\langle DOP\rangle_{worst\,site}$ are within bounds, several other statistics were calculated which provide insight into the availability of the GPS constellation throughout the world. Included in these statistics are the annual means of the daily global average DOP and the $\langle DOP\rangle_{worst\,site}$ values. These values are presented in Table 3.11, with values for 2014 through 2016 provided for comparison. The average number of satellites and the fewest satellites visible across the grid are calculated as part of the DOP calculations. Also shown in Table 3.11 are the annual means of the global average number of satellites visible to grid cells on a 111 km $\times$ 111 km (latitude by longitude) global grid and the annual means of the number of satellites in the worst-site grid cell (defined as seeing the fewest number of satellites). It should be noted that the worst site for each of these values was not only determined independently from day-to-day, it was also determined independently for each metric. That is to say, it is not guaranteed that the worst site with respect to Horizontal DOP (HDOP) is the same as the worst site with respect to PDOP. For all quantities shown in Table 3.11 the values are very similar across all four years.

There are a few other statistics that can add insight regarding the GPS system availability. The primary availability metric requires that the globally averaged PDOP be in-bounds at least 98% of the time. There are two related values: the number of days for which the PDOP is in bounds and the 98^{th} percentile of the daily globally averaged PDOP values. Similarly, calculations can be done for $\langle DOP\rangle_{worst\,site}$ criteria of having the PDOP ≤ 6 greater than 88% of the time. Table 3.12 presents these values.

Table 3.12 shows that the average DOP values for 2017 are nearly identical to previous years.

Table 3.11: Additional DOP Annually-Averaged Visibility Statistics

	$\langle DOP\rangle$				$\langle DOP\rangle_{worst\,site}$			
	2014	2015	2016	2017	2014	2015	2016	2017
Horizontal DOP	0.86	0.85	0.83	0.83	0.99	0.97	0.94	0.94
Vertical DOP	1.39	1.37	1.34	1.35	1.73	1.72	1.68	1.68
Time DOP	0.81	0.80	0.78	0.78	0.94	0.92	0.89	0.89
Position DOP	1.64	1.62	1.58	1.59	1.89	1.89	1.84	1.83
Geometry DOP	1.83	1.81	1.77	1.77	2.10	2.10	2.04	2.04
Number of visible SVs	10.31	10.33	10.39	10.49	4.99	5.28	5.93	5.95

Table 3.12: Additional PDOP Statistics

	2014	2015	2016	2017
Percentage of Days with the $\langle PDOP\rangle \leq 6$	100.00	100.00	100.00	100.00
Percentage of Days with the $\langle PDOP\rangle$ at Worst Site ≤ 6	100.00	100.00	100.00	100.00
98^{th} Percentile of $\langle PDOP\rangle$	1.67	1.65	1.63	1.60
88^{th} Percentile of $\langle PDOP\rangle_{worst\,site}$	1.91	1.92	1.89	1.84

Behind the statistics are the day-to-day variations. Figure 3.10 provides a time history of the four PDOP metrics considering all satellites for 2017. Four metrics are plotted:

- Daily Global Average PDOP: $\langle PDOP\rangle$
- Average Worst Site PDOP: $\langle PDOP\rangle_{worst\,site}$
- Average PDOP at Worst Site: $\langle PDOP_{worst\,site}\rangle$
- Absolute Worst PDOP: $PDOP_{abs.\,worst}$

$PDOP_{abs.\,worst}$ is the only quantity that does not include averaging. As such, $PDOP_{abs.\,worst}$ is the quantity most sensitive to events such as SV outages and to short-duration periods of higher PDOP as SVs drift within the constellation. In addition, the fact that the PDOP evaluation is conducted on a five minute cadence coupled with the fact that the SV ground tracks advance four minutes per day means a period of higher PDOP that lasts less than five minutes can be alternately observed/not-observed on successive days as the two cadences interact. An example of this is seen at the end of April and in December where the $PDOP_{abs.\,worst}$ exhibits daily oscillations. During this time, a very short-duration period of localized somewhat higher PDOP is coming in-and-out of view as it overlaps (or does not overlap) with the five minute evaluation cadence. The period becomes long enough to regularly be noted for the period from May to early December, then closes up once more.

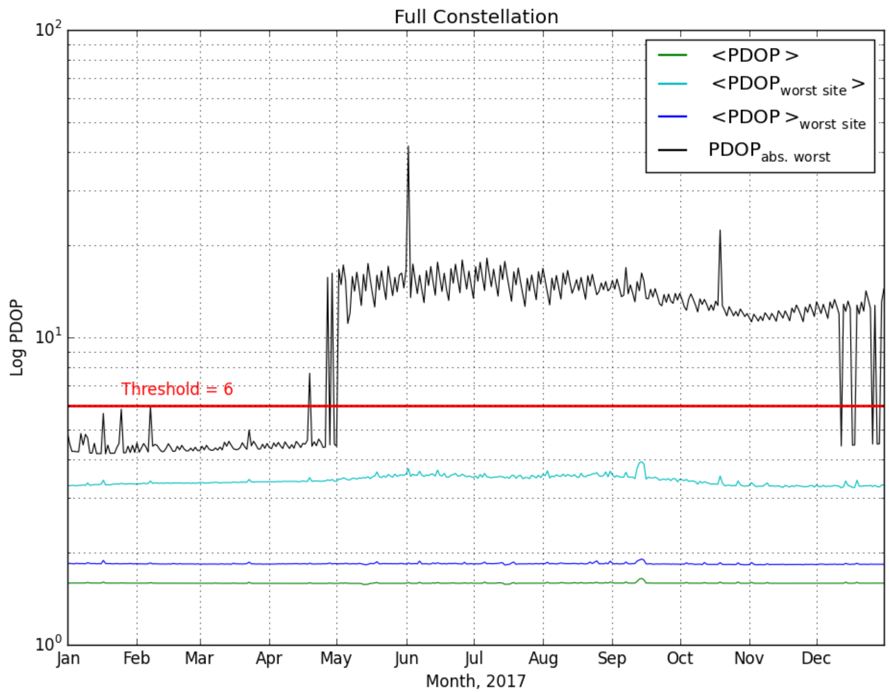

Figure 3.10: Daily PDOP Metrics Using All SVs, 2017

3.5.3 Position Service Availability

The positioning and timing availability standards are stated in Table 3.8-2 of SPSPS08 as follows:

- *"≥ 99% Horizontal Service Availability, average location"*
- *"≥ 99% Vertical Service Availability, average location"*
- *"≥ 90% Horizontal Service Availability, worst-case location"*
- *"≥ 90% Vertical Service Availability, worst-case location"*

The conditions and constraints associated with the standards include the specification of a 17 m horizontal 95^{th} percentile threshold and a 37 m vertical 95^{th} percentile threshold.

These are derived values as described in the sentence preceding SPSPS08 Table 3.8-2:

> *"The commitments for maintaining PDOP (Table 3.8-1) and SPS SIS URE accuracy (Table 3.4-1) result in support for position service availability standards as presented in Table 3.8-2."*

Because the commitments for PDOP and constellation SPS SIS URE have not only been met, but exceeded, this assertion in the SPSPS08 implies that the position and timing availability standards have also been fulfilled. A direct assessment of these metrics was not undertaken.

3.5.4 Position Accuracy

The positioning accuracy standards are stated in Table 3.8-3 of SPSPS08 as follows:

- *"≤ 9 m 95% Horizontal Error Global Average Position Domain Accuracy"*
- *"≤ 15 m 95% Vertical Error Global Average Position Domain Accuracy"*
- *"≤ 17 m 95% Horizontal Error Worst Site Position Domain Accuracy"*
- *"≤ 37 m 95% Vertical Error Worst Site Position Domain Accuracy"*

These are derived values as described in the sentence preceding SPSPS08 Table 3.8-3:

> *"The commitments for maintaining PDOP (Table 3.8-1) and SPS SIS URE accuracy (Table 3.4-1) result in support for position service availability standards as presented in Table 3.8-3."*

Since the commitments for PDOP and constellation SPS SIS URE have been met, the position and timing accuracy standards have also been fulfilled.

While this answer is technically correct, it is not very helpful. Position and time determination are the primary reasons that GPS exists. At the same time, position accuracy is a particularly difficult metric to evaluate due to the fact that GPS provides the SIS, but the user is responsible for appropriately processing the SIS to determine a position.

Section 2.4.5 of SPSPS08 provides usage assumptions for the SPS PS and some of the notes in Section 2.4.5 are relevant to the question of position determination. The following is quoted from Section 2.4.5:

> *"The performance standards in Section 3 of this SPS PS do not take into consideration any error source that is not under direct control of the Space Segment or Control Segment. Specifically excluded errors include those due to the effects of:*
>
> - *Signal distortions caused by ionospheric and/or tropospheric scintillation*
> - *Residual receiver ionospheric delay compensation errors*
> - *Residual receiver tropospheric delay compensation errors*

- *Receiver noise (including received signal power and interference power) and resolution*
- *Multipath and receiver multipath mitigation*
- *User antenna effects*
- *Operator (user) error"*

In addition, at the beginning of Section 3.8, the SPSPS08 explains that in addition to the error exclusions listed in Section 2.4.5, the following assumptions are made regarding the SPS receiver:

"The use of a representative SPS receiver that:

- *is designed in accordance with IS-GPS-200*
- *is tracking the SPS SIS from all satellites in view above a* 5° *mask angle... It is assumed the receiver is operating in a nominal noise environment...*
- *accomplishes satellite position and geometric range computations in the most current realization of the WGS 84 Earth-Centered, Earth-Fixed (ECEF) coordinate system.*
- *generates a position and time solution from data broadcast by all satellites in view*
- *compensates for dynamic Doppler shift effects on nominal SPS ranging signal carrier phase and C/A code measurements.*
- *processes the health-related information in the SIS and excludes marginal and unhealthy SIS from the position solution.*
- *ensures the use of up-to-date and internally consistent ephemeris and clock data for all satellites it is using in its position solution.*
- *loses track in the event a GPS satellite stops transmitting a trackable SIS.*
- *is operating at a surveyed location (for a time transfer receiver)."*

To address these standards, the following approach was adopted for computing a set of accuracy statistics:

1. 30 s GPS observations were collected from the NGA GPS monitor station network and a similar set of 31 IGS stations. This decision addressed the following concerns:
   (a) All stations selected collect dual-frequency observations. Therefore the first-order ionospheric effects can be eliminated from the results.
   (b) All stations selected collect weather observations. The program that generates the positions uses the weather data to eliminate first order tropospheric effects.

(c) The receiver thermal noise will not be eliminated, but both the NGA and IGS stations are generally using the best available equipment, so effects will be limited.

(d) Similarly, multipath cannot be eliminated, but both networks use antennas designed for multipath reduction, and station sites are chosen to avoid the introduction of excessive multipath.

(e) Antenna phase center locations for such stations are very well known. Therefore, position truth is readily available.

(f) Despite the similarities, the two networks are processed separately for a variety of reasons.

i. The NGA GPS network use receivers capable of tracking the Y-code and therefore have somewhat better SNR for individual observations. By contrast, most of the IGS monitor stations average their observations over 30 s.

ii. The NGA GPS network uses a single receiver which limits the number of receiver-specific traits, but leaves the possibility that a systemic problem could impact all receivers. The IGS network uses a variety of receivers, which is some proof against systemic problems from a single receiver, but requires that the processing address a variety of receiver-specific traits.

iii. The NGA network is operated and maintained by a single organization. Changes are rare and well-controlled. The IGS network is cooperative in nature. While policies are in place to encourage operational standards changes in station behavior are not as well-coordinated.

2. Process the data using a comprehensive set of broadcast ephemerides collected as described in Appendix B.2.

3. Process the collected observations using the PRSOLVE program of the ARL:UT-hosted open source GPS Toolkit (GPSTk)[12]. Note:

(a) PRSOLVE meets the relevant requirements listed above. For example, SV positions are derived in accordance with IS-GPS-200, the elevation mask is configurable, weather data is used to estimate tropospheric effects, and WGS 84 [13] conventions are used. Data from unhealthy SVs were removed from PRSOLVE using an option to exclude specific satellites.

(b) PRSOLVE is highly configurable. Several of the items in the preceding list of assumptions are configuration parameters to PRSOLVE.

(c) Any other organization that wishes to reproduce the results should be able to do so. (Both the algorithm and the data are publically available.)

4. Process the collected 30 s observations in two ways:

(a) Use all SVs in view without data editing in an autonomous pseudorange solution to generate 30 s position residuals at all sites.

(b) Use a receiver autonomous integrity monitoring (RAIM) algorithm (another PRSOLVE option) to remove outlier pseudorange measurements from which a "clean" set of 30 s position residuals is generated at all sites. The RAIM algorithm used by PRSOLVE is dependent on several parameters, the two most important of which are the RMS limit on the post-fit residuals (default: 3.0 m) and the number of SVs that can be eliminated in the RAIM process (default: unlimited). This analysis was conducted using the default values.

5. Compute statistics on each set of data independently.

We conducted the elevation angle processing with a 5° minimum elevation angle in agreement with the standard.

This process yields four sets of results organized as detailed in Table 3.13.

Table 3.13: Organization of Positioning Results

Case	Constellation Considered	Data Editing Option	Data Source
1	All in View	RAIM	IGS Data
2			NGA Data
3		None	IGS Data
4			NGA Data

Once the solutions are computed, two sets of statistics were developed. The first set is a set of daily average values across all stations. In the second set, the worst site is determined on a day-to-day basis and the worst site 95^{th} percentile values are computed.

These are empirical results and should not be construed to represent a proof that the metrics presented in the standard have been met. Instead, they are presented as a means of corroboration that the standards have been met through the fulfillment of the more basic commitments of PDOP and SPS SIS URE.

3.5.4.1 Results for Daily Average

Using the approach outlined above, position solutions were computed at each 30 s interval for data from both the NGA and IGS stations. In the nominal case in which all stations are operating for a complete day, this yields 2880 solutions per station per day. Truth positions for the IGS stations were taken from the weekly Station Independent Exchange format (SINEX) files. Truth locations for the NGA stations were taken from station locations defined as part of the latest WGS 84 adjustment with corrections for station velocities applied.

Residuals between estimated locations and the truth locations were computed (using PRSOLVE options) in the form of North, East and Up components in meters. The horizontal residual was computed from the RSS of the North and East components, and the vertical residual was computed from the absolute value of the Up component. As a result, the residuals will have non-zero mean values. The statistics on the residuals were compiled across all stations in a set for a given day. Figures 3.11-3.14 show the daily average for the horizontal and vertical residuals corresponding to the options shown in Table 3.13.

The statistics associated with the processing are provided in Table 3.14. The table contains the mean, median, maximum, and standard deviation of the daily values across 2017. The results are organized in this fashion to facilitate comparison of the same quantity across the various processing options. The results are expressed to the centimeter level of precision. This choice of precision is based on the fact that the truth station positions are known only at the few-centimeter level.

The following general observations may be drawn from the charts and the supporting statistics in Table 3.14:

- Outliers - Figure 3.12 shows a number of large outliers for the IGS averages computed with a simple pseudorange solution and no data editing. The outliers are distributed among several stations. These outliers are largely missing from Figure 3.11. This indicates the importance of conducting at least some level of data editing in the positioning process.

- Mean & Median values - The means and medians of the position residuals given in Table 3.14 are nearly identical for the NGA data sets, suggesting that if there are any 30 s position residual outliers, they are few in number and not too large. The means for the RAIM solutions from IGS are approximately 10% higher than the medians. The means and medians for the IGS data set solutions with no data editing are significantly different. This is consistent with the outliers observed in Figure 3.11 and Figure 3.12 and with the maximum and standard deviation values for the IGS data set solutions with no editing. This suggests that there are some large 30 s position residuals in the epoch-by-epoch results for these data sets.

- Maximum values and Standard Deviation - The values shown in Table 3.14 for the IGS data sets are quite a bit larger than the corresponding values for the NGA data sets. Once again, this suggests that there are some large 30 s position residuals in the epoch-by-epoch results for these data sets.

- Differences between NGA and IGS results - The mean magnitude of the position residual as reported in Table 3.14 is slightly smaller for the NGA stations than for the IGS stations. There are a number of differences between the two station sets. The NGA station set is more homogeneous in that the same receiver model is used throughout the data processed for this analysis, the data are derived from full-code tracking, and a single organization prepared all the data sets using a single set of algorithms. By contrast, the IGS data sets come from a variety of receivers and were prepared and submitted by a variety of organizations. These differences likely account for the greater variability in the results derived from the IGS data sets.

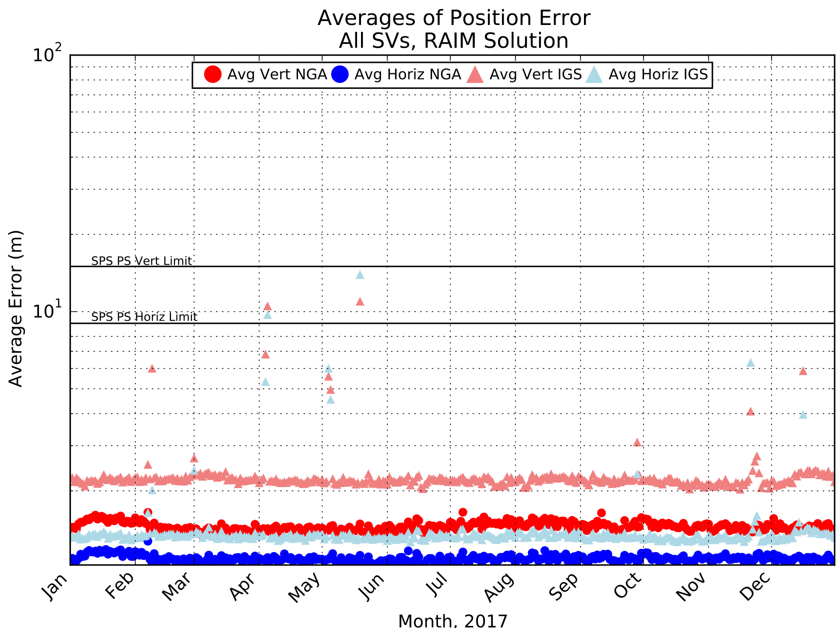

Figure 3.11: Daily Averaged Position Residuals Computed Using a RAIM Solution

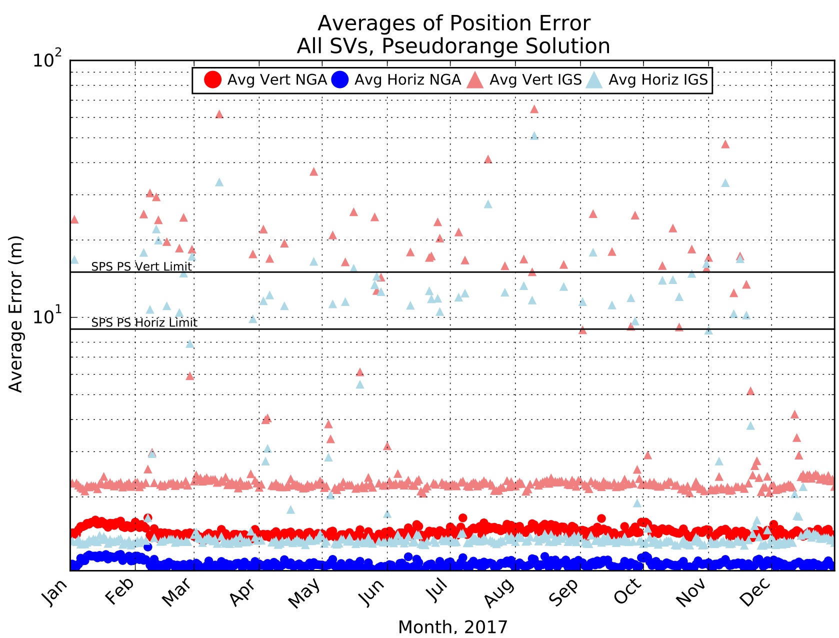

Figure 3.12: Daily Averaged Position Residuals Computed Using No Data Editing

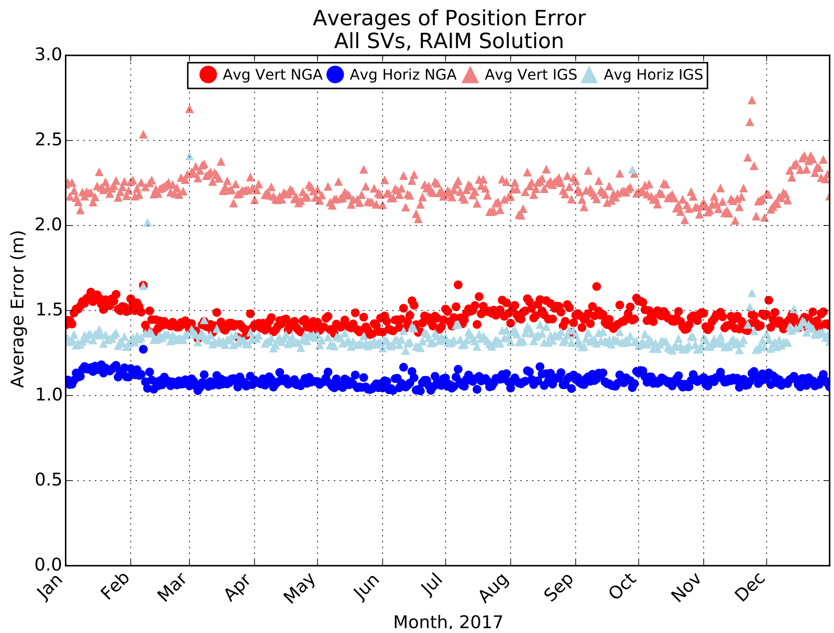

Figure 3.13: Daily Averaged Position Residuals Computed Using a RAIM Solution (enlarged)

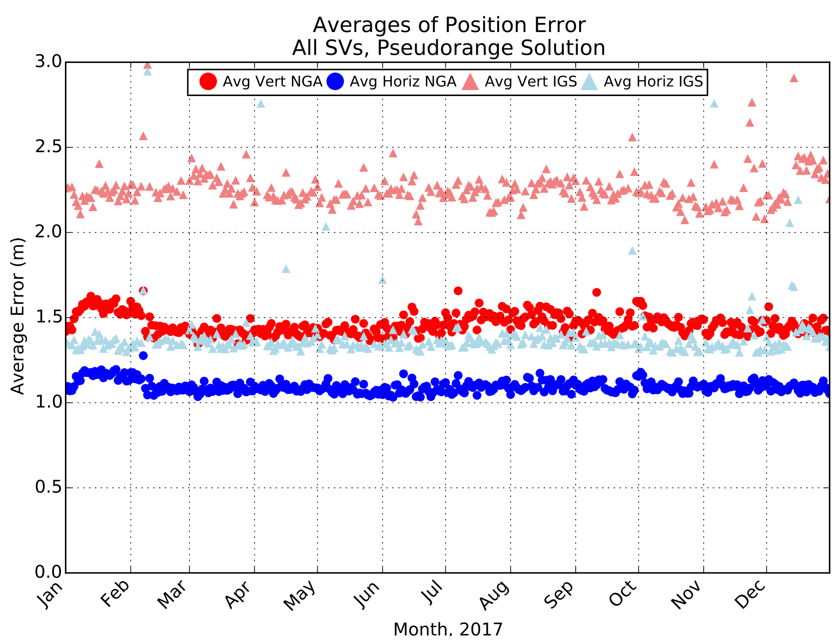

Figure 3.14: Daily Averaged Position Residuals Computed Using No Data Editing (enlarged)

Table 3.14: Daily Average Position Errors for 2017

Statistic	Data Source	Horizontal		Vertical	
		IGS	NGA	IGS	NGA
Mean (m)	RAIM	1.45	1.09	2.31	1.45
	No Editing	3.27	1.10	4.98	1.46
Median (m)	RAIM	1.33	1.09	2.20	1.44
	No Editing	1.36	1.09	2.25	1.45
Maximum (m)	RAIM	13.95	1.27	10.97	1.65
	No Editing	51.02	1.28	64.80	1.66
Std. Dev. (m)	RAIM	0.92	0.03	0.77	0.06
	No Editing	5.40	0.03	7.92	0.06

3.5.4.2 Results for Worst Site 95$^{\text{th}}$ Percentile

The edited and non-edited 30 s position residuals were then processed (independently) to determine the worst site 95th percentile values. In this case, the 95th percentile was determined for each station in a given set, and the worst of these was used as the final 95th percentile value for that day. Figures 3.15-3.18 show these values for the various processing options described in the previous section. The plots are followed by tables of the statistics for the mean, median, maximum, and standard deviation of the daily worst site 95th percentile values. Some general observations on the results are included following the tables.

The statistics associated with the worst site 95th percentile values are provided in Table 3.15. The table contains the mean, median, maximum, and standard deviation of the daily values across 2017. As before, the results are organized in this fashion to facilitate comparison of the same quantity across the various processing options. Values are reported with a precision of one centimeter due to (a.) the magnitude of the standard deviation and (b.) the fact that the station positions are known only at the few-centimeter level.

Most of the observations from the daily averaged position residuals hold true in the case of the results for the worst site 95th percentile case. However, there are a few additional observations to be drawn from Figures 3.15-3.18 and Table 3.15:

- Comparison to threshold - The values for both mean and median of the worst 95th percentile for both horizontal and vertical errors are well within the standard for both solutions. Compared to the thresholds of 17 m 95th percentile horizontal and 37 m 95th percentile vertical these results are outstanding.

- Comparison between processing options - The statistics for the RAIM solutions are slightly better than the statistics for the pseudorange solutions with respect to mean and median. However, the maximum values for the IGS data with no editing exceed the 95th percentile error worst site assertion. This illustrates the importance of some form of data editing.

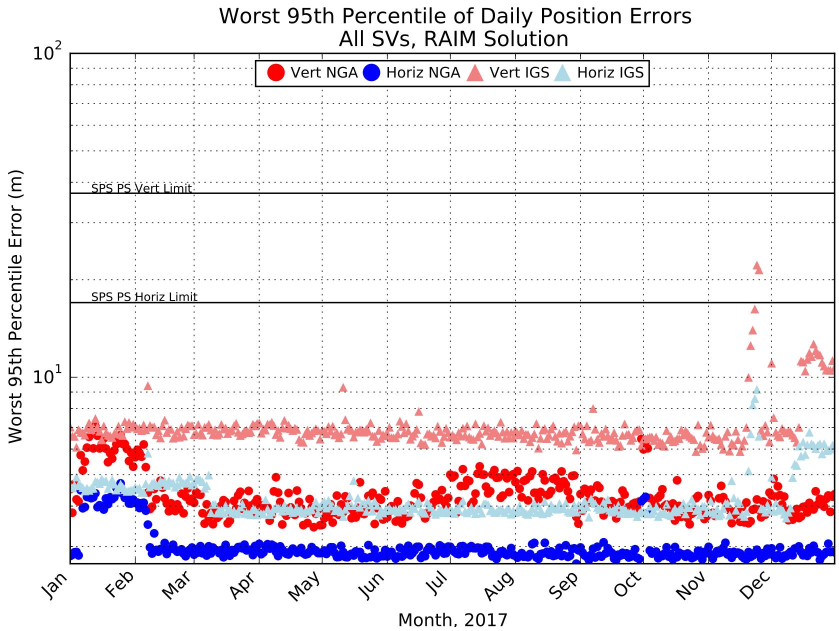

Figure 3.15: Worst Site 95^{th} Daily Averaged Position Residuals Computed Using a RAIM Solution

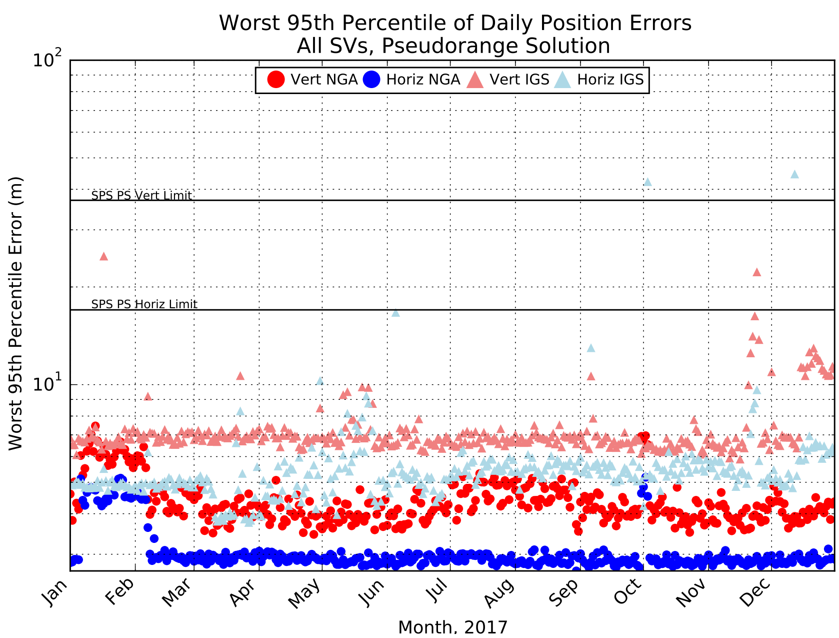

Figure 3.16: Worst Site 95^{th} Daily Averaged Position Residuals Computed Using No Data Editing

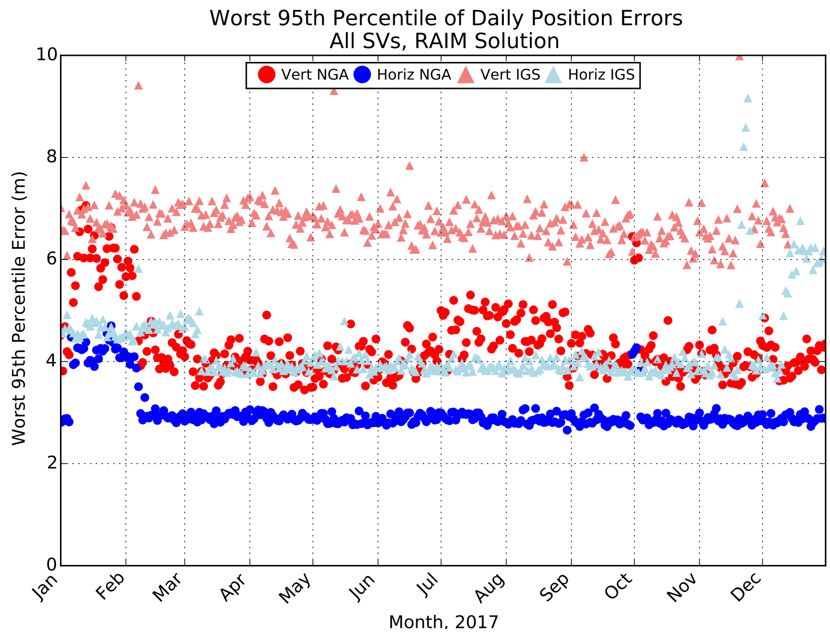

Figure 3.17: Worst Site 95^{th} Daily Averaged Position Residuals Computed Using a RAIM Solution (enlarged)

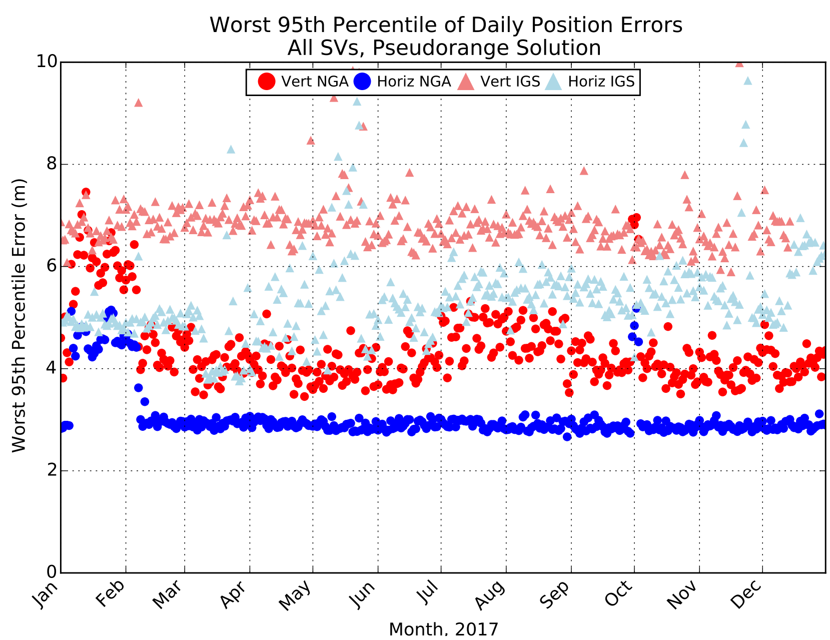

Figure 3.18: Worst Site 95^{th} Daily Averaged Position Residuals Computed Using No Data Editing (enlarged)

Table 3.15: Daily Worst Site 95^{th} Percentile Position Errors for 2017

Statistic	Data Source	Horizontal		Vertical	
		IGS	NGA	IGS	NGA
Mean (m)	RAIM	4.24	3.01	7.11	4.33
	No Editing	5.61	3.07	7.27	4.39
Median (m)	RAIM	3.95	2.88	6.75	4.13
	No Editing	5.27	2.89	6.83	4.19
Maximum (m)	RAIM	9.16	4.70	22.20	7.06
	No Editing	44.60	5.18	24.91	7.46
Std. Dev. (m)	RAIM	0.71	0.40	1.66	0.69
	No Editing	3.01	0.53	1.83	0.72

3.5.5 Time Accuracy

The timing accuracy standard is stated in Table 3.8-3 of SPSPS08 as follows:

- *"$\leq$ 40 nsec 95% Error Time Transfer Domain Accuracy"* (SIS only)

Conditions and Constraints:

- *Defined for a time transfer solution meeting the representative user conditions*
- *Standard based on a measurement interval of 24 hours averaged over all points in the service volume.*

The equation for time transfer accuracy relative to UTC(USNO) in GPS is found in the SPSPS08, Appendix B.2.2. Time transfer dilution of precision (TTDOP) is $1/\sqrt{\text{N}}$, where N is the number is satellites visible to the user[1]. The User UTC(USNO) Error (UUTCE) calculation was performed for each day of the year.

This computation was done only for satellites that are "good" (see 2. below). To meet the requirement of an average over all points in the service volume a worldwide grid with 425 points was created (see Figure 3.19). Since time transfer accuracy can be dependent on which SVs are in view of a given location, the grid was selected to provide a representative sampling of possible user locations around the world with a variety of possible SV combinations. The grid has 10° separation in latitude, and 10° separation in longitude at the equator. The longitude spacing for latitudes away from the equator was selected to be as close as possible to the distance between longitude points along the equator while maintaining an even number of intervals. This yields a spacing of roughly 1100km.

Statistics were performed for each day over the grid of 425 points and time step of 15 minutes (96 time points), resulting in 40800 points to determine the 95^{th} percentile UUTCE value.

[1] *as per conversation with Mr. Karl Kovach, author of the SPS PS, 31 August 2017*

The computation steps are:

1. Compute satellite positions for each time point in day using the broadcast ephemeris,
2. For each time and grid point, find visible satellites (above 5° elevation) that are good: healthy, trackable, operational, and have no NANU at each given time,
3. For each time and grid point, determine the appropriate UTCO data set ($UTCO_i$). The appropriate data set is the valid data set that has the latest reference time (t_{ot}) of all valid data sets received at that location at that time.

   Calculate $UTCOE_i = UTCO_i - USNO$, where $USNO$ is the daily truth value,
4. For each time and grid point, get the Instantaneous SIS URE for each visible satellite, then take the mean of all values ($UERE_i$) and assign as the value for that time and grid point,
5. Calculate all UUTCE values for the day (# of grid points * # of times = 40800), find 95% containment of all values. $UUTCE_i = \sqrt{(UERE_i * TTDOP_i/c)^2 + (UTCOE_i)^2)}$

The daily UUTCE results over all grid points and times per day are shown in Figure 3.20. All of these results are well below 40 nsec. Therefore this assertion is met.

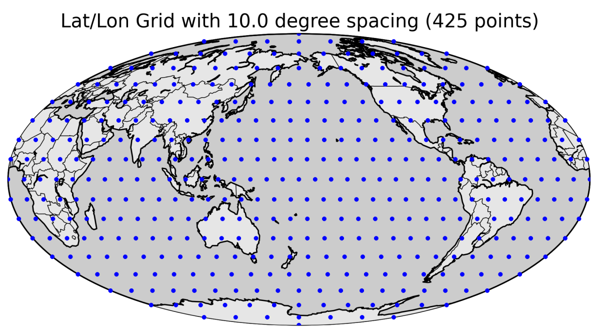

Figure 3.19: 10° Grid for UUTCE Calculation

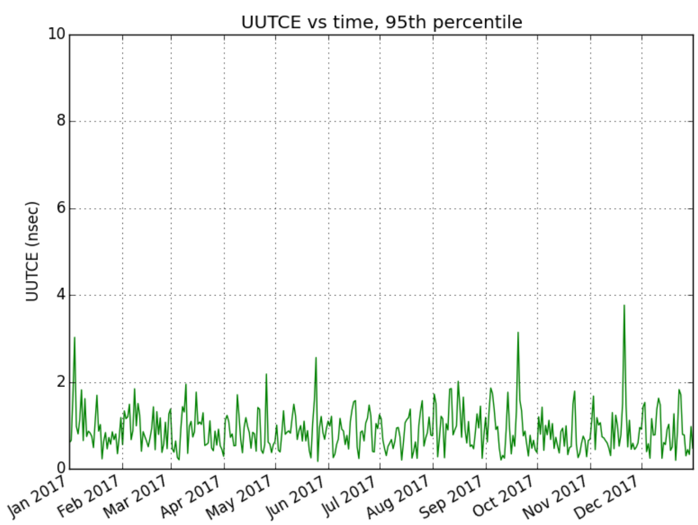

Figure 3.20: UUTCE 95^{th} Percentile Values

Chapter 4

Additional Results of Interest

4.1 Frequency of Different SV Health States

Several of the assertions require examination of the health information transmitted by each SV. We have found it useful to examine the rate of occurrence for all possible combinations of the six health bits transmitted in subframe 1.

Table 4.1 presents a summary of health bit usage in the ephemerides broadcast during 2017. Each row in the table presents a summary for a specific SV. The summary across all SVs is shown at the bottom. The table contains the count of the number of times each unique health code was seen, the raw count of unique sets of subframes 1, 2, and 3 collected during the year, and the percentage of sets of subframe 1, 2, and 3 data that contained specific health codes. Only two unique health settings were observed throughout 2017: binary 000000_2 (0x00) and binary 111111_2 (0x3F).

4.2 Age of Data

The Age of Data (AOD) represents the elapsed time between the observations that were used to create the broadcast navigation message and the time when the contents of subframes 1, 2, and 3 are available to the user to estimate the position of a SV. The accuracy of GPS (at least for users that depend on the broadcast ephemeris) is indirectly tied to the AOD because the prediction accuracy degrades over time (see Section 3.1.2). This is especially true for the clock prediction. It has been recognized that reducing the AOD improves position, velocity, or time (PVT) solutions for autonomous users; however, there is an impact in terms of increased operations tempo at 2^{nd} Space Operations Squadron (2 SOPS).

Note that there is no need for a GPS receiver to refer to AOD in any PVT computation other than the optional application of the navigation message correction table (NMCT). (See IS-GPS-200 Section 20.3.3.5.1.9 for a description of the NMCT.) The AOD is computed here to validate that the operators at 2 SOPS are not modifying the operational tempo to maintain the URE accuracy described in Section 3.1.

Table 4.1: Frequency of Health Codes

SVN	PRN	Count by Health Code		Total # SF 1, 2, 3 Collected	Percent of Time by Health Code		Operational Days for 2017	Avg # SF 1, 2, 3 per Operational Day
		0x3F	0x00		0x3F	0x00		
41	14	4	4748	4752	0.1	99.9	365	13.0
43	13	7	4745	4752	0.1	99.9	365	13.0
44	28	4	4782	4786	0.1	99.9	365	13.1
45	21	8	4742	4750	0.2	99.8	365	13.0
46	11	6	4747	4753	0.1	99.9	365	13.0
47	22	6	4746	4752	0.1	99.9	365	13.0
48	07	57	4703	4760	1.2	98.8	365	13.0
50	05	9	4742	4751	0.2	99.8	365	13.0
51	20	4	4748	4752	0.1	99.9	365	13.0
52	31	9	4743	4752	0.2	99.8	365	13.0
53	17	7	4756	4763	0.1	99.9	365	13.0
54	18	8	4748	4756	0.2	99.8	365	13.0
55	15	8	4742	4750	0.2	99.8	365	13.0
56	16	7	4737	4744	0.1	99.9	365	13.0
57	29	10	4753	4763	0.2	99.8	365	13.0
58	12	7	4750	4757	0.1	99.9	365	13.0
59	19	4	4740	4744	0.1	99.9	365	13.0
60	23	8	4743	4751	0.2	99.8	365	13.0
61	02	7	4749	4756	0.1	99.9	365	13.0
62	25	5	4744	4749	0.1	99.9	365	13.0
63	01	4	4755	4759	0.1	99.9	365	13.0
64	30	2	4749	4751	0.0	100.0	365	13.0
65	24	0	4807	4807	0.0	100.0	365	13.2
66	27	2	4750	4752	0.0	100.0	365	13.0
67	06	4	4751	4755	0.1	99.9	365	13.0
68	09	3	4756	4759	0.1	99.9	365	13.0
69	03	4	4752	4756	0.1	99.9	365	13.0
70	32	4	4747	4751	0.1	99.9	365	13.0
71	26	5	4748	4753	0.1	99.9	365	13.0
72	08	0	4765	4765	0.0	100.0	365	13.1
73	10	0	4752	4752	0.0	100.0	365	13.0
All SVs		213	147240	147453	0.1	99.9	365	404.0

The daily average AOD throughout 2017 is shown in Table 4.2, along with values for the previous three years. Details on how AOD was computed are provided in Appendix B.3. The daily average AOD for the constellation and for each block is illustrated in Figure 4.1. The AOD is generally constant throughout 2017, which indicates that any variations in the URE results discussed earlier are not due to changes in operations tempo at 2 SOPS.

Table 4.2: Age of Data of the Navigation Message by SV Type

	Average Age of Data (hrs)			
	2014	2015	2016	2017
Full Constellation	11.6	11.6	11.9	12.1
Block II/IIA	11.1	11.6	11.7	–
Block IIR/IIR-M	11.7	11.7	11.9	12.1
Block IIF	11.6	11.4	11.8	12.1

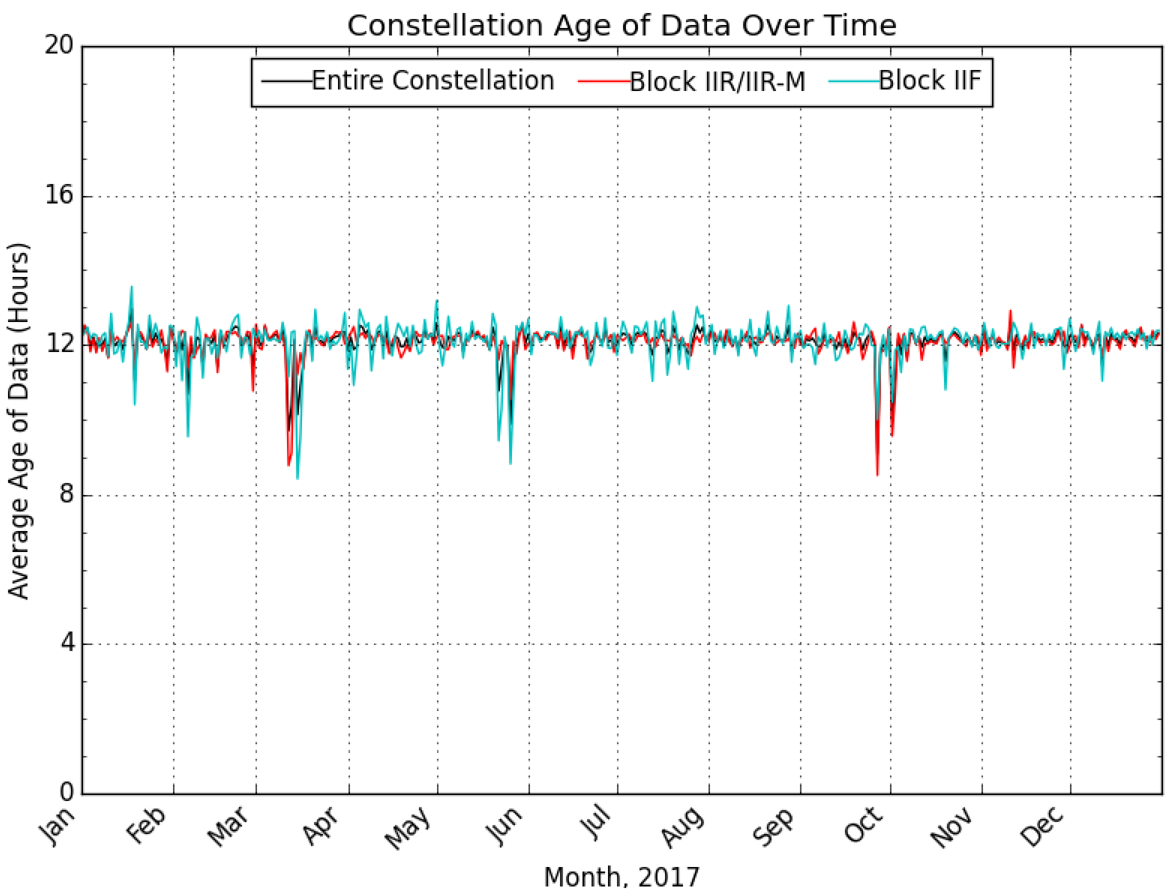

Figure 4.1: Constellation Age of Data for 2017

4.3 User Range Accuracy Index Trends

Tables 4.3 and 4.4 present a summary of the analysis of the URA index values throughout 2017. The total number of navigation messages examined differs from the health summary in Section 4.1 as only URA index values corresponding to health settings of 0x00 are included in this analysis. Both the absolute count and the count as a percentage of the total are shown.

The vast majority of the values are 0, 1, or 2 (over 99.9%). Index values between 3 and 5 were very rare. No values over 5 were observed.

4.4 Extended Mode Operations

IS-GPS-200 defines Normal Operations as the period of time when subframe 1, 2, and 3 data sets are transmitted by the SV for periods of two hours with a curve fit interval of four hours (IS-GPS-200 Section 20.3.4.4). This definition is taken to be the same as the definition of Normal Operations in SPSPS08 for the URE metrics. To determine if any SV operated in other than Normal Operations at any time in 2017, the broadcast ephemerides were examined to determine if any contained fit interval flags set to 1. (See IS-GPS-200 20.3.3.4.3.1 for definition of the fit interval flag.)

The analysis found a total of 43 examples of extended operations for satellites set healthy. The examples were distributed across 36 days. The average time of an occurrence was 55 minutes. The minimum duration was 60 seconds and the maximum duration was 6 hours 40 minutes. These results are summarized in Table 4.5.

Given the relative rarity of occurrence, the URE values for the periods summarized in Table 4.5 are included in the statistics presented in Section 3.1.1, even though a strict interpretation of the SPSPS08 would suggest that they be removed. However, the SVs involved were still set healthy and (presumably) being used by user equipment, it is appropriate to include these results to reflect performance seen by the users.

Examination of the ephemerides from past years reveals that 2017 is not an anomaly. Such periods have been found in all years checked (back to 2005).

Past discussions with the operators have revealed several reasons for these occurrences. Some are associated with Alternate MCS (AMCS) testing. When operations are transitioned from the MCS to the AMCS (and reverse) it is possible that SVs nearing the end of their daily cycle may experience a longer-than-normal upload cycle. Other occurrences may be caused by delays due to ground antenna maintenance or due to operator concentration on higher-priority issues with the constellation at the time.

Table 4.3: Distribution of URA Index Values

SVN	PRN	URA Index						Total # SF 1, 2, 3 examined[a]	Avg # SF 1, 2, 3 per Oper. Day[a]	Oper. Days for 2017
		5	4	3	2	1	0			
41	14					260	4488	4748	13.0	365
43	13				1	416	4328	4745	13.0	365
44	28			3	979	1165	2635	4782	13.1	365
45	21				81	867	3794	4742	13.0	365
46	11				1	744	4002	4747	13.0	365
47	22			1	5	89	4651	4746	13.0	365
48	07				1	303	4399	4703	13.0	363
50	05				3	106	4633	4742	13.0	365
51	20					63	4685	4748	13.0	365
52	31			5	1	378	4359	4743	13.0	365
53	17				2	915	3839	4756	13.0	365
54	18			4	8	128	4608	4748	13.0	365
55	15				1	357	4384	4742	13.0	365
56	16			5	1	331	4400	4737	13.0	365
57	29				4	688	4061	4753	13.0	365
58	12			2	3	250	4495	4750	13.0	365
59	19				1	300	4439	4740	13.0	365
60	23		1	6	1	337	4398	4743	13.0	365
61	02		2	5	34	176	4532	4749	13.0	365
62	25		2	2	4	381	4355	4744	13.0	365
63	01				5	243	4507	4755	13.0	365
64	30					382	4367	4749	13.0	365
65	24				1	1146	3660	4807	13.2	365
66	27					389	4361	4750	13.0	365
67	06			4	1	141	4605	4751	13.0	365
68	09			4	4	330	4418	4756	13.0	365
69	03		5	2	87	767	3891	4752	13.0	365
70	32	1	5	1	9	385	4346	4747	13.0	365
71	26					357	4391	4748	13.0	365
72	08				1	511	4253	4765	13.1	365
73	10					98	4654	4752	13.0	365
All SVs		1	15	44	1239	13003	132938	147240	403.4	365

[a] *Only sets of SF 1,2,3 that include a healthy indication are included.*

Table 4.4: Distribution of URA Index Values As a Percentage of All Collected

SVN	PRN	URA Index					
		5	4	3	2	1	0
41	14					5.5	94.5
43	13					8.8	91.2
44	28			0.1	20.5	24.4	55.1
45	21				1.7	18.3	80.0
46	11					15.7	84.3
47	22				0.1	1.9	98.0
48	07					6.4	93.5
50	05				0.1	2.2	97.7
51	20					1.3	98.7
52	31			0.1		8.0	91.9
53	17					19.2	80.7
54	18			0.1	0.2	2.7	97.1
55	15					7.5	92.5
56	16			0.1		7.0	92.9
57	29				0.1	14.5	85.4
58	12				0.1	5.3	94.6
59	19					6.3	93.6
60	23			0.1		7.1	92.7
61	02			0.1	0.7	3.7	95.4
62	25				0.1	8.0	91.8
63	01				0.1	5.1	94.8
64	30					8.0	92.0
65	24					23.8	76.1
66	27					8.2	91.8
67	06			0.1		3.0	96.9
68	09			0.1	0.1	6.9	92.9
69	03		0.1		1.8	16.1	81.9
70	32		0.1		0.2	8.1	91.6
71	26					7.5	92.5
72	08					10.7	89.3
73	10					2.1	97.9
Constellation Average		0.0	0.0	0.0	0.8	8.8	90.3

Notes: Values smaller than 0.1 are not shown. Constellation averages are weighted by the number of observations.

Table 4.5: Summary of Occurrences of Extended Mode Operations

SVN	PRN	# of Occurrences		Duration (minutes)	
		Healthy	Unhealthy	Healthy	Unhealthy
41	14	1	0	8	0
43	13	3	0	309	0
44	28	1	0	13	0
45	21	1	0	73	0
46	11	1	0	10	0
47	22	1	0	2	0
48	07	1	0	24	0
50	05	2	0	154	0
51	20	2	0	85	0
53	17	3	0	63	0
54	18	1	0	42	0
55	15	1	0	400	0
56	16	1	0	12	0
57	29	1	0	15	0
59	19	2	0	92	0
60	23	1	0	24	0
61	02	1	0	137	0
62	25	1	0	101	0
63	01	2	0	128	0
65	24	1	0	4	0
66	27	2	0	78	0
67	06	2	0	122	0
68	09	1	0	6	0
69	03	1	0	93	0
70	32	4	0	160	0
71	26	3	0	51	0
72	08	2	0	148	0
Totals		43	0	2354	0

Appendix A

URE as a Function of AOD

This appendix contains supporting information for the results presented in Section 3.1.2. Charts of SIS RMS URE vs. AOD charts similar to Figures 3.4-3.7 are presented for each GPS SV. The charts are organized by SV Block and by ascending SVN within each block.

These charts are based on the same set of 30 s Instantaneous RMS SIS URE values used in Section 3.1.1. For each SV, a period of 48 hours of AOD was divided into a set of 192 bins, each 15 minutes of AOD in duration. An additional bin was added for any AOD that appeared beyond 48 hours. All of the 30 s URE values for the year for a given SV were grouped according to AOD bin. The values in each bin were sorted and the 95^{th} percentile and the maximum were determined. Once the analysis was complete, it was clear that most bins beyond the 26 hour mark contained too few points to be considered statistically relevant. Therefore, when the number of points in a bin falls below 10% of the number of points in most populated bin, the bin is not used for plotting purposes. The problem with bins with low counts is that, in our experience, the results tend to dominated by one or two very good or very bad observations and this can lead to erroneous conclusions about behavior.

The figures on the following pages each show two curves:

- Blue: 95^{th} percentile SIS RMS URE vs. AOD (in hours)
- Green: the count of points in each bin as a function of AOD

Note that for most SVs, the green curve has a well-defined horizontal plateau that begins near zero AOD, continues for roughly 24 hours, and then drops quickly toward zero. The location of the right-hand drop of the green curve toward zero provides an estimate of the typical upload period for the SV. In cases where the SV is uploaded more frequently, the shape of the green curve will vary reflecting that difference.

A.1 Notes

This section contains some notes on SV-specific behavior observed in the following charts.

- SVN 44/PRN 28: This is the most obvious example of a SV that is being uploaded more frequently than normal. The fact that it is being uploaded more frequently is based on the shape of the dashed green curve which indicates the number of points in each AOD bin. The scale for this curve is on the right-hand vertical axis. The green curve does not exhibit the plateau seen in most plots but instead has a downward slope in the number of points as the AOD increases. If the SV were consistently being uploaded at a given interval, there would still be a plateau, only shorter than the typical plateau. For example, if an SV were being uploaded every 12 hours, one would expect a plateau from somewhere around an hour AOD out to 12 hours AOD. The near linear trend implies that the upload time for this SV is variable over a fairly large range.

- SVN 65/PRN 24: This Block IIF shows indications of occasional contingency uploads. This conclusion is based on the manner in which the SIS URE value line tends to flatten as it approaches the 3 m magnitude and the fact that the number of points starts to decline far earlier than the other Block IIF SVs. This is consistent with the higher 95^{th} percentile URE shown in Table 3.1 and Figure 3.1. It is likely related to the fact that SVN 65/PRN 24 is using a Cesium frequency reference. SVN 72/PRN 8 (which also uses a Cesium frequency reference) shows similar but less pronounced characteristics.

A.2 Block IIR SVs

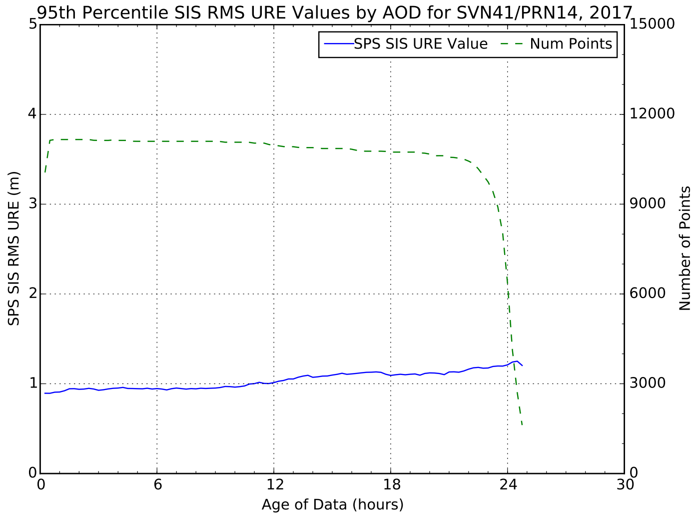

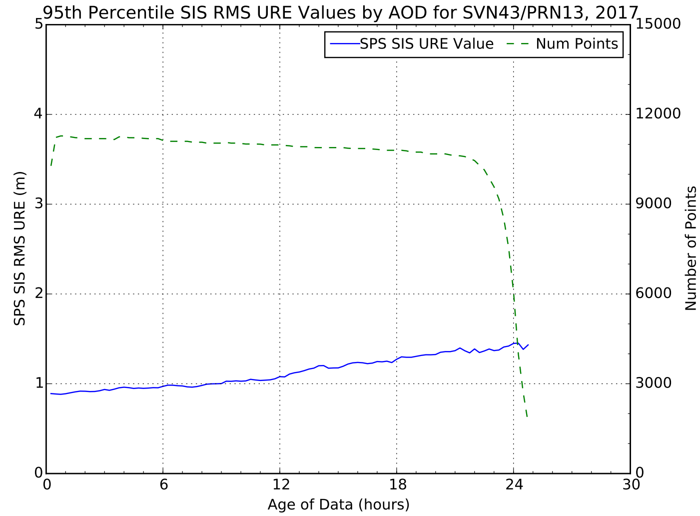

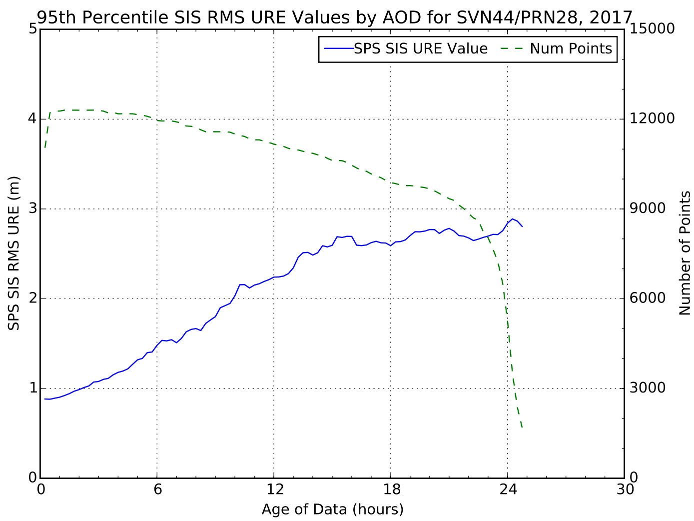

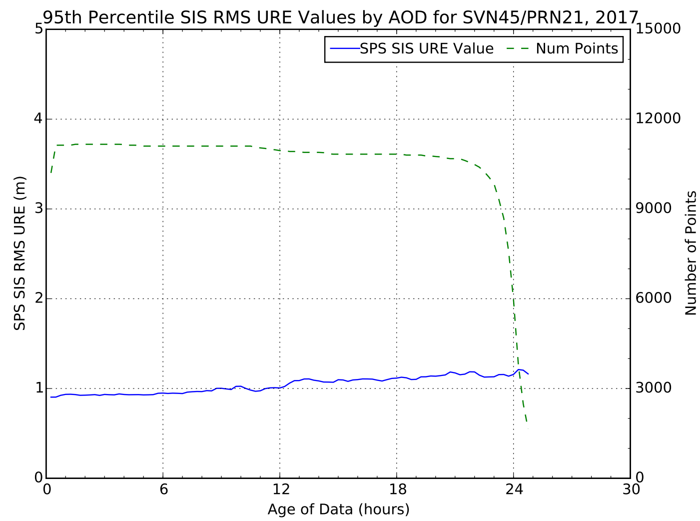

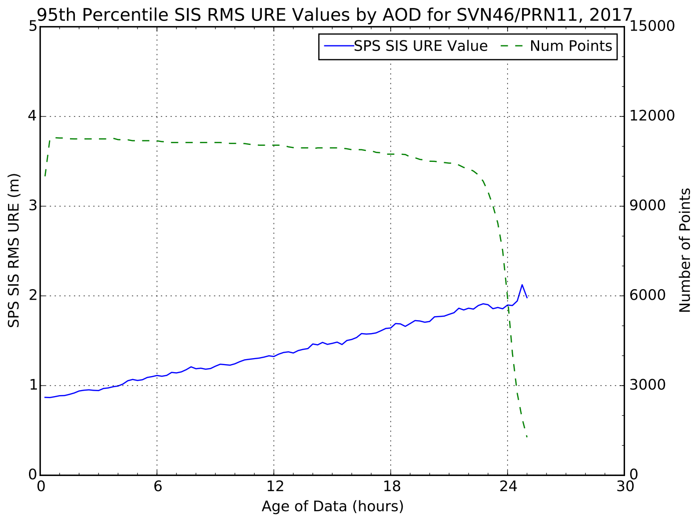
95th Percentile SIS RMS URE Values by AOD for SVN46/PRN11, 2017
SPS SIS URE Value
Num Points
SPS SIS RMS URE (m)
Number of Points
Age of Data (hours)

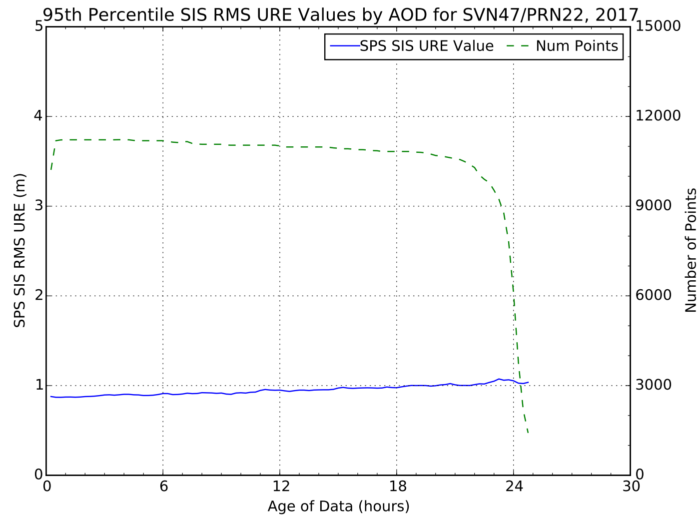
95th Percentile SIS RMS URE Values by AOD for SVN47/PRN22, 2017
SPS SIS URE Value
Num Points
SPS SIS RMS URE (m)
Number of Points
Age of Data (hours)

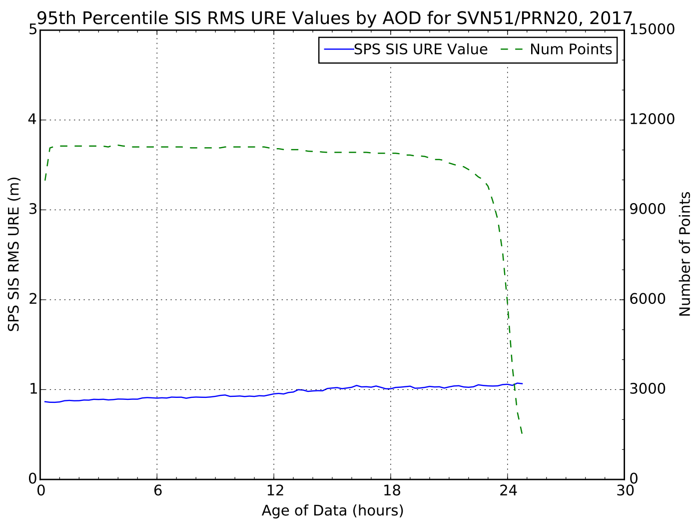
95th Percentile SIS RMS URE Values by AOD for SVN51/PRN20, 2017
SPS SIS URE Value
Num Points
SPS SIS RMS URE (m)
Number of Points
Age of Data (hours)

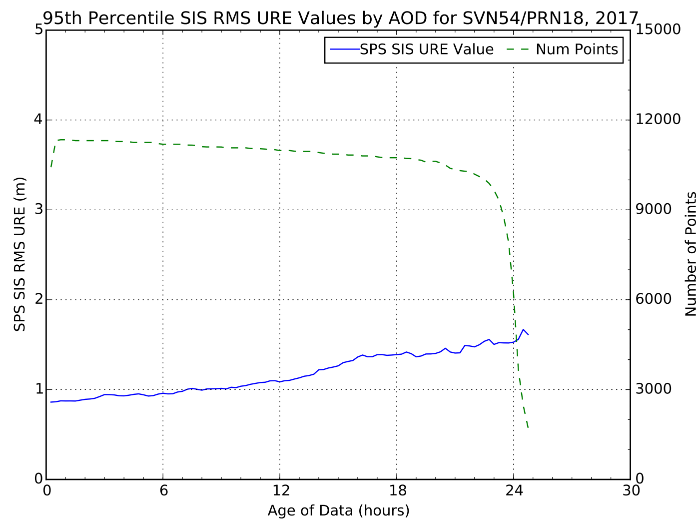
95th Percentile SIS RMS URE Values by AOD for SVN54/PRN18, 2017
SPS SIS URE Value
Num Points
SPS SIS RMS URE (m)
Number of Points
Age of Data (hours)

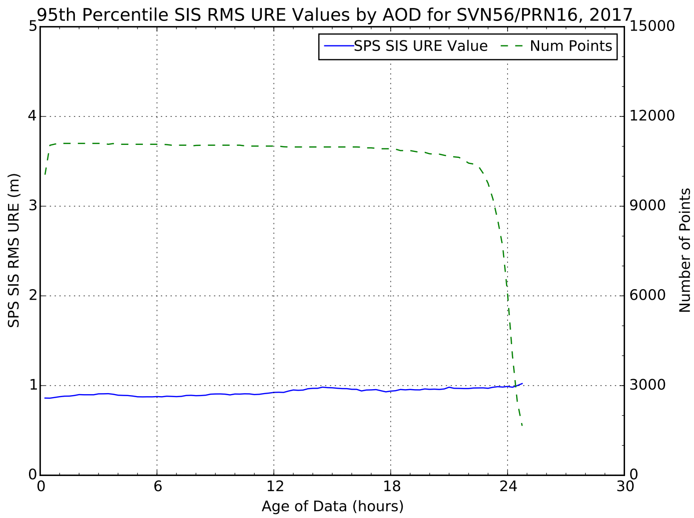
95th Percentile SIS RMS URE Values by AOD for SVN56/PRN16, 2017
SPS SIS URE Value
Num Points
SPS SIS RMS URE (m)
Number of Points
Age of Data (hours)

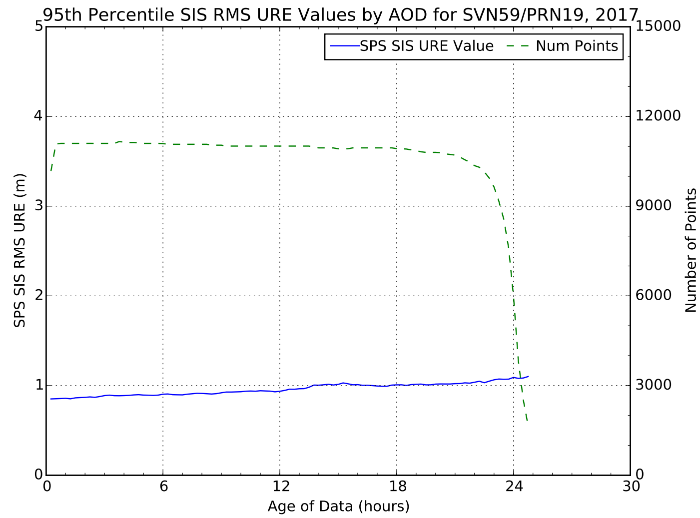
95th Percentile SIS RMS URE Values by AOD for SVN59/PRN19, 2017
SPS SIS URE Value
Num Points
SPS SIS RMS URE (m)
Number of Points
Age of Data (hours)

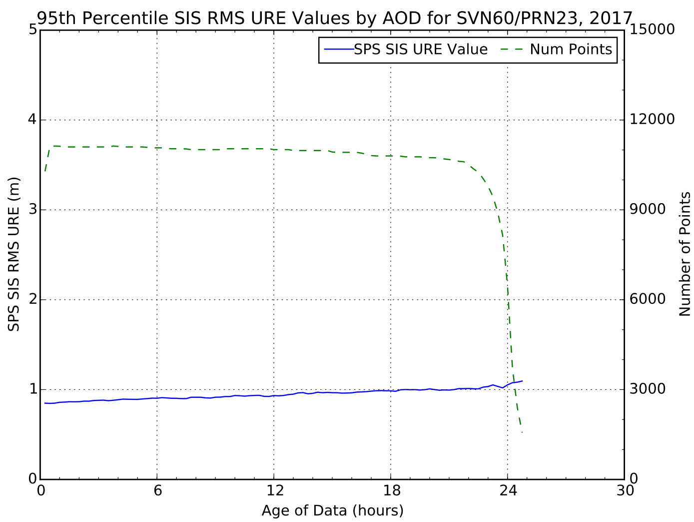
95th Percentile SIS RMS URE Values by AOD for SVN60/PRN23, 2017
SPS SIS URE Value
Num Points
SPS SIS RMS URE (m)
Number of Points
Age of Data (hours)

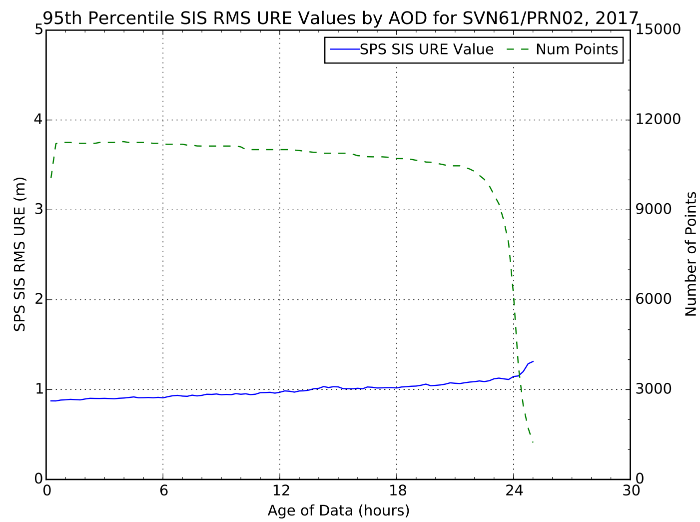
95th Percentile SIS RMS URE Values by AOD for SVN61/PRN02, 2017
SPS SIS URE Value
Num Points
SPS SIS RMS URE (m)
Number of Points
Age of Data (hours)

A.3 Block IIR-M SVs

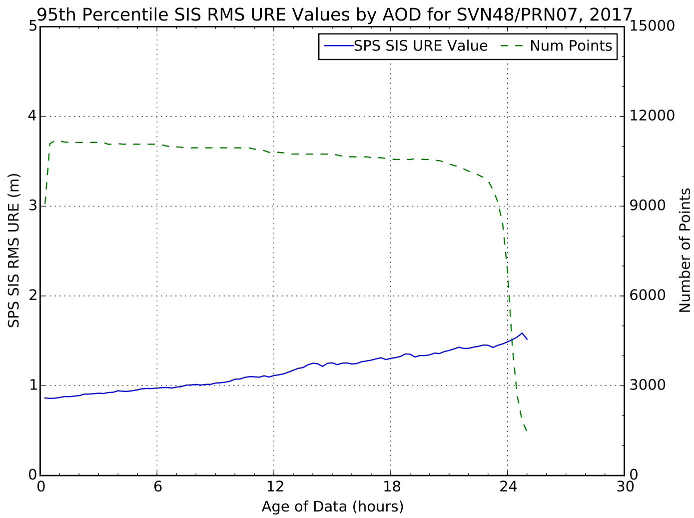

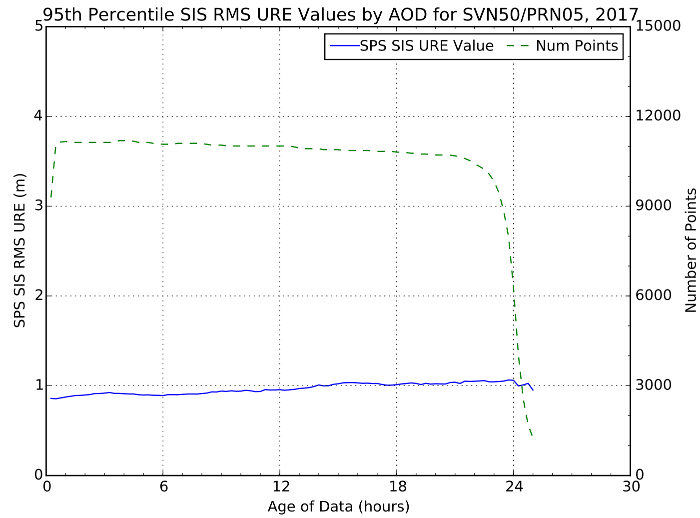

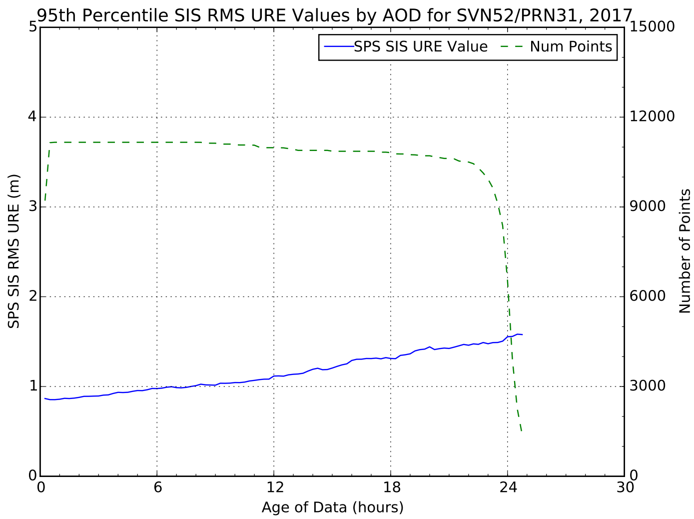

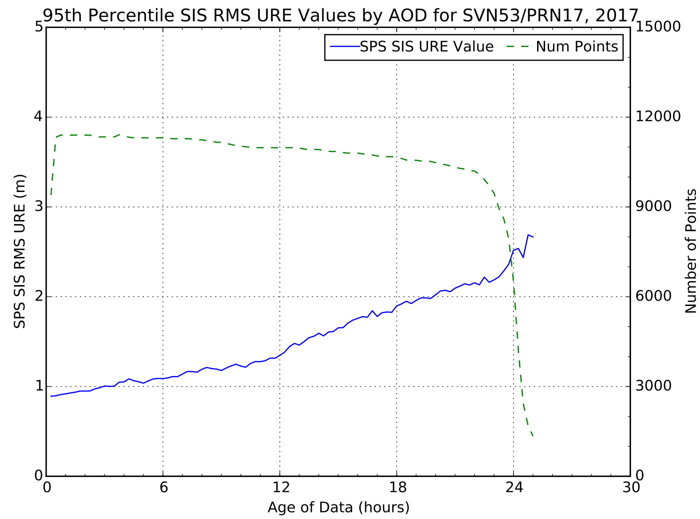

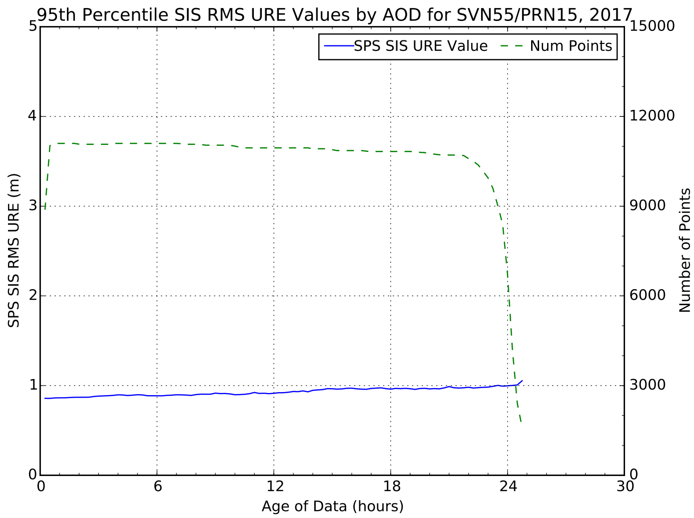
95th Percentile SIS RMS URE Values by AOD for SVN55/PRN15, 2017
SPS SIS URE Value
Num Points
SPS SIS RMS URE (m)
Number of Points
Age of Data (hours)
0
1
2
3
4
5
0
3000
6000
9000
12000
15000
0
6
12
18
24
30

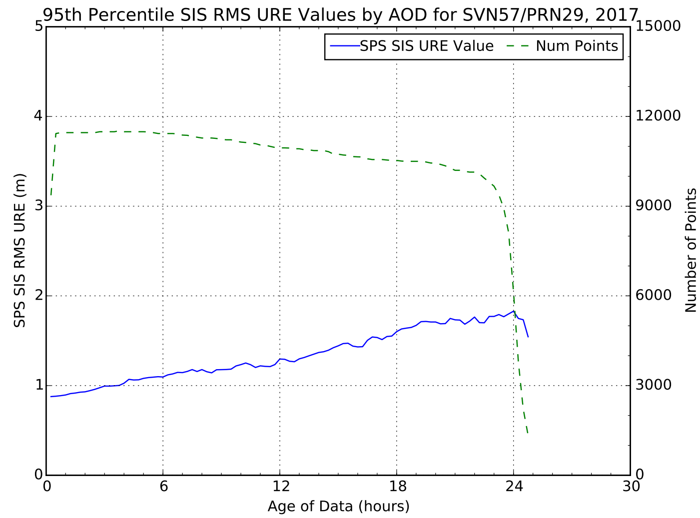
95th Percentile SIS RMS URE Values by AOD for SVN57/PRN29, 2017
SPS SIS URE Value
Num Points
SPS SIS RMS URE (m)
Number of Points
Age of Data (hours)
0
1
2
3
4
5
0
3000
6000
9000
12000
15000
0
6
12
18
24
30

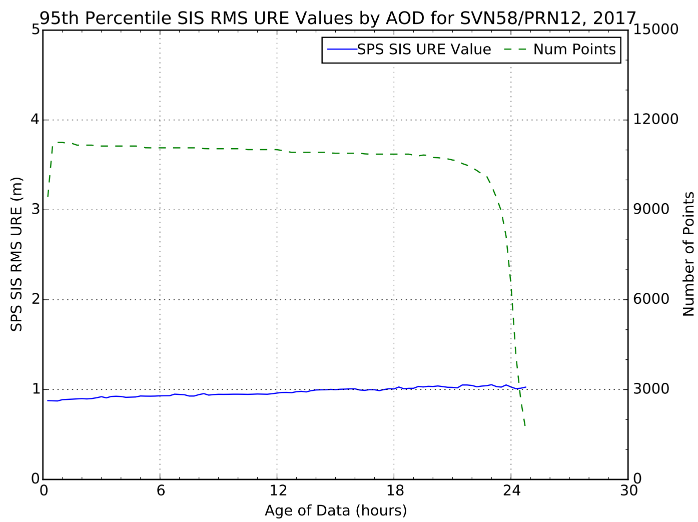
95th Percentile SIS RMS URE Values by AOD for SVN58/PRN12, 2017
SPS SIS URE Value
Num Points
SPS SIS RMS URE (m)
Number of Points
Age of Data (hours)
0
1
2
3
4
5
0
3000
6000
9000
12000
15000
0
6
12
18
24
30

A.4 Block IIF SVs

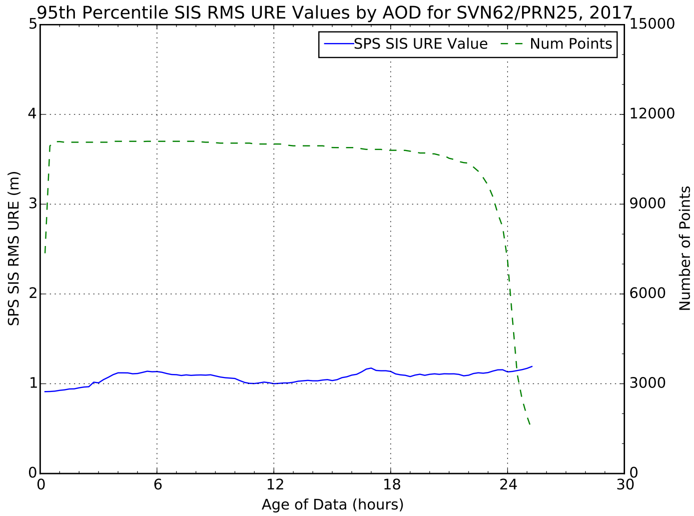

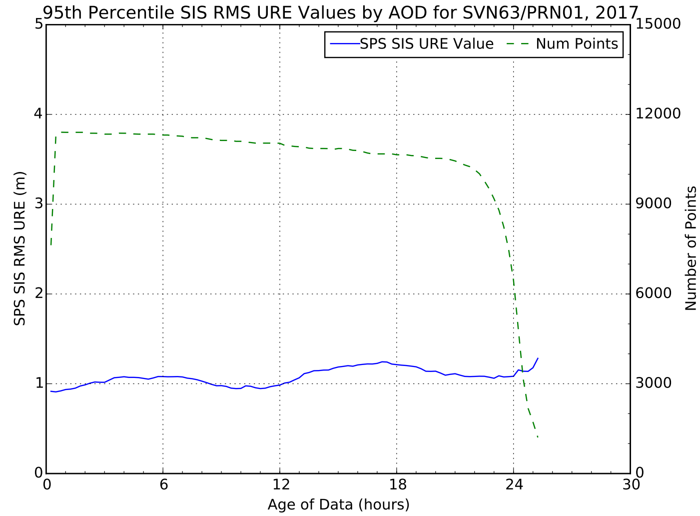

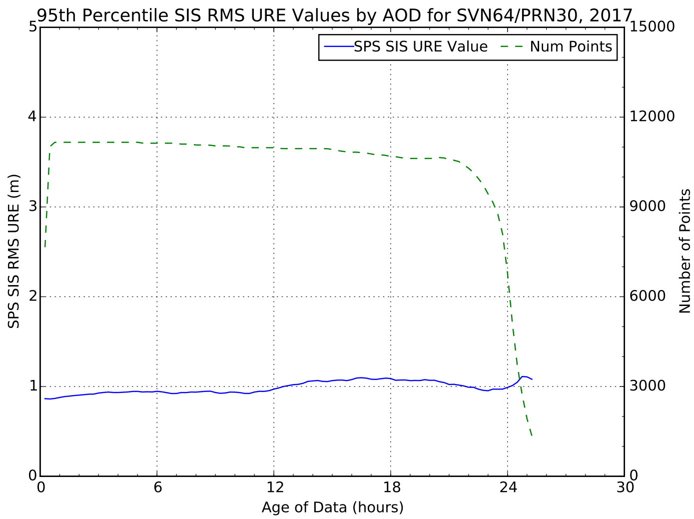

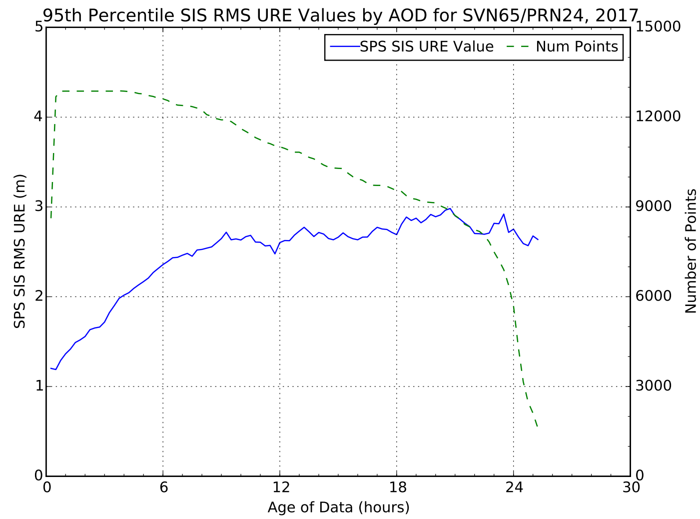

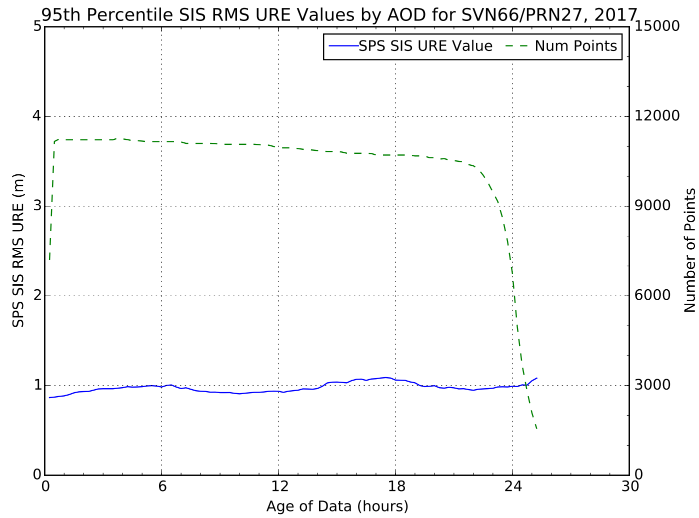
95th Percentile SIS RMS URE Values by AOD for SVN66/PRN27, 2017
SPS SIS URE Value
Num Points
SPS SIS RMS URE (m)
Number of Points
Age of Data (hours)

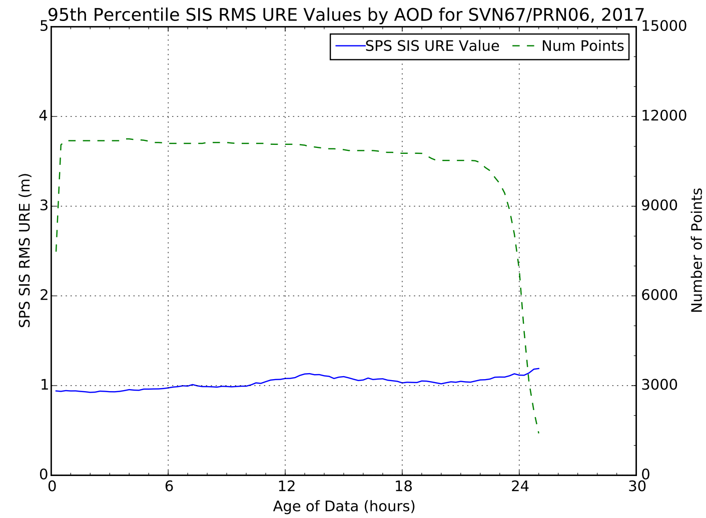
95th Percentile SIS RMS URE Values by AOD for SVN67/PRN06, 2017
SPS SIS URE Value
Num Points
SPS SIS RMS URE (m)
Number of Points
Age of Data (hours)

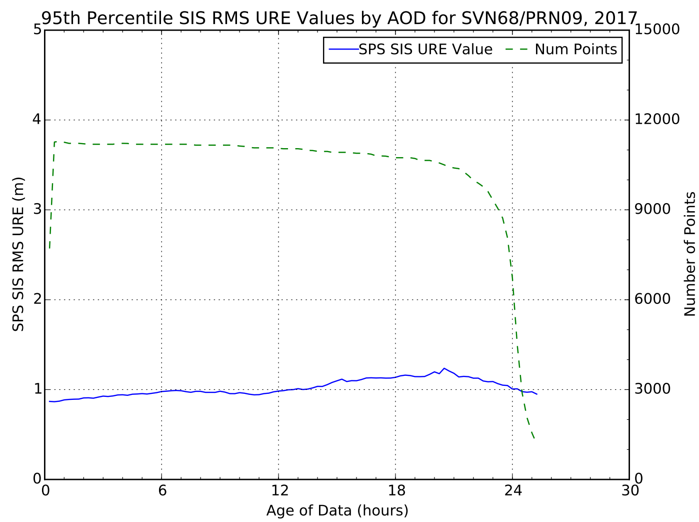
95th Percentile SIS RMS URE Values by AOD for SVN68/PRN09, 2017
SPS SIS URE Value
Num Points
SPS SIS RMS URE (m)
Number of Points
Age of Data (hours)

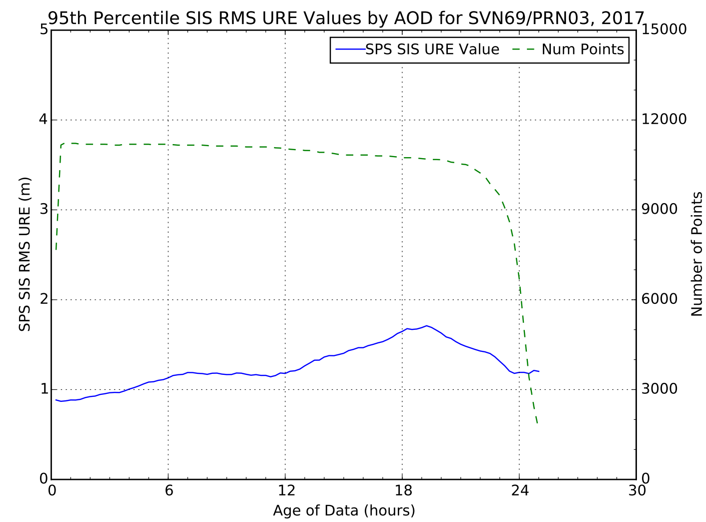
95th Percentile SIS RMS URE Values by AOD for SVN69/PRN03, 2017
SPS SIS URE Value
Num Points
SPS SIS RMS URE (m)
Number of Points
Age of Data (hours)

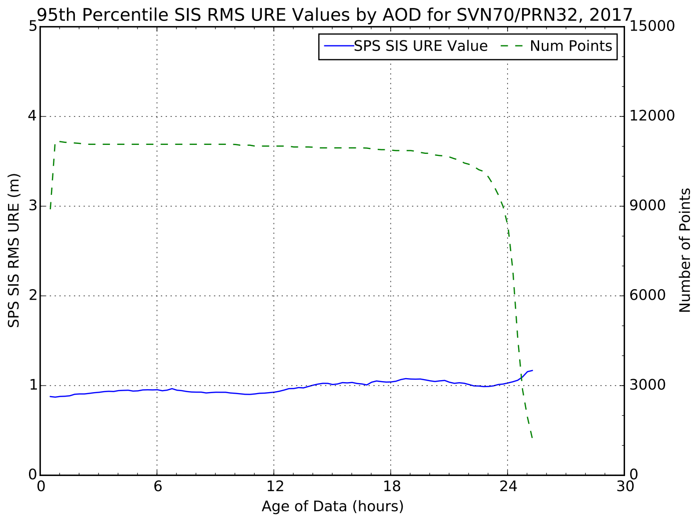
95th Percentile SIS RMS URE Values by AOD for SVN70/PRN32, 2017
SPS SIS URE Value
Num Points
SPS SIS RMS URE (m)
Number of Points
Age of Data (hours)

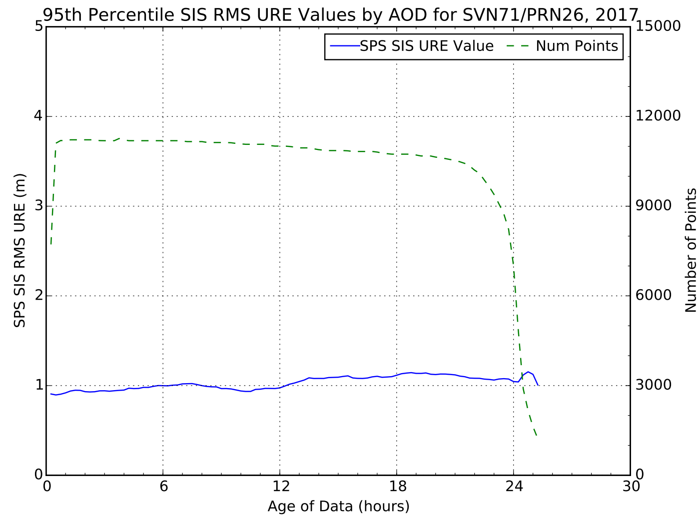
95th Percentile SIS RMS URE Values by AOD for SVN71/PRN26, 2017
SPS SIS URE Value
Num Points
SPS SIS RMS URE (m)
Number of Points
Age of Data (hours)

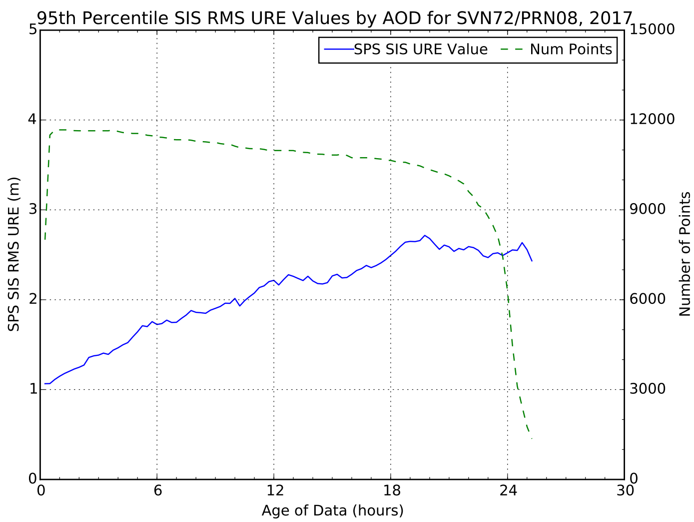
95th Percentile SIS RMS URE Values by AOD for SVN72/PRN08, 2017
SPS SIS URE Value
Num Points
SPS SIS RMS URE (m)
Number of Points
Age of Data (hours)

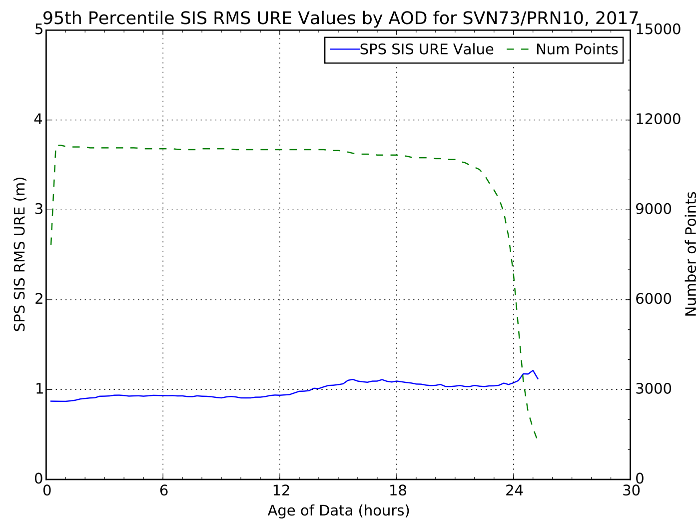
95th Percentile SIS RMS URE Values by AOD for SVN73/PRN10, 2017
SPS SIS URE Value
Num Points
SPS SIS RMS URE (m)
Number of Points
Age of Data (hours)

Appendix B

Analysis Details

B.1 URE Methodology

URE represents the accuracy of the broadcast navigation message. There are a number of error sources that affect the URE, including errors in broadcast ephemeris and timing.

Two methods to URE analysis are provided in this report. The first method (Section B.1.2) uses separate statistical processes over space and time to arrive at a URE. The second method (Section B.1.3) derives the URE by a single statistical process but is more computationally demanding.

B.1.1 Clock and Position Values for Broadcast and Truth

The URE values in this report are derived by comparison of the space vehicle (SV) clock and position representations as computed from the broadcast Legacy Navigation (LNAV) message data (BCP) against the SV truth clock and position data (TCP) provided by a precise orbit calculated after the time of interest.

The broadcast LNAV message data used in the calculations were collected by the National Geospatial-Intelligence Agency (NGA) MSN (Section B.2). The broadcast LNAV messages provide a set of parameters for an equation which can be evaluated at any time for which the parameters are valid. Our process evaluates the parameters at either a 30 s or 5 min cadence (depending on the process).

The TCP values are computed from the archived NGA products. The NGA products used in the calculations are the antenna phase center (APC) precise ephemeris files available from the NGA public website [14]. The NGA products are published in tabular SP3 format, with positions and clocks provided at a 5 min cadence. When TCP data are needed at a 5 min cadence, a simple table look-up is sufficient. When TCP data are needed at a 30 s cadence, a Lagrange interpolation scheme is used, in which the five points prior to and after the estimation time are used to estimate the SV position. Clock interpolation is handled via a linear interpolation between adjacent points.

B.1.2 95th Percentile Global Average in the SPS PS

The SPSPS08 specifications for URE suggest averaging across the service volume visible to a GPS SV at any specified point in time. The process is illustrated in Figure B.1.

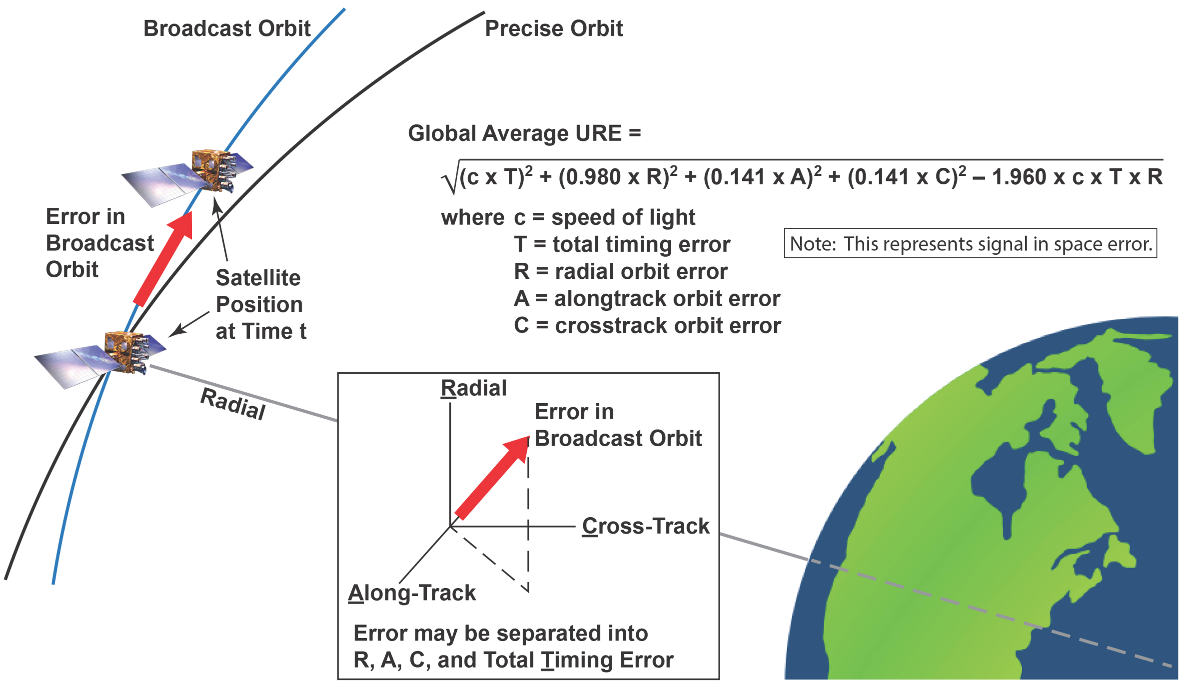

Figure B.1: Global Average URE as defined in SPS PS

The equation shown in Figure B.1 is Equation A-1 of SPSPS08 Section A.4.11. This expression allows the computation of the URE from known errors.

For purposes of this report, the Instantaneous RMS SIS URE values were generated at 30 s intervals for all of 2017. The URE was formed by differencing the BCP and TCP to obtain the radial, along-track, cross-track, and time errors at each epoch. These errors were used as inputs to the SPSPS08 Equation A-1.

After the Instantaneous RMS SIS URE values were computed, values for periods when each SV was unhealthy or not broadcasting were discarded. The remaining values were then grouped by monthly period for each SV and sorted; the maximum and the 95th percentile values within a given month were identified for each SV. This is the basis for Table 3.2. The monthly grouping corresponds closely to the 30 day period suggested in the SPSPS08 for URE Accuracy over all AODs while being more intuitive to the reader.

B.1.3 An Alternate Method

The previous method computes an SIS Instantaneous RMS URE (an average over space) for a given SV at a 30 s cadence over a month, then selects a 95^{th} percentile value from that set. That is to say, two different statistical processes are combined.

An alternate method is to compute the SIS Instantaneous URE for a large number of locations at each time point and store those results. For each SV, this is done for a series of time points at a selected cadence, and the collection of SIS Instantaneous URE values at each time point are stored. Once the values for all the time points for a month have been computed, the absolute values of SIS Instantaneous URE values for all time points are gathered together in a monthly set. The 95^{th} percentile value is selected from that set.

This method uses an approximation of an equidistant grid over the portion of the Earth visible to the SV with a spacing of roughly 550 km (5° latitude on the surface of the Earth). Considering those points at or above a 5° elevation angle with respect to the SV, this yields a set of 577 SIS Instantaneous URE values for each SV for each evaluation time. Figure B.2 illustrates this set of grid points for a particular SV-time shown as a projection onto the surface of the Earth.

This was done at a cadence of 5 min for each SV for all of 2017 and all 577 values were stored for all time points. Sets of values corresponding to each month were extracted (approximately 5 million values per SV-month). The absolute values and 95^{th} percentile values for each month were selected as the result for the SV-month. This is the basis for Table 3.3.

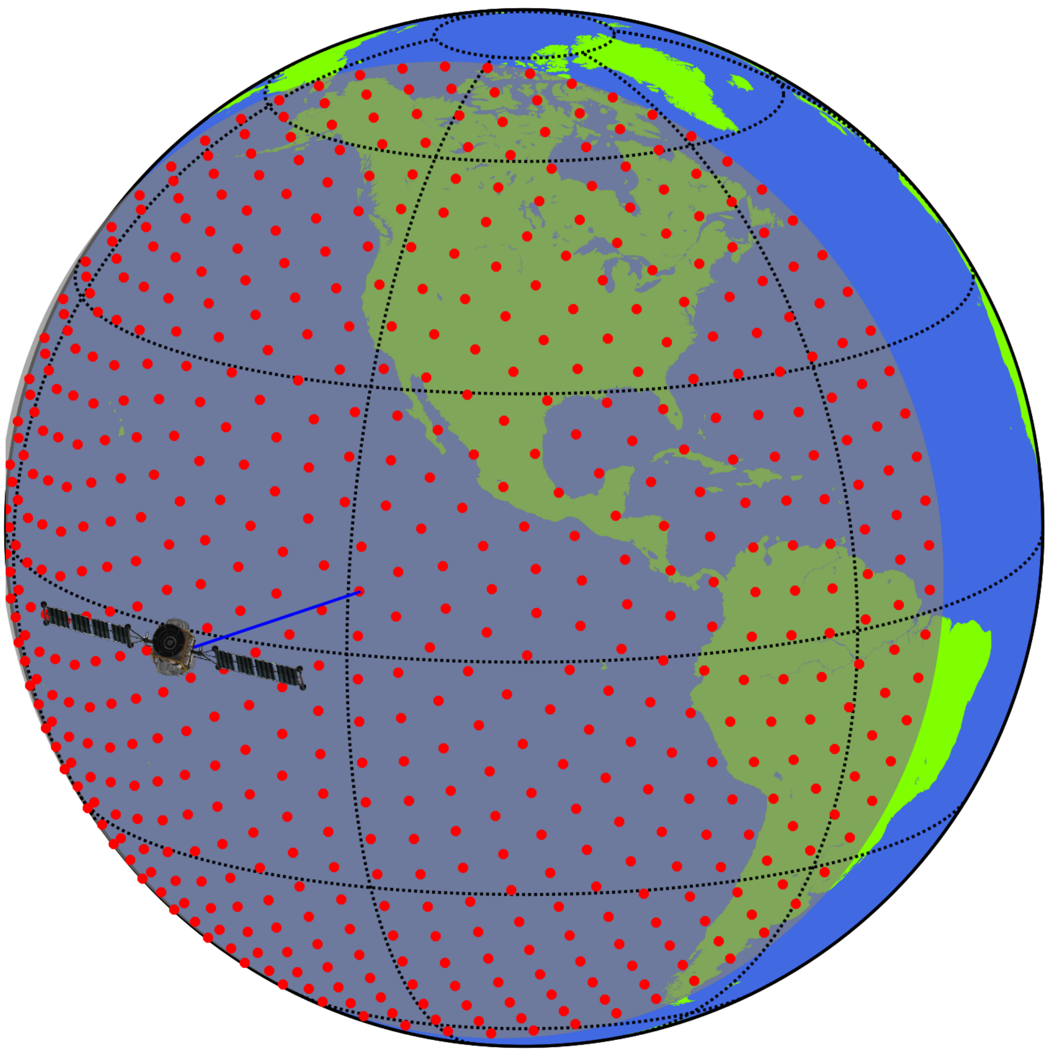

Figure B.2: Illustration of the 577 Point Grid

B.1.4 Limitations of URE Analysis

There are a number of subtleties in this method to computing URE accuracies, and the following paragraphs detail some of these.

The methods described in Sections B.1.1-B.1.3 work well when the estimated URE accuracy is below the required thresholds, as it verifies that the system is operating as expected. However, experience has shown that when an actual problem arises, the use of this procedure, without other cross-check mechanisms, can create some issues and may lead to incorrect results. Consider the following two cases.

- In cases where an SV is removed from service for reasons that invalidate the broadcast ephemeris (such as a clock run-off) we need to compare the time at which the removal from service occurred with the time at which any of the URE accuracy bounds were exceeded to assess whether a violation of the SPS PS metrics occurred. However, because we have relied on the interpolation process to generate 30 s values, we cannot obtain an accurate estimate of the time at which the URE bound was exceeded. As a general rule, the UREs computed in our process should be reviewed when they are contained between two SP3 epochs, one of which contains a clock event.
- When an SV is set unhealthy or cannot be tracked, the PE may provide misleading results. The analyst preparing the PE has several options for handling discontinuities that occur during outages. Therefore, the URE values generated near such events may be incorrect. As a result, it is necessary to avoid accepting UREs into the statistical process under conditions in which the SV could not be tracked or was set unhealthy. This has been done for all the results presented here.

In all cases, when an apparent violation of the URE limits is encountered, we choose to reconcile the analysis described above with the behavior of ORDs formed from the data collected at NGA and IGS sites. Because the observational data used is collected at a 30 s cadence, we obtain a much higher resolution insight into the details of the actual event than we do with the interpolated PE.

B.2 Selection of Broadcast Navigation Message Data

Several of the processes used in deriving the results in this report are dependent on the broadcast navigation message data. In most cases the data needed are the clock, ephemeris, and integrity data (CEI Data) contained in subframes 1, 2, and 3 of the GPS legacy navigation message (LNAV). These data are most often required in order to derive the position and/or health status of the transmitting SV.

The goal in selecting the CEI Data for a given SV at a given time of interest is to reproduce what the user would have experienced had they been collecting data from that SV at that time. To accomplish this, the process must have access to a complete time-history of navigation message data and it must properly select specific sets of CEI Data from that time-history.

The navigation message data supporting this analysis were collected from the National Geospatial-Intelligence Agency (NGA) GPS Monitor Station Network (MSN) [4]. The MSN has complete dual-station visibility to all GPS SVs (and generally much better). The redundant data sets at each navigation message epoch are cross-compared in order to best determine what was actually broadcast from each SV at each navigation message epoch. The MSN data collection process is designed to capture the earliest transmission of each unique set of CEI data. The data are stored in a format that retains all the transmitted bits. As part of the analysis associated with the production of this report, any gaps in the data set are investigated and filled if practical. The results is an archived time-history of the unique CEI Data sets transmitted by the constellation.

Wherever the analysis process requires CEI Data for a given SV at a given time, it selects the CEI Data set from the archive that corresponds to what was being transmitted from the SV at that time. During periods in which new data is being transmitted (data set cutovers), the preceding CEI Data set is used until the time the new CEI Data set had been completely transmitted and available to the user.

It must be recognized that this may be an inexact reproduction of the experience of any given user. Users may experience delays in the receipt of newly transmitted navigation message data due to obstructions, atmospheric issues, or receiver problems. However, this process is deterministic and reproducible.

B.3 AOD Methodology

The AOD was calculated by finding the upload times based on the t_{oe} offsets as defined in IS-GPS-200 Section 20.3.4.5 and then examining the t_{nmct} under the following assumptions:

- A complete set of the subframe 1, 2, and 3 data broadcast by all SVs of interest is available throughout the time period of interest.
- The term t_{nmct} defined in IS-GPS-200 Section 20.3.3.4.4 represents the time of the Kalman state used to derive the corresponding navigation message.

Given these assumptions, the AOD at any point in time can be determined by the following process:

- Working backward from the time of interest to finding the time when the most recent preceding upload was first broadcast
- Finding the AOD offset (AODO) of the associated subframe 2
- Subtracting the AODO from the t_{oe} (as described in IS-GPS-200 20.3.3.4.4) to determine the time of the Kalman state parameters
- Calculating the difference between the time of interest and the Kalman state parameter time

The search for the preceding upload is necessary because the AODO has a limited range and is not sufficient to maintain an accurate count for a complete upload cycle.

The results of this algorithm are generally consistent with the results provided by MCS analysis. The first assumption is fulfilled by the NGA MSN archive. The remaining assumptions were discussed with systems engineers supporting 2 SOPS and are believed to be valid.

The exception to this process is PRN 32. Any SV assigned to PRN 32 presents a minor problem for this analysis. This problem is limited to the type of performance analysis presented in this report. There is no similar concern for a GPS receiver. The AOD values are based on the AODO field in subframe 2. The definition of the AODO field is tied to how AODO is used to determine the age of the data in the NMCT. PRN 32 can never be represented in the NMCT due to the design of the navigation message. Therefore, the AODO field for PRN 32 is never reset to zero at a new upload but remains at the "all ones" state. Therefore, the AOD for PRN 32 cannot be independently derived from the navigation message data. For purposes of this report we examined all upload cutovers through 2017 for all SVs except SVN 70/PRN 32. For each upload cutover we computed the AOD at the time of the upload cutover. We then computed the mean of these samples to determine an average AOD at the time of the upload cutover. There were 11650 samples with an average AOD of 982 sec (about 16 minutes). We assumed this average holds true for SVN 70/PRN 32 and conducted the analysis accordingly.

Appendix C

PRN to SVN Mapping for 2017

Throughout the report, SVs have been referred to by both PRN and SVN. The PRN to SVN mapping is time dependent as PRN assignments change. Keeping track of this relationship has become more challenging over the past few years as the number of operational SVs is typically very close to the number of available PRNs. As a result, the relationships have been changing several times throughout a year. Therefore it is useful to have a summary of the PRN to SVN mapping as a function of time. Figure C.1 presents that mapping for 2017. SVNs on the right vertical axis appear in the order in which they were assigned the PRN values in 2017. Colored bars indicate the range of time each relationship was in effect. Start and end times of relationships are indicated by the dates at the top of the chart.

These data are assembled from the NANUs and the operational advisories, and confirmed by discussion with the Aerospace Corp. staff supporting 2SOPS.

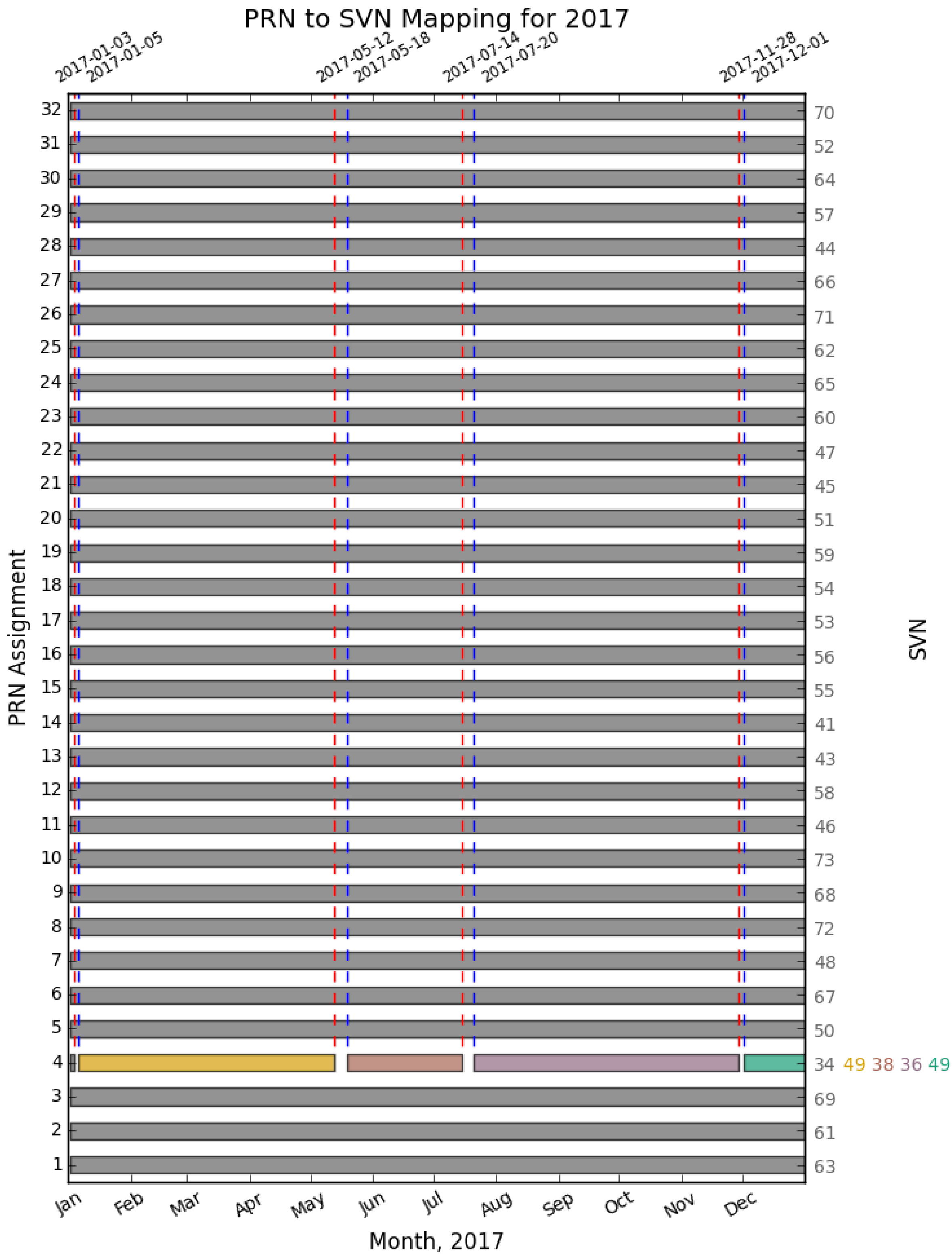

Figure C.1: PRN to SVN Mapping for 2017

Appendix D

NANU Activity in 2017

Several sections in the report make use of NANUs. It is useful to have a time history of the relevant NANUs sorted by SVN. This makes it convenient to determine which NANU(s) should be examined if an anomaly is observed for a particular satellite at a particular time.

Figure D.1 presents a plot of the NANU activity in 2017. Green bars are scheduled outages and red bars represent unscheduled outages. Gray bars represent SVs that have been decommissioned. No satellites were decommissioned in 2017. Yellow bars indicate scheduled outages with notice of less than 48 hours. NANU numbers are indicated next to each bar. In the event there is more than one NANU for an outage, the last NANU number is displayed.

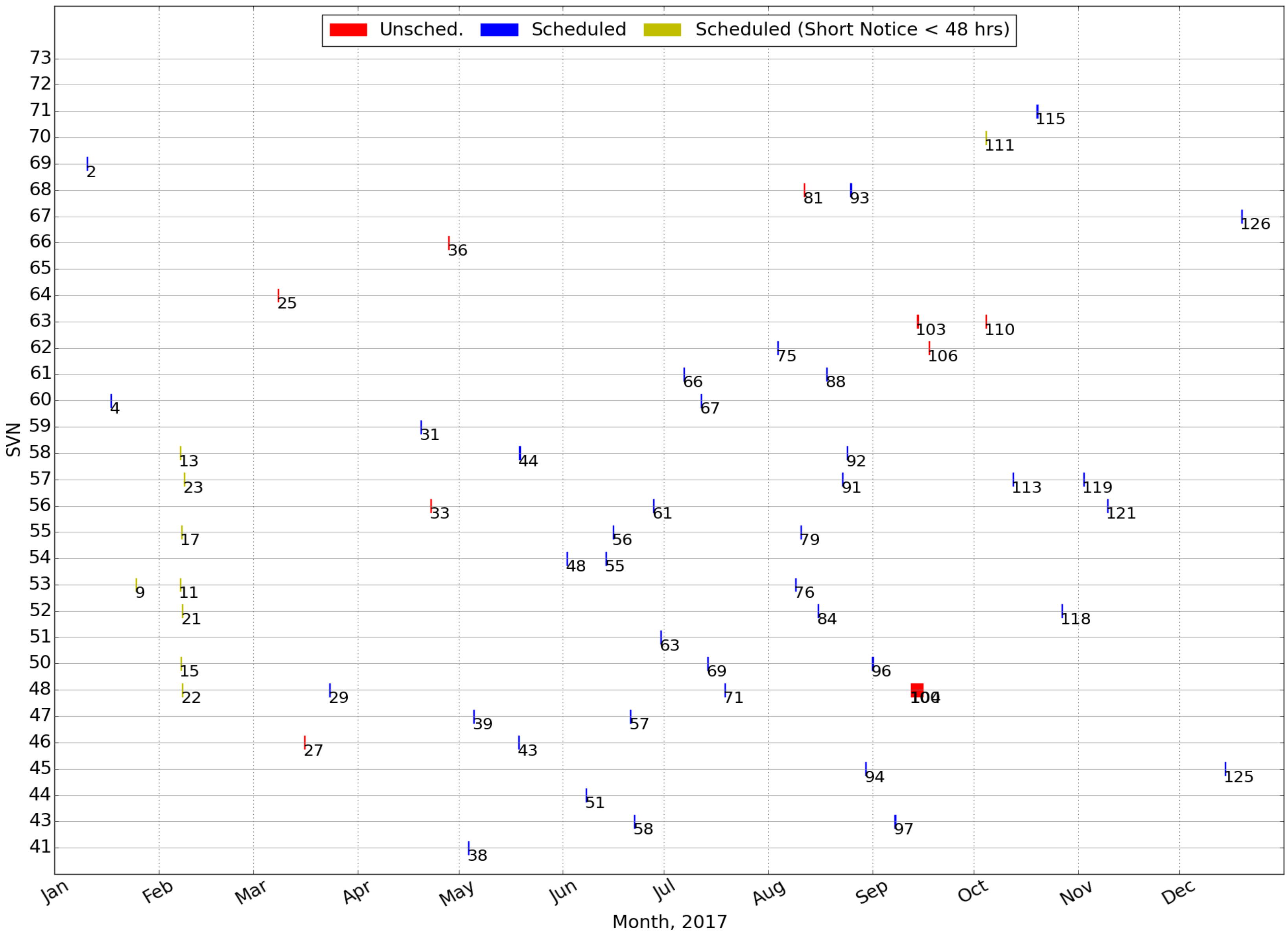

Figure D.1: Plot of NANU Activity for 2017

Appendix E

SVN to Plane-Slot Mapping for 2017

Several assertions are related to the performance of the constellation as defined by the plane-slot arrangement specified in the performance standard. Evaluation of these assertions requires information on the plane-slot occupancy during the year.

Information on plane-slot assignment is included in the operational advisory (OA) provided by 2 SOPS to the United States Coast Guard (USCG) Navigation Center and defined in ICD-GPS-240. This is a publicly available document and is one of few ways the public is informed of slot assignments. However, the format of the OA does not permit it to clearly convey the status of expanded slots. The format is limited to a letter representing the plane and a number representing the slot. There is no provision of the "fore/aft" designation. The OA designations are also cluttered by use of numbers greater than the number of defined slots. These are "slots of convenience" defined by the operators but have no fixed meaning in terms of position within the constellation. As a result, interpretation of the OA is challenging.

For the past several years, the plane-slot assignments have been provided to ARL:UT by Aerospace Corporation analysts supporting 2 SOPS. The assignments are provided as a set of daily plane-slot relationships. This information source is not publicly available.

Both of these sources are limited in that only a single satellite may be designated as being present in a slot at a given moment. In fact, as satellites are moved within the constellation, there exists occasional periods when more than one SV may be present within the defined boundaries of a slot. From the user's point of view, if a satellite transmitting a healthy signal is present within the slot boundaries, the slot should be counted as occupied.

Figure E.1 provides a graphical illustration of the plane-slot relationships throughout 2017. The contents of Figure E.1 are primarily drawn from the information provided by Aerospace Corporation and cross-checked against the Operational Advisories. In the cases where an SV is decommissioned or a new SV is launched, the appropriate NANUs were also checked to confirm dates. In some cases, multiple satellites fall within the same slot definition for a period of time. These special cases did not occur in 2017. The dates when satellites are judged to be present in a slot location are noted only when a change occurs in the plane-slot during the year. This allows the reader to determine when multiple satellites occupied the same slot.

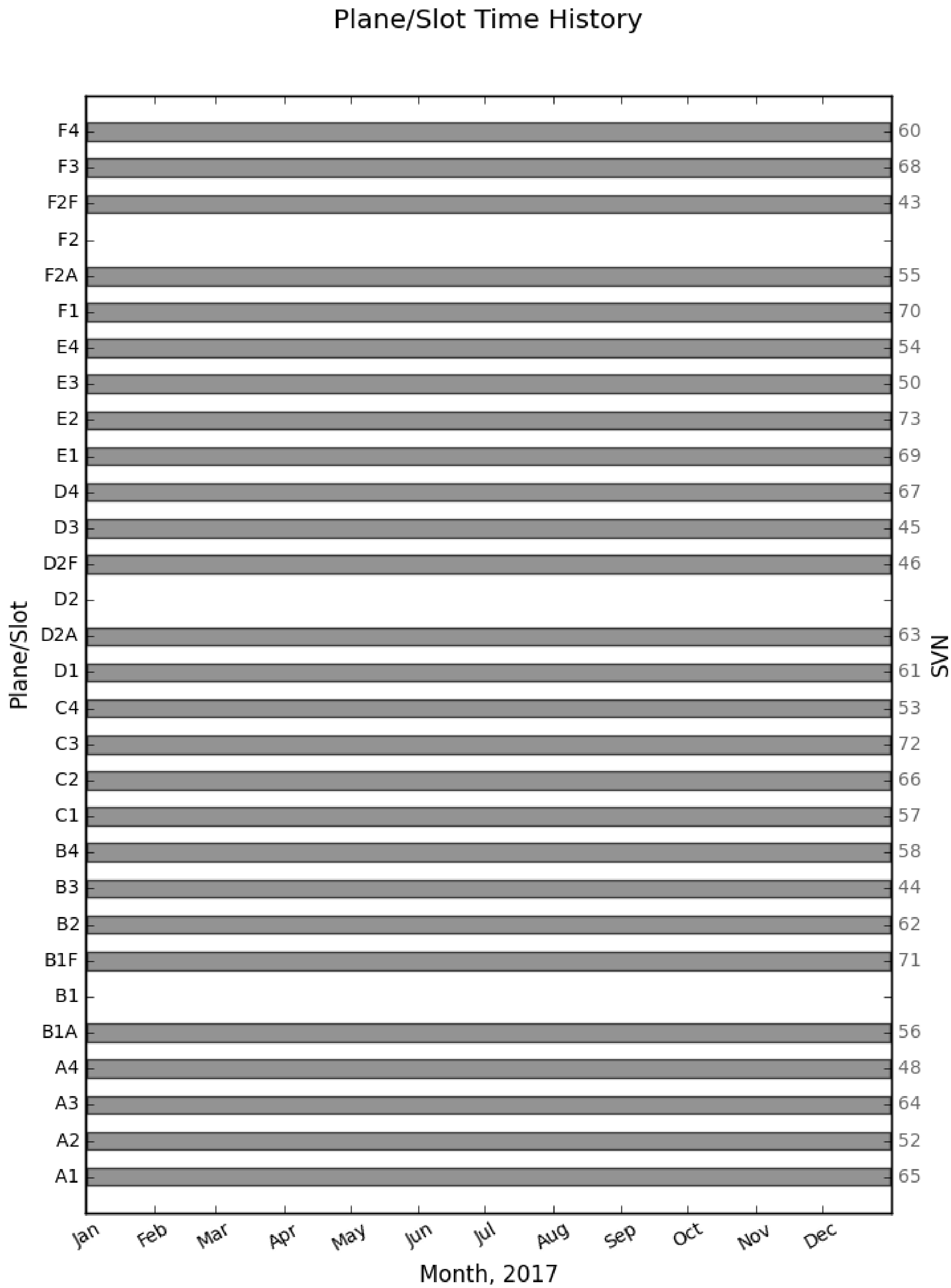

Figure E.1: Time History of Satellite Plane-Slots for 2017

Appendix F

Translation of URE Statistics Among Signals

The URE process described in Appendix B is based on the data broadcast in subframes 1, 2, and 3 of the navigation message and the NGA PE. Both of these estimates of the satellite orbits and clock offsets are referenced to the dual-frequency P(Y)-code signal. Therefore, the URE results are directly related to the Precise Positioning Service (PPS) dual-frequency performance. This appendix explains how these results have been interpreted to apply to the SPS assertions.

The PPS dual-frequency results may be mapped to SPS equivalent results by considering the effects of both the group delay differential and the intersignal bias (ISB) between the P(Y)-code and the C/A-Code on L1.

F.1 Group Delay Differential

As described in IS-GPS-200 Section 3.3.1.7, the group delay through the satellite transmission hardware is accounted for in the satellite clock offset. However, there remains a group delay differential effect that comes about due to the fact that the signals passing through the different frequency chains experience slightly different delays. An estimate of the group delay differential is transmitted to the users in the navigation message using the T_{GD} term in subframe 1. Note that T_{GD} is not the group delay differential but the group delay differential scaled to account for the difference between a dual-frequency observation and a single-frequency observation. This is described in IS-GPS-200 Section 20.3.3.3.3.2. This distinction will be relevant below when comparisons to other estimates are discussed.

IS-GPS-200 Section 3.3.1.7.2 states that the random plus non-random variations about the mean of the differential delay shall not exceed 3.0 nsec (95% probability). While this establishes an upper bound on the uncertainty, it does not represent actual performance. The quantization in the T_{GD} term is 0.5 nsec. Therefore, even with perfect estimation, the floor on the uncertainty would be on the order of 0.25 nsec.

If one assumes that T_{GD} is correct and that the user equipment properly applies the correction, then the single-frequency results would be aligned with the dual-frequency results to within that quantization error. However, once the satellite is on orbit it is not possible to directly observe T_{GD}. Instead it must be estimated, and the estimates are subject to a variety of factors including receiver group delay differential effects and ionospheric dispersion. This uncertainty has the effect of inflating the PPS dual-frequency results when these results are interpreted in terms of the PPS single-frequency or SPS services. In fact, because the errors are not directly observable, the best that can be done is to examine the repeatability in the estimate or the agreement between independent estimates and consider these as proxies for the actual uncertainty.

Since 1999, the T_{GD} values have been estimated by Jet Propulsion Laboratory (JPL) and provided to 2 SOPS on a quarterly basis. Shortly before this process was instituted there was a study of the proposed estimation process and a comparison of the estimates to those independently developed by two other sources [15]. The day-to-day uncertainty in the JPL estimates appeared to be about 0.3 nsec and the RMS of the differences between the three processes (after removal of a bias) was between 0.2 nsec and 0.7 nsec.

The Center For Orbit Determination (CODE) at the University of Bern estimates the P1-P2 bias [16]. CODE provides a group delay differential estimate for each SV every month. CODE does not provide details on the estimation process, but it must include a constraint that the group differential delay averaged over the constellation is zero as all sets of monthly values exhibit a zero mean.

A comparison of the CODE estimates and the T_{GD} values (scaled by the group differential delay values) shows a ∼5 nsec bias between the estimates. This bias can be removed as we are comparing mean-removed vs non-mean removed values. After the bias across the constellation is removed, the level of agreement between the scaled T_{GD} values and the monthly CODE estimates is between 0.1 nsec and 0.8 nsec RMS.

Considering all these factors, for the purpose of this analysis the uncertainty in the T_{GD} is assumed to be 0.5 nsec RMS.

F.2 Intersignal Bias

The ISB represents the difference between two signals on the same frequency. This bias is due to differences in the signal generation chain coupled with dispersive effects in the transmitter due to the differing bandwidths of the signals. It is not possible to observe these effects directly. When examining the signal structure at the nanosecond level the chip edges are not instantaneous transitions with perfectly vertical edges but exhibit rise times that vary by signal. Therefore, measuring the biases requires assumptions about the levels at which one decides a transition is in progress. These assumptions will vary between receivers.

There is no estimate of the ISB provided in the GPS legacy navigation message. However, CODE estimates the bias between the L1 P(Y)-code and the L1 C/A-code [16]. An estimate is provided for each SV every month. When this adjustment process was developed, these estimates were examined for each month in 2013. The monthly mean across all SVs is zero, suggesting the estimation process is artificially enforcing a constraint. The RMS of the monthly values across the constellation is 1.2 nsec for each month. Because there is no estimate of the ISB, this RMS value represents an estimate of the error C/A users experience due to the ISB.

F.3 Adjusting PPS Dual-Frequency Results for SPS

The PPS dual-frequency and SPS cases are based on a different combination and a different code. Therefore, the uncertainties in both T_{GD} and ISB must be considered. The PPS dual-frequency URE results are all stated as 95^{th} percentile (2-sigma) values. This means that the RMS errors estimated in Sections F.1 and F.2 must be multiplied by 1.96 (effectively 2, given that the amount of uncertainty in the values).

If it is assumed that these errors are uncorrelated, the total error may be estimated as:

$$\begin{aligned}
\text{Total error} &= \sqrt{((2 * \mathrm{T_{GD}}\text{ uncertainty})^2 + (2 * \text{ISB uncertainty})^2)} \\
&= \sqrt{((2 * 0.5\text{ nsec})^2 + (2 * 1.2\text{ nsec})^2)} \\
&= \sqrt{(1\text{ nsec}^2 + 5.76\text{ nsec}^2)} \\
&= 2.6\text{ nsec}
\end{aligned} \tag{F.3.1}$$

Converted to equivalent range at the speed of light and given only a single significant digit is justified, the total error is about 0.8 m. This adjustment may then be combined with the PPS dual-frequency result in a root-sum-square manner.

Appendix G

Acronyms and Abbreviations

Table G.1: List of Acronyms and Abbreviations

2 SOPS	-	2^{nd} Space Operations Squadron
AMCS	-	Alternate Master Control Station
AOD	-	Age of Data
AODO	-	Age of Data Offset
ARL:UT	-	Applied Research Laboratories, The University of Texas at Austin
BCP	-	Broadcast Clock and Position
CEI	-	Clock, Ephemeris, and Integrity
CMPS	-	Civil Monitoring Performance Specification
CODE	-	Center For Orbit Determination
DECOM	-	Decommission
DOP	-	Dilution of Precision
ECEF	-	Earth-Centered, Earth-Fixed
FAA	-	Federal Aviation Administration
FCSTDV	-	Forecast Delta-V
FCSTEXTD	-	Forecast Extension
FCSTMX	-	Forecast Maintenance
FCSTRESCD	-	Forecast Rescheduled
FCSTUUFN	-	Forecast Unusable Until Further Notice
GNSS	-	Global Navigation Satellite System

GPS	-	Global Positioning System
GPSTK	-	GPS Toolkit
HDOP	-	Horizontal Dilution Of Precision
IGS	-	International GNSS Service
IODC	-	Issue of Data, Clock
IODE	-	Issue of Data, Ephemeris
ISB	-	Intersignal Bias
JPL	-	Jet Propulsion Laboratory
LNAV	-	Legacy Navigation Message
LSB	-	Least Significant Bit
MCS	-	Master Control Station
MSB	-	Most Significant Bit
MSI	-	Misleading Signal Information
MSN	-	Monitor Station Network
NANU	-	Notice Advisory to Navstar Users
NAV	-	Navigation Message
NGA	-	National Geospatial-Intelligence Agency
NMCT	-	Navigation Message Correction Table
NTE	-	Not to Exceed
OA	-	Operational Advisory
ORD	-	Observed Range Deviation
PDOP	-	Position Dilution of Precision
PE	-	Precise Ephemeris
PPS	-	Precise Positioning Service
PRN	-	Pseudo-Random Noise
PVT	-	Position, Velocity, and Time
RAIM	-	Receiver Autonomous Integrity Monitoring
RINEX	-	Receiver Independent Exchange Format

RMS	-	Root Mean Square
SA	-	Selective Availability
SINEX	-	Station Independent Exchange Format
SIS	-	Signal-in-Space
SMC/GP	-	Space and Missile Systems Center Global Positioning Systems Directorate
SNR	-	Signal-to-Noise Ratio
SP3	-	Standard Product 3
SPS	-	Standard Positioning Service
SPS PS(SPSPS08)	-	2008 Standard Positioning Service Performance Standard
SV	-	Space Vehicle
SVN	-	Space Vehicle Number
TCP	-	Truth Clock and Position
T_{GD}	-	Group Delay
UNUNOREF	-	Unusable with No Reference
UNUSUFN	-	Unusable Until Further Notice
URA	-	User Range Accuracy
URAE	-	User Range Acceleration Error
URE	-	User Range Error
URRE	-	User Range Rate Error
USCG	-	United States Coast Guard
USNO	-	U.S. Naval Observatory
UTC	-	Coordinated Universal Time
UTCOE	-	UTC Offset Error
UUTCE	-	User UTC(USNO) Error
WGS 84	-	World Geodetic System 1984
ZAOD	-	Zero Age of Data

Bibliography

[1] U.S. Department of Defense. Standard Positioning Service Performance Standard, 4th Edition. `http://www.gps.gov/technical/ps/2008-SPS-performance-standard.pdf`, 2008.

[2] U.S. Department of Defense. Navstar GPS Space Segment/Navigation User Interfaces, IS-GPS-200, Revision G, September 2012.

[3] John M. Dow, R.E. Neilan, and C. Rizos. The International GNSS Service in a changing landscape of Global Navigation Satellite Systems. *Journal of Geodesy*, 2009.

[4] B. Renfro, D. Munton, and R. Mach. Around the World for 26 Years - A Brief History of the NGA Monitor Station Network. In *Proceedings of the Institute of Navigation International Technical Meeting*, Newport Beach, CA, 2012.

[5] U.S. Coast Guard. GPS Constellation Status. `https://www.navcen.uscg.gov/?Do=constellationStatus`.

[6] U.S. Naval Observatory. Block II Satellite Information. `ftp://tycho.usno.navy.mil/pub/gps/gpstd.txt`, January 2017.

[7] U.S. Naval Observatory. Daily GPS-UTC Comparison data. `ftp://tycho.usno.navy.mil/pub/gps/gps15m/gps_utc_1day.hist`.

[8] W. Gurtner and L. Estey. RINEX: The Receiver Independent Exchange Format Version 2.11, 2006.

[9] U.S. Department of Defense. Navstar GPS Control Segment to User Support Community Interfaces, ICD-GPS-240, Revision A, January 2010.

[10] U.S. Department of Transportation. Global Positiong System (GPS) Civil Monitoring Performance Specification, DOT-VNTSC-FAA-09-08, April 2009.

[11] P. Misra and P. Enge. *Global Positioning System: Signals, Measurements, and Performance*. Ganga-Jamuna Press, revised second edition, 2012.

[12] B. Tolman et al. The GPS Toolkit - Open Source GPS Software. In *Proceedings of the 17th International Technical Meeting of the Satellite Division of the Institute of Navigation (ION GNSS 2004)*, Long Beach, CA, 2004.

[13] NIMA Technical Report TR8350.2. Department of Defense World Geodetic System 1984, Its Definition and Relationships With Local Geodetic Systems, July 1997.

[14] National Geospatial-Intelligence Agency. NGA Antenna Phase Center Precise Ephemeris products. `ftp://ftp.nga.mil/pub2/gps/pedata`.

[15] Colleen H. Yinger, William A. Feess, Ray Di Esposti, The Aerospace Corporation, Andy Chasko, Barbara Cosentino, Dave Syse, Holloman Air Force Base, Brian Wilson, Jet Propulsion Laboratory, Maj. Barbara Wheaton, and SMC/CZUT. GPS Satellite Interfrequency Biases, June 1999.

[16] Center for Orbit Determination Europe. GPS satellite bias estimates for 2013. `ftp://ftp.aiub.unibe.ch/CODE/2013`, 2013.